EG&G Idaho, Inc.

FORM EG&G-398
(Rev. 11-79)

INTERIM REPORT

Accession No. _____

Report No. EGG-LOFT-5093

Contract Program or Project Title:

LOFT Experimental Program Division

Subject of this Document:

Large Break Transient Calculations ir a Commercial
PWR and LOFT Prototypicality Assessment

Type of Document:

Analysis results report

Author(s):

Lambert Winters

Date of Document:

April 1980

Responsible NRC Individual and NRC Office or Division:

G. D. McPherson, Acting Chief, LOFT Research Branch,
Division of Reactor Safety Research, USNRC

EG&G Idaho, Inc.
Idaho Falls, Idaho **83415**

Prepared for the
U.S. Nuclear Regulatory Commission
Washington, D.C.
Under DOE Contract No. **DE-AC07-76ID01570**
NRC FIN No. A6048

INTERIM REPORT

8005270 368

NRC Research and Technical
Assistance Report
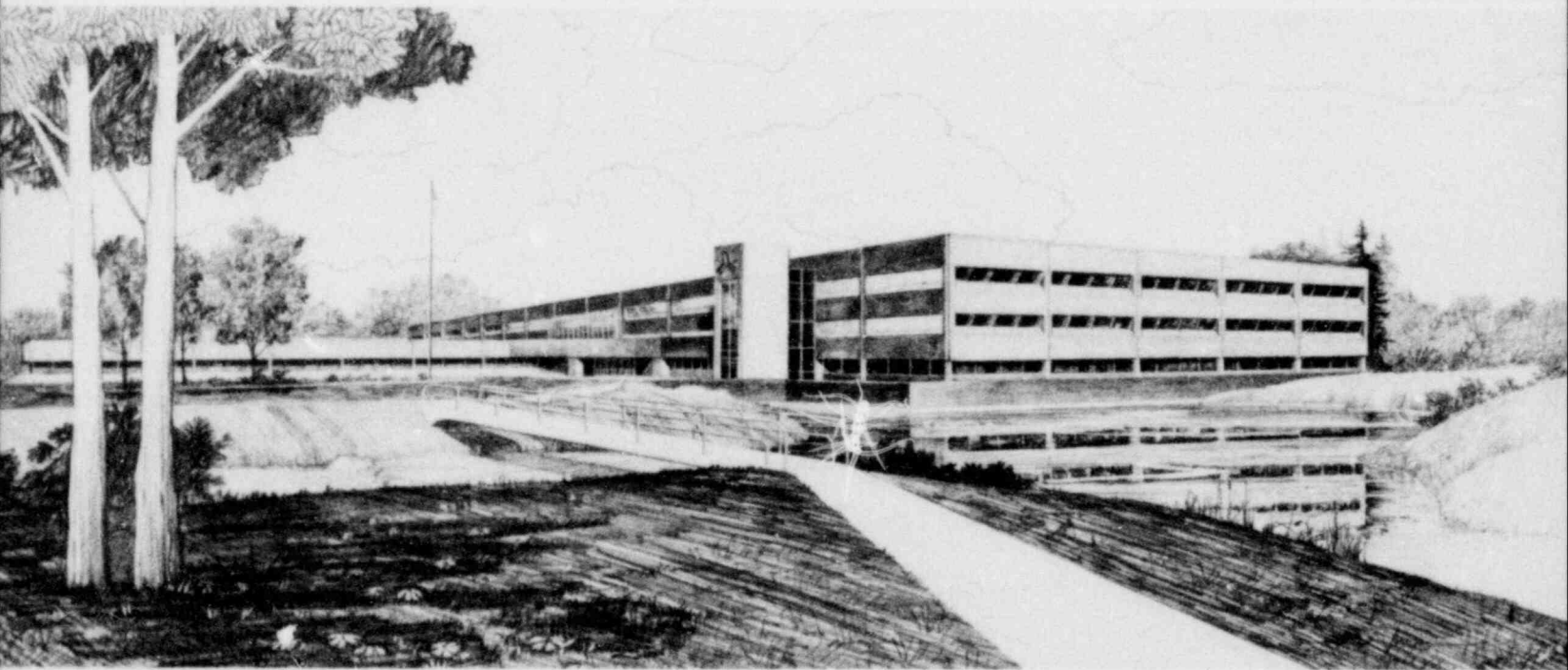
LARGE BREAK TRANSIENT CALCULATIONS IN A
COMMERCIAL PWR AND LOFT PROTOTYPICALITY

ASSESSMENT

SYSTEM (OO)

Lambert Winters

U.S. Department of Energy

Idaho Operations Office • Idaho National Engineering Laboratory

This is an informal report intended for use as a preliminary or working document
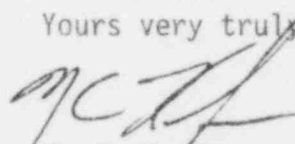
EG&G Idaho

May 5, 1980

Mr. R. E. Tiller, Director
Reactor Operations and Programs Division
Idaho Operations Office - DOE
Idaho Falls, Idaho 83401

REPORT TRANSMITTAL - Kau-58-80

Dear Mr. Tiller:

The report, "Large Break Transient Calculations in a Commercial
PWR and LOFT Prototypicality," is transmitted for your informa-
tion. This report serves to document those studies with the
RELAP4/MOD6 code that were done to determine the scaling relation-
ships between Loss-of-Fluid Test (LOFT) and the commercial pres-
surized water reactor (PWR) for large pipe break areas. Some of
the results were included in Research Information Letter No. 63.
The results are also being included in a paper requested by Nuclear
Technology.

Yours very truly,

N. C. Kaufman
Director, LOFT

VTB:tc

cc: R. W. Kiehn (w/o enc.)

EG&G Idaho, Inc.

FORM EG&G-229
(Rev. 01-80)

LOFT TECHNICAL REPORT

Title Large Break Transient Calculations in a Commercial PWR	LTR No. EGG-LOFT-5093
and LOFT Prototypicality	
Author Lambert Winters	Released By LOFT CDCS
	Date May 7, 1980
Performing Organization LOFT Experimental Programs	Project System Engineer
LOFT Review and Approval LTSD Mgr.	NA

For LOFT Experimental Program signatures, see Page ii

ABSRACT

For Absract, see page iii.

DISPOSITION OF RECOMMENDATIONS

No disposition required.

LARGE BREAK TRANSIENT CALCULATIONS IN A COMMERCIAL
PWR AND LOFT PROTOTYPICALITY ASSESSMENT

Approved:

S. A. Naff

Manager
Program Planning and Test Evaluation Branch

S. A. Naff

Manager
LOFT Experimental Program Division

ABSTRACT

This report presents results of calculations which predict the thermal-hydraulic response of a large pressurized water reactor (Zion 1 plant designed by Westinghouse Electric Corporation) to a hypothesized loss-of-coolant accident (LOCA). The calculations were performed using the RELAP4/MOD6 computer code, and the results are compared with large break loss-of-coolant experiments performed in the Loss-of-Fluid Test (LOFT) facility. The comparison indicates that the response of the LOFT facility to a LOCA is prototypical of Zion 1 response. Additional calculations (sensitivity studies) show that the response of Zion 1 to a large break LOCA is almost unaffected by changes in steam generator geometry and pressurizer water level. These calculations also show that the operation mode of the pumps during the accident is very important to the core mass flow behavior.

CONTENTS

FIGURES

TABLES

SUMMARY

This report documents results of calculations which predict the thermal-hydraulic response of a large pressurized water reactor (Zion 1 plant designed by Westinghouse Electric Corporation) to a hypothetical loss-of-coolant accident (LOCA). These calculations were performed for three 200% double-ended cold leg break LOCAs initiated at plant conditions corresponding to Loss-of-Fluid Test (LOFT) large break Experiments L2-2 and L2-3 (completed) and Experiment L2-4 (proposed).

The RELAP4/MOD6 computer code was used for this analysis. The analytical models used best-estimate predictive mechanisms and are described.

Results of the Zion 1 LOCA calculations are compared with data from LOFT Experiments L2-2 and L2-3. This comparison indicates that the response of the LOFT facility to a LOCA is prototypical of Zion 1 response.

Additional calculations (sensitivity studies) show that the response of Zion 1 to a 200% double-ended cold leg break LOCA would be almost unaffected by changes in steam generator geometry and pressurizer water level. These calculations also show that the pump operating mode during an accident would be very important to the core mass flow behavior.

1. INTRODUCTION

This report presents results of calculations, using the RELAP4 computer code, which predict the thermal-hydraulic response of a large pressurized water reactor (LPWR) to a hypothetical loss-of-coolant accident (LOCA). The LOCA calculations were performed to evaluate prototypicality of large break (200% double-ended cold leg break) loss-of-coolant experiments performed in the Loss-of-Fluid Test (LOFT) facility[1] for simulating LOCAs in a LPWR. The Zion 1 plant, a currently operational LPWR built by Westinghouse Electric Corporation, was chosen as the subject for the calculations. LOFT large break Experiments L2-2 and L2-3 provided a comparison for the calculated results.

Basically, three calculations were done for Zion 1: One of the calculations was done at approximately 70% nominal power, and one at approximately 110% nominal power. These two power level conditions, together with nominal plant coolant mass flow, furnish the Zion 1 plant with the same temperature difference across the core as in LOFT Experiments L2-2 and L2-3, respectively. A third calculation was done with an increased mass flow (130% of the nominal mass flow) and with a power level of about 150% of the nominal power which gives a plant condition comparable with the proposed LOFT Experiment L2-4. The calculations were done only for the blowdown phase and a part of the refill phase; there is no analysis of the reflood phase. In this report, the data from LOFT Experiments L2-2 and L2-3 are compared with the first two Zion 1 calculations.

In addition to the three basic calculations, specific sensitivity studies were done. These studies are divided into three major parts: The first part gives the sensitivity of calculated parameters to some RELAP4 input options. The second part consists of a pair of calculations which investigate the influence of the pressurizer level and the steam generator design on a LPWR LOCA calculation. The remaining sensitivity calculations give the sensitivity of the system behavior during a LOCA for different plant conditions. Some of these studies can be used in defining future experiments in the LOFT large break experiment series.

Sections 1.1 and 1.2 of this introduction give brief descriptions of the Zion 1 plant and of the analytical model used for the calculations, respectively. Section 2 describes the calculational techniques, and Section 3 presents the calculational results. The calculated and experimental data are compared in Section 4. Results of the sensitivity studies are presented in Section 5. Section 6 contains the conclusions reached from this analysis.

1.1 Description of the Reference Plant

The plant chosen for this study was the Zion 1 reactor, a 15 x 15 four-loop pressurized water reactor designed by Westinghouse Electric Corporation. The Zion 1 plant was chosen for these calculations because a basic RELAP4 model of the plant was available,[2] eliminating the very time consuming work of gathering all the geometrical information needed. The Zion 1 plant is considered to be representative of LPWRs; therefore, the results of the calculations should be considered as typical for a LPWR of that type.

All the information used in the calculations, geometries, nuclear data, and other characteristics, were taken from an earlier study on the Zion 1 plant described in Reference 2. The nominal operating conditions for the plant are given in Table 1.

TABLE 1. NOMINAL OPERATING CONDITIONS FOR ZION 1

Operational Parameter	Value
Core power [MW(t)]	3 238
Peak power density (kW/m)	35.8
Core coolant flow (kg/s)	18 296
Core coolant inlet temperature (K)	550
System pressure (MPa)	15.5

1.2 Analytical Model

All the calculations have been done with the RELAP4/MOD6 (Update 4)[3,a] code which has had a few minor updates. Some corrections were made in the heat transfer subroutines (HTS2 and HTS4) and also in the Wilson bubble rise subroutine. The RELAP4 blowdown system calculation was used to generate boundary conditions for the RELAP4/MOD6 "hot pin" calculations.

2. CALCULATIONAL TECHNIQUES

The technical bases for the calculations are presented. The intent is to describe the analytical methods and models which were used in the calculations; however, only the more significant basic equations are discussed. Basically, the same models and methods were used in these calculations as were used in the RELAP4 predictions for LOFT Experiments L2-2, L2-3, and L2-4.[4] All the models used should be recognized as best estimate models.

2.1 RELAP4 System Input Model

The nodalization and models for the RELAP4 system input model are described in this section.

2.1.1 Nodalization

The RELAP4 system input model consists of 42 control volumes, 60 junctions, and 17 heat slabs. The nodalization for the system model was basically the same as the nodalization used in the recent RELAP4 models for LOFT.[4,5] A schematic of the system model is shown in Figure 1. A brief description of each control volume is given in Table 2. Some major points concerning the nodalization follow.

---

a. RELAP4/MOD6 (Update 4), Idaho National Engineering Laboratory Configuration Control Number H01017IB.
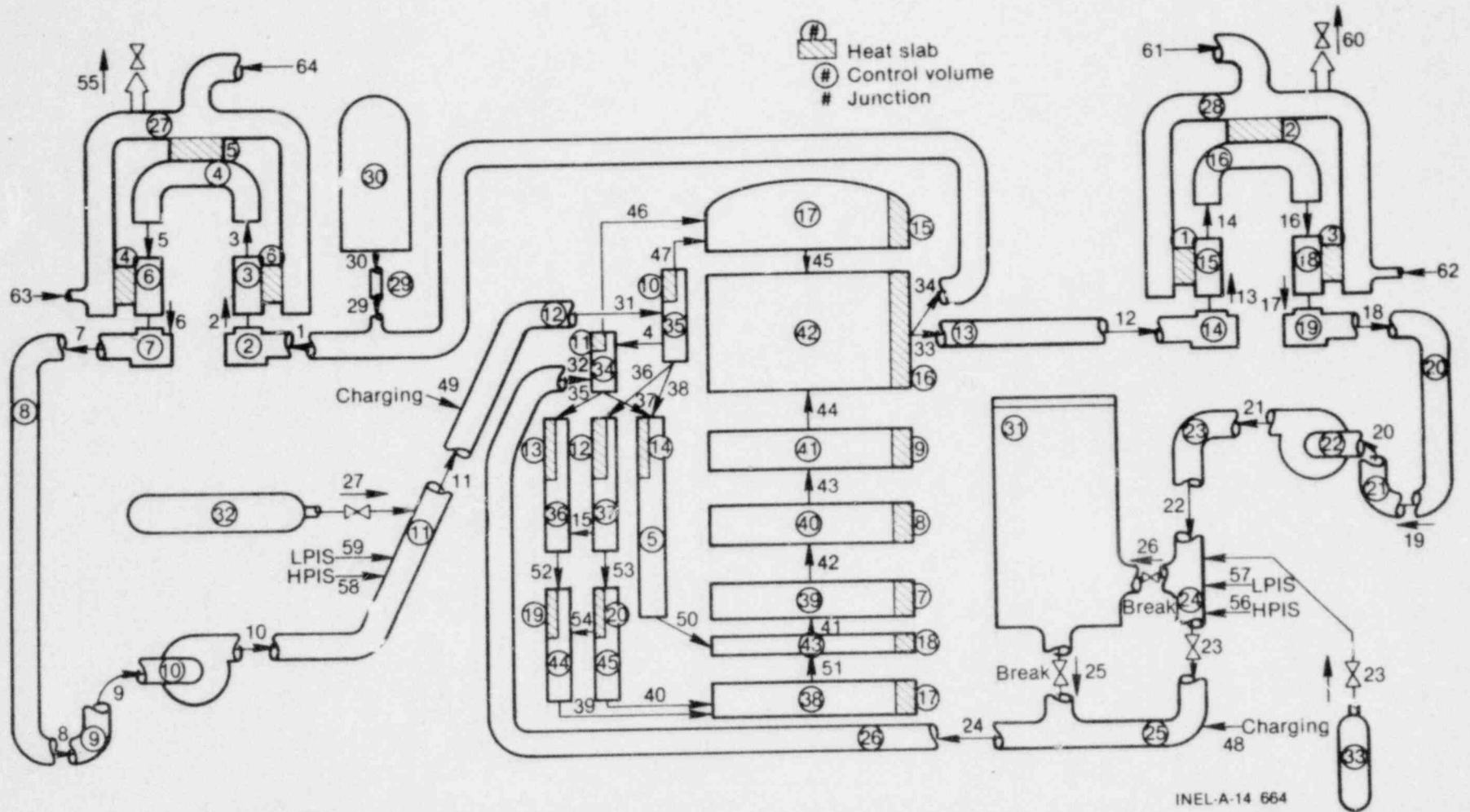
Figure 1. RELAP4 model schematic diagram for a LPWR.

INEL-A-14 664

TABLE 2. DESCRIPTION OF CONTROL VOLUMES FOR RELAP4 SYSTEM INPUT MODEL

Control Volume	Description
1, 8, 9, 11, and 12	Intact loop piping
2	Inlet plenum of intact loop steam generator
3, 4, and 6	Intact loop steam generator tubes
7	Outlet plenum of intact loop steam generator
10	Intact loop primary coolant pump
13, 20, 21, 23, 24, 25, and 26	Broken loop piping
14	Inlet plenum of broken loop steam generator
15, 16, and 18	Broken loop steam generator tubes
19	Outlet plenum of broken loop steam generator
22	Broken loop primary coolant pump
34 and 35	Downcomer inlet annulus
36 and 37	Upper part of downcomer
44 and 45	Lower part of downcomer
38 and 43	Lower plenum
39, 40, and 41	Core
42	Upper plenum
17	Upper head
5	Core bypass
27	Secondary side of intact loop steam generator
28	Secondary side of broken loop steam generator
30	Pressurizer
29	Pressurizer surge line
32	Intact loop accumulator
33	Broken loop accumulator (not used)
31	Containment

The "split-downcomer" model was used for this analysis since it allows a realistic description of the penetration of emergency core coolant (ECC) water into the reactor vessel downcomer. In this model, the downcomer was axially divided into an upper annulus and two axial stacked volumes with the circumference of each volume split into two volumes (three-fourths of the volume was located on the intact loop side and one-fourth of the volume on the broken loop side of the downcomer). A more complete description of the split downcomer model is given in Reference 6.

The core was divided in three axial stacked volumes; each volume contains a heat slab representing the fuel rods.

The pressurizer and the surge line of the pressurizer were modeled as two separate volumes. This is in contrast with the nodalization used in the RELAP4 LOFT model[4], where the surge line and pressurizer were modeled as one volume.

The upper plenum of the reactor vessel was modeled as one volume. A sensitivity study[2] of the nodalization of the upper plenum shows that test results are not influenced by modeling the upper plenum with only one volume. The temperature of the fluid in the reactor vessel upper head was taken as equal to the sum of the cold leg fluid temperature plus 60% of the core inlet-to-outlet fluid temperature difference.

The LOCAs evaluated in all cases were 200% double-ended cold leg breaks. Initiation of the LOCAs was controlled by three valves (Junctions 23, 25, and 26 shown in Figure 1). At time t = 0, the LOCAs were initiated by simultaneously opening Valves 25 and 26 and closing Valve 23. The valves in Junctions 25 and 26 have flow areas respectively equal to the cold leg and hot leg piping of the broken loop. The coolant flowed through these two discharge valves into the containment reservoir. The containment reservoir of the reactor plant was modeled as a control volume with the pressure given as a function of time.

The ECC injection can be made into either the broken loop or intact loop, as shown in Figure 1. However, for all the calculations, the ECC injection systems on the broken loop side were turned off. This was done by setting Junctions 56, 57, and 48 to zero and closing the valve in Junction 28 during the transient. There are two reasons to turn off the ECC systems on the broken loop side as follows:

1. For RELAP4 calculations, instantaneous equilibrium in the volumes is assumed. After injection of cold water from the accumulator was started, the pressure in Volume 24 decreased fast. After a short time, the pressure was lower than the containment pressure, and reverse flow from the containment to the hot leg broken loop occurred. This caused instabilities and a considerable increase in central processing unit (CPU) time on the computer.

2. The LOFT facility has ECC injection only in the intact loop. The broken loop ECC system of Zion 1 was turned off to make the Zion 1 calculation similar to LOFT experiment conditions.

2.1.2 Models

The compressible flow equation (MVMIX=0) was used for almost all the junctions. The incompressible (MVMIX=3) flow equation was used only for the cross-flow junctions in the downcomer, the junctions connected with the core bypass, the ECC junctions, and the junctions on the secondary side of the steam generator.

All the volumes were assumed to contain homogeneous fluid except the upper head, pressurizer, and inlet and outlet plena of the steam generator. For these volumes, the Wilson bubble rise model was applied. Complete phase separation was used in the accumulator. In the secondary side of the steam generator, a bubble rise model consistent with the heat transfer rate and mass flow was chosen.

The Henry-Fauske critical flow model was specified in the subcooled region, and the homogeneous equilibrium model (HEM) was specified in the saturated region with a transition region from 0.0 to 0.25% quality. The multiplier (contraction coefficient) used in the critical flow model was 1.0. In RELAP4, the critical flow tables are given as a function of the upstream stagnation properties. However, RELAP4 calculates the static properties and uses these properties in the critical flow tables. Earlier studies showed that the cold leg break flow was influenced by this phenomena. An artificially large flow area was applied to the two control volumes upstream of the break in the cold leg. This was done in an attempt to model the stagnation properties in the volume upstream of this break junction. The two volumes (Volumes 25 and 26 in Figure 1) were given a flow area four times larger than the actual flow area, and the hydraulic diameter was changed to conserve the friction loss in the volumes.

A slip model was applied to the vertically oriented junctions outside the core. Horizontal slip was not applied.

Pump characteristics of head, torque, and two-phase flow behavior were taken from the "BE/EM study."[2] An assumption in the calculations is that off-site power was maintained throughout the accident so both pumps continued to operate.

The several ECC systems for the Zion 1 model were modeled in different ways. The low-pressure injection system (LPIS), high-pressure injection system (HPIS), and the charging systems were modeled as fill junctions with the flow rate given as a function of the system pressure. Volume 32 in Figure 1 represents the accumulator. The nitrogen gas in the accumulator volume was modeled as an air head with a polytropic expansion model ($pv^n = c$, $n = 1.401$). There was ECC injection only in the intact loop; fill junctions 56, 57, and 48 were set at zero; and the valve in Junction 28 was closed during the transient.

Heat slabs were used in the core (heat generation), in the steam generators (heat transfer between primary and secondary side), and in the reactor vessel (representing the stored energy in the metal structures). Figure 1 gives the location of the different heat slabs. The RELAP4/MOD6 blowdown correlations (subroutine HTS2) were used with Condie-Bengston III as the film boiling correlation and the modified Tong-Young correlation for transition boiling. In the core, the W-3, Hsu-Beckner, and modified Zuber correlations[a] were used as departure from nucleate boiling (DNB) correlations. In the steam generator secondary side, the natural convection option was used.

All the nuclear data concerning reactivity, scram, etc., were taken from the "BE/EM study" report.[2] The axial power profile for the system calculations gives a close representation of a "middle-of-life" core. In Figure 2, the shape of the power profile is given as a function of the axial position in the core. This shape is the same for the three system calculations.

---

a. All the correlations used in this analysis are incuded in RELAP4/MOD6 and are described in Reference 3.
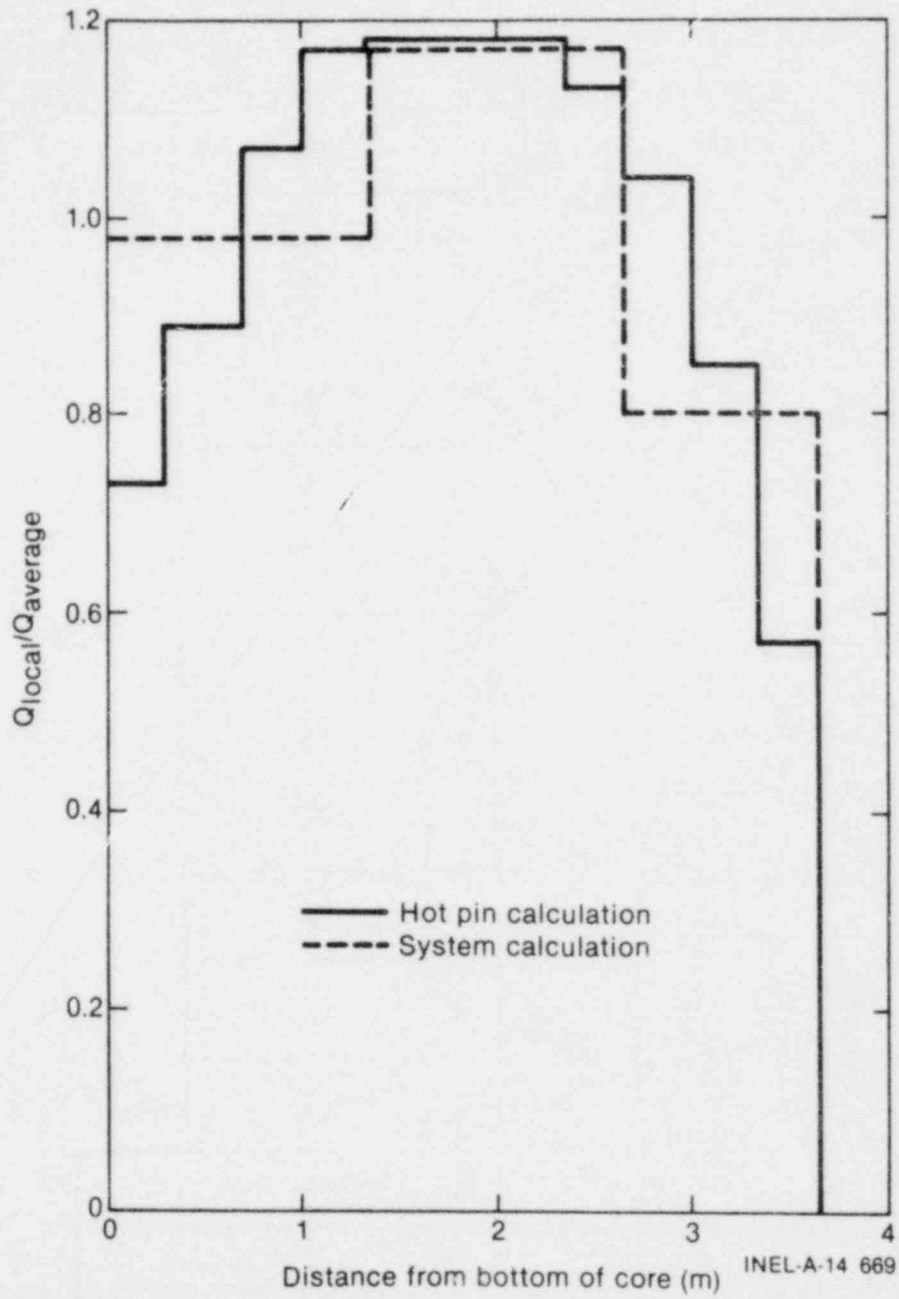
Figure 2. Power profile in core for hot pin and system calculation.

The three basic system calculations are referred to in this report as the 70% power case, 110% power case, and 150% power case, where:

1. For the 70% power case, the temperature difference across the core was 23.9 K and the total core generated power was 2296.63 MW, which is about 70% of the nominal power of the reactor.

2. For the 110% power case, the temperature difference across the core was 35.8 K and the total core generated power was 3540 MW, which is about 110% nominal power of the reactor.

3. For the 150% power case, the temperature difference across the core was also 35.8 K, but the core flow was increased 35%. The generated power was 4760.74 MW, which is about 150% nominal power of the reactor.

Table 3 gives the maximum linear heat generation rate (MLHGR) for the three core parts for the three calculations. The peaking factor, maximum linear heat generation divided by average linear heat generation, for the three calculations is 1.17.

TABLE 3. MLHGR AT THREE LOCATIONS IN THE CORE FOR ZION 1 CALCULATIONS

Heat Slab Number	Location in Core	MLHGR (kW/m)		
		70% Power	110% Power	150% Power
7	Bottom	15.56	23.98	32.25
8	Middle	18.68	28.79	38.72
9	Top	12.82	19.76	26.57

The fuel rods were modeled as three regions: the UO_2 pellets, the gap, and the zirconium cladding. The McDonald-Broughton gap conductance model and the Cathcart-Pawel zirconium-steam reaction model were the major selected options used in the system calculations.

Table 4 gives a review of the main initial conditions used in the calculations. All calculations simulated a 200% double-ended cold leg break LOCA.

TABLE 4. INITIAL PLANT CONDITIONS FOR ZION 1 CALCULATIONS

Parameter	Initial Conditions		
	70% Power	110% Power	150% Power
Power [MW(t)]	2 296.63	3 540.0	4 760.74
Maximum power density (kW/m)	18.68	28.79	38.72
Axial peaking factor	1.17	1.17	1.17
Core inlet temperature (K)	549.8	549.8	549.8
ΔT across core (K)	23.9	35.8	35.8
Upper head fluid temperature (K)	564.2	571.3	571.3
Core mass flow (kg/s)	18 395	18 395	24 713
Pressurizer pressure (MPa)	15.42	15.43	15.43
Accumulator pressure (MPa)	4.21	4.21	4.21

2.2 RELAP4 Hot Pin Input Model

The nodalization and models for the RELAP4 hot pin input model are described in this section.

2.2.1 Nodalization

The RELAP4 blowdown system calculation was used to generate the time-dependent boundary conditions in the upper and lower plenum for a detailed RELAP4 calculation of a specific fuel rod (referred to as the hot pin calculation). Figure 3 is a schematic of the model for the hot pin calculation. The model consists of 14 control volumes, 13 junctions, and 11 heat slabs. Volumes 1 and 14 represent the lower and upper plenum, respectively, for which the time-dependent conditions were taken from a tape generated by the system calculation. The heat slabs represent one fuel rod. The flow area of the core volumes is equal to a square with dimensions of the pitch of the fuel rods minus the area of one fuel rod (pitch, 0.0143 m; diameter of fuel rod, 0.01072 m). The spacer grids of a fuel bundle are situated in
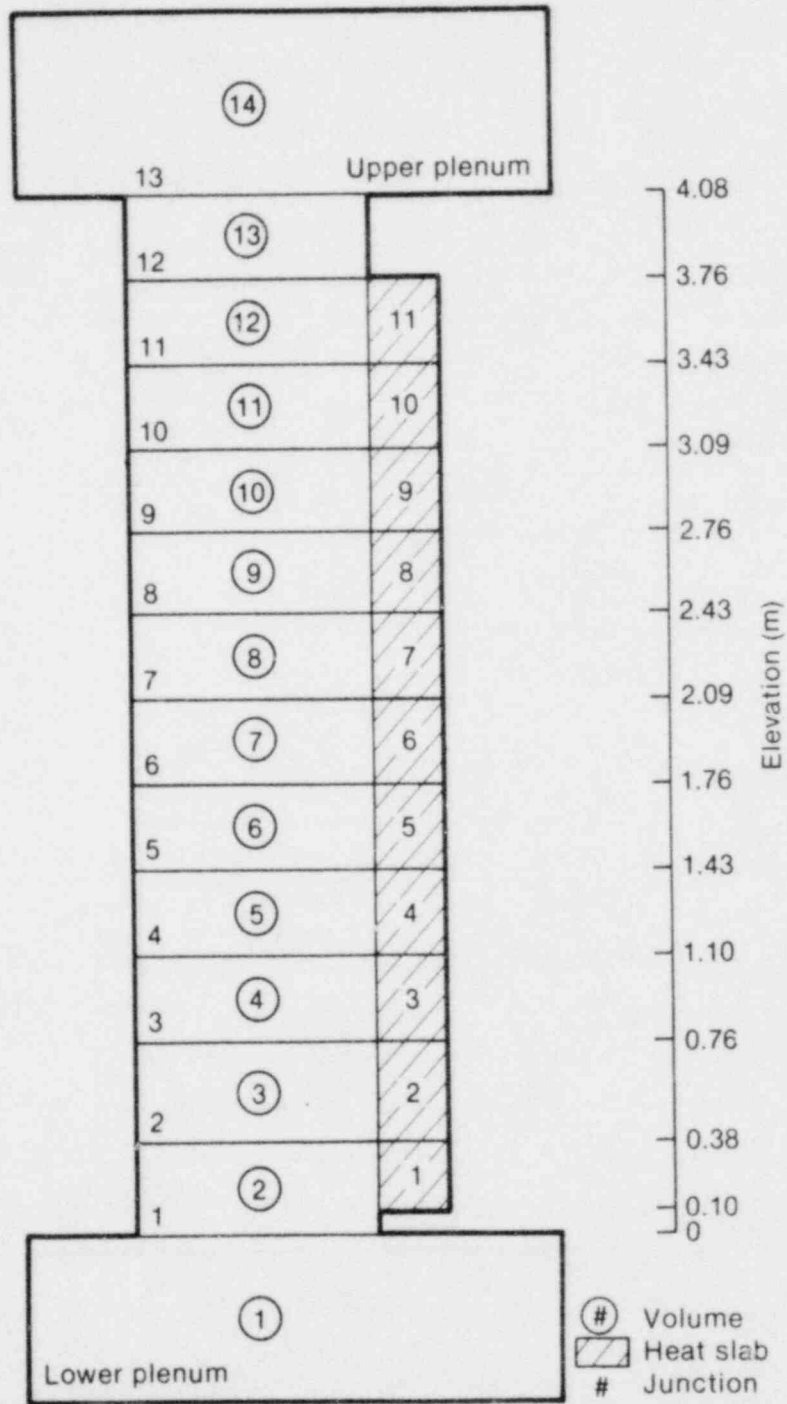
Figure 3. Hot pin fuel rod model schematic diagram.

Junctions 3, 5, 7, 9, and 11 and are specified by a form loss coefficient
in these junctions. A brief description of the control volumes is given in
Table 5.

TABLE 5. DESCRIPTION OF CONTROL VOLUMES FOR RELAP4 HOT PIN INPUT MODEL

Control Volume	Description
1	Upper part of lower plenum
2 through 12	Core volumes with heat generation
13	Outlet volume of the core
14	Upper plenum volume

2.2.2 Models

Basically, the models used for this RELAP4/MOD6 hot pin calculation are
the same as the models used for the system calculation. The compressible
flow equation was used in all the junctions, and all the volumes were assumed
to be homogeneous.

The heat transfer options used were the same as for the system
calculation. The RELAP4/MOD6 blowdown heat transfer package used the Condie-
Bengston correlation as the film boiling correlation and the modified Tong-
Young correlation for transition boiling. In the core, the W-3,
Hsu-Beckner, and modified Zuber correlations were used to predict DNB.

The 3.66-m-long core was divided into a stack of 11 heat slabs. The
power generated by each heat slab corresponded to the calculated power dis-
tribution for a single rod. In Figure 2, the power profile for the hot pin
calculation is given as a function of the axial location; this shape is the
same for all hot pin calculations and is representative for a "middle-of-
life" core. The peaking factor, F_z, for the power in this calculation is
1.18 (F_z = maximum linear heat generation in the hot channel divided by
the mean linear heat generation in the hot channel). The total power gene-
rated in the hot pin was taken as 37% higher than the power generated per
fuel pin in the system calculation. The peaking factor, F_R, in the core
is 1.60 (F_R = maximum linear heat generation in the hot channel divided by

13

the mean linear heat generation in the average core). In Table 6, the MLHGR
for the different heat slabs is given for the three basic calculations.

TABLE 6. MLHGR AT 11 LOCATIONS IN THE CORE FOR ZION 1 CALCULATIONS

Heat Slab Number	MLHGR (kW/m)		
	70% Power	110% Power	150% Power
1 (bottom)	15.80	24.35	32.75
2	19.31	29.76	40.02
3	23.20	35.76	48.09
4	25.28	38.97	52.41
5	25.49	39.29	52.84
6	25.56	39.40	52.99
7	25.47	39.26	52.80
8	24.42	37.64	50.62
9	22.44	34.59	46.52
10	18.48	28.48	38.30
11 (top)	12.39	19.10	25.69

The temperatures used in the RELAP4 input for the fluid volumes are
related to the heat input from the hot pin. Therefore, there was a tempera-
ture jump across Junction 13 because Volume 13 had a temperature set by the
heat input from the hot pin while Volume 14, with conditions taken from the
system calculation, had a temperature set by the average core power genera-
tion. Due to the temperature differences in the core between the hot pin
and the system calculations, the fluid properties differed slightly. In
order to get the same pressure drop across the core, small changes in the
initial mass flux were made in the hot pin calculation compared to the system
calculation.

3. CALCULATIONAL RESULTS

This section gives results from the RELAP4 system and hot pin calcula-
tions for the three Zion 1 LOCA cases (70, 110, and 150% power cases).

3.1 System Calculations

Three basic system calculations were done: the 70% power case (Δt across the core, 23.9 K), the 110% power case (Δt across the core, 35.8 K), and the 150% power case (Δt across the core, 35.8 K with a higher initial core mass flow). The blowdown calculations were discontinued between 30 and 32.5 s after initiation of the blowdown. Around this time, there was an increase in computer CPU time due to water packing in the lower part of the reactor vessel downcomer. Table 7 gives the sequence of events as calculated for the three system calculations.

TABLE 7. CALCULATED SEQUENCE OF EVENTS FOR ZION 1 CALCULATIONS

Event	Time After Rupture (s)		
	70% Power	110% Power	150% Power
Blowdown initiated	0.0	0.0	0.0
Reactor scrammed	0.53	0.53	0.53
HPIS plus charging flow started	1.4	1.4	1.4
Pressurizer empty	9.3	9.3	9.3
Accumulator started	15.5	15.0	14.7
LPIS flow started	25.0	23.0	22.1

The total liquid mass in the reactor vessel, the maximum amount of water the vessel can contain below the bottom of the core, and the total liquid mass delivered by the ECC systems are given as a function of time in Figure 4. An extrapolation of the liquid mass in the reactor vessel shows that somewhere between 33 and 37 s, there will be enough water in the vessel to fill it to the bottom of the heated core; therefore, this should be a reasonable time to start a reflood calculation. The difference between the increase in mass inventory in the vessel and mass delivered by the ECC systems was bypassed to the cold leg broken loop. From 23 s into the transient until the end of the calculations, the average amount of bypassed ECC water was 42% for the 70% power calculation and 35% for the 110 and 150% power calculations.
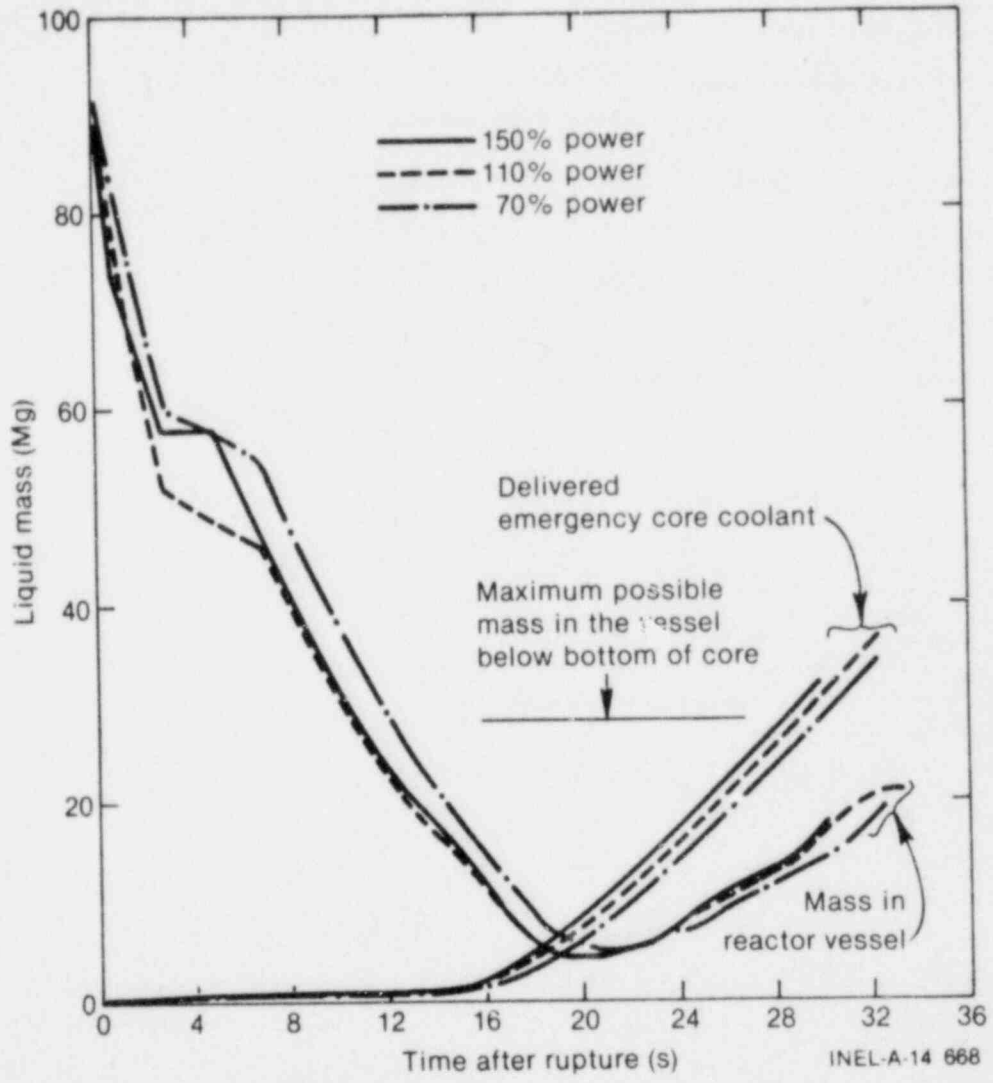
Figure 4. Liquid mass in reactor vessel for Zion 1 calculations.

The average core flow is given in Figure 5, and the inlet and outlet flow
of the core is given in Figures 6 and 7, respectively. Due to the high break
flows shown in Figures 8 and 9 there was an immediate flow reversal in the
core inlet flow (Figure 6) while the flow at the core exit decreased but did
not reverse. Therefore, the stagnation point of the flow was in the core
region. At about 0.5 s, the core started voiding, see Figure 10; from this
time on all the core flows decrease in the direction of zero flow. The
cladding temperatures of the three core parts are given in Figures 11, 12,
and 13. After about 1 s (for the 70% power calculation, 1.5 to 2.0 s), the
cladding temperatures increased steeply, because of the low flow, and
proceeded almost immediately to film boiling due to the high void fraction in
the core (first dryout of the core). At about 2 s, the whole core stagnated
and the void fraction in the core was greater than 0.96. The cold leg flow
from and to the downcomer and the average core flow are given for the three
calculations in Figures 14, 15, and 16. Moreover, in these figures, the
difference of the two cold leg flows is given. These figures also illustrate
that the increasing positive core flow after 2.5 s was caused by the cold leg
break flow being smaller than the pump flow delivery. This increasing core
flow caused a rewetting of the core and a fast decrease in cladding
temperature. A return to nucleate boiling in all cases, except for the two
.op parts of the core in the 110% power calculation, is shown. In the 110%
power calculation, the positive core flow was not large enough to cause a
return to nucleate boiling, as witnessed in the 70% power calculation,
because of the higher stored energy. In the 150% power calculation, the
higher positive core flow (due to the higher pump speed) caused a complete
return to nucleate boiling for the entire core. The decrease in positive
core flow at about 5 s was initiated by the intact loop pump, which started
to degrade at this point (Figure 17 gives the pump head for the intact loop
pumps). From about 5 s until somewhere between 10 and 15 s, there was a
steady decrease in core flow and voiding began in the downcomer and lower
plenum. During this time, the void fraction in the core increased
(Figure 10) and between 9 and 14 s (top of the core earlier than bottom)
there was a second dryout. The accumulator flow started at approximately
15 s, and this caused a low pressure (due to instantaneous equilibrium in
RELAP4) in the cold leg intact loop. This low pressure was able to

EGG-LOFT 5093
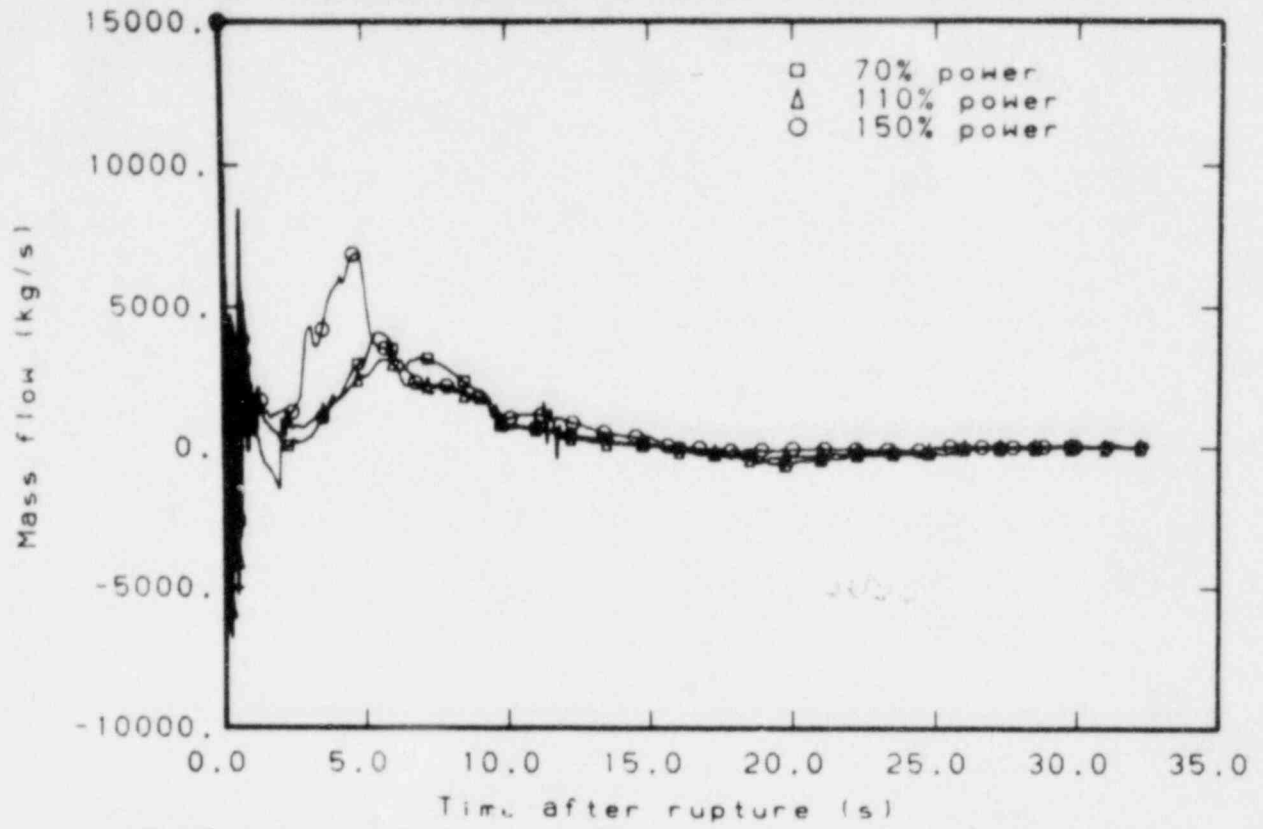
Figure 5. Average mass flow in the core for Zion 1 calculations.
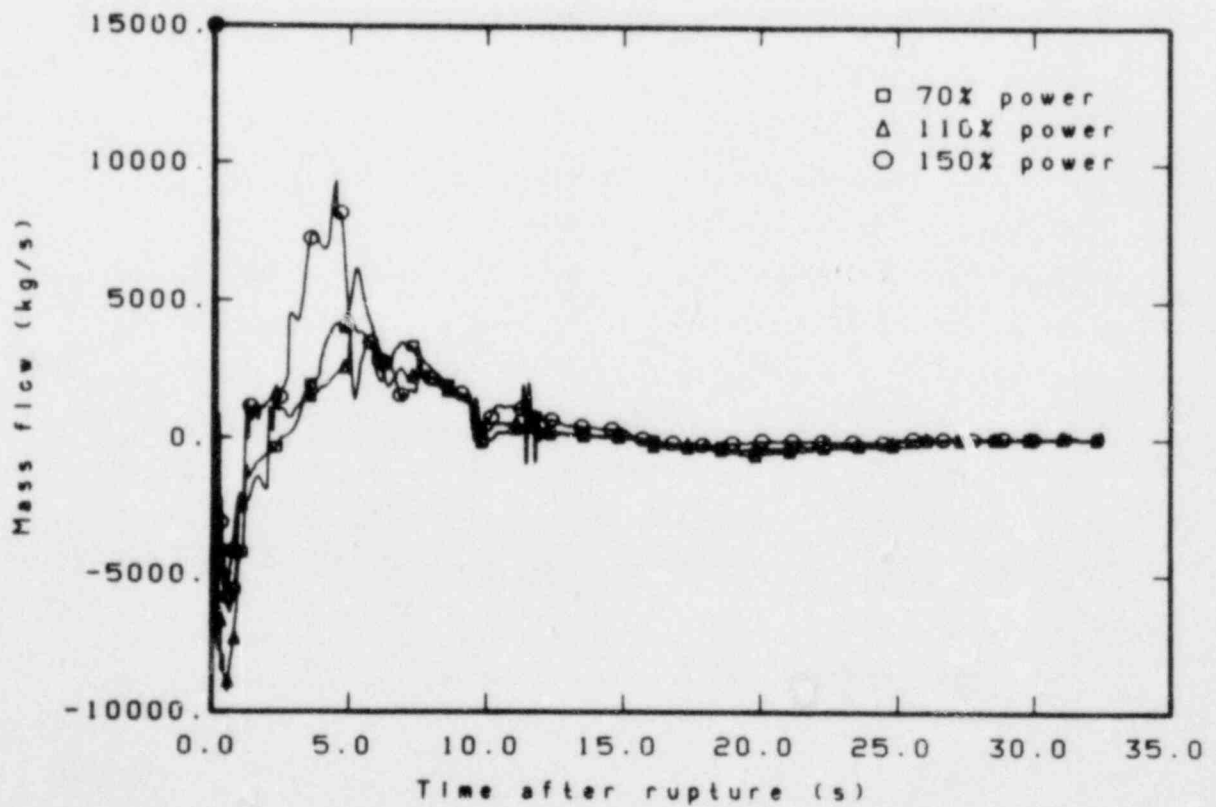
Figure 6. Mass flow at the core inlet for Zion 1 calculations.

18
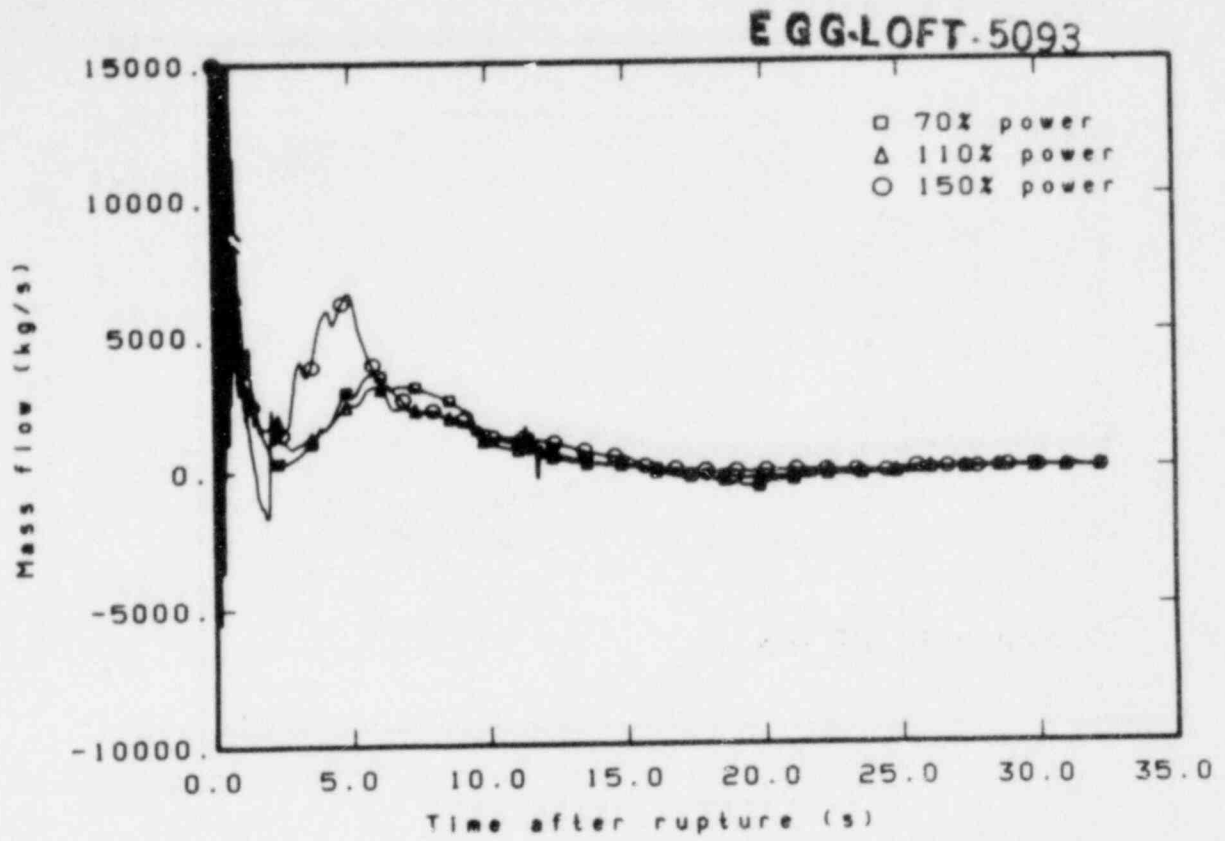
Figure 7.   Mass flow at the core outlet for Zion 1 calculations.
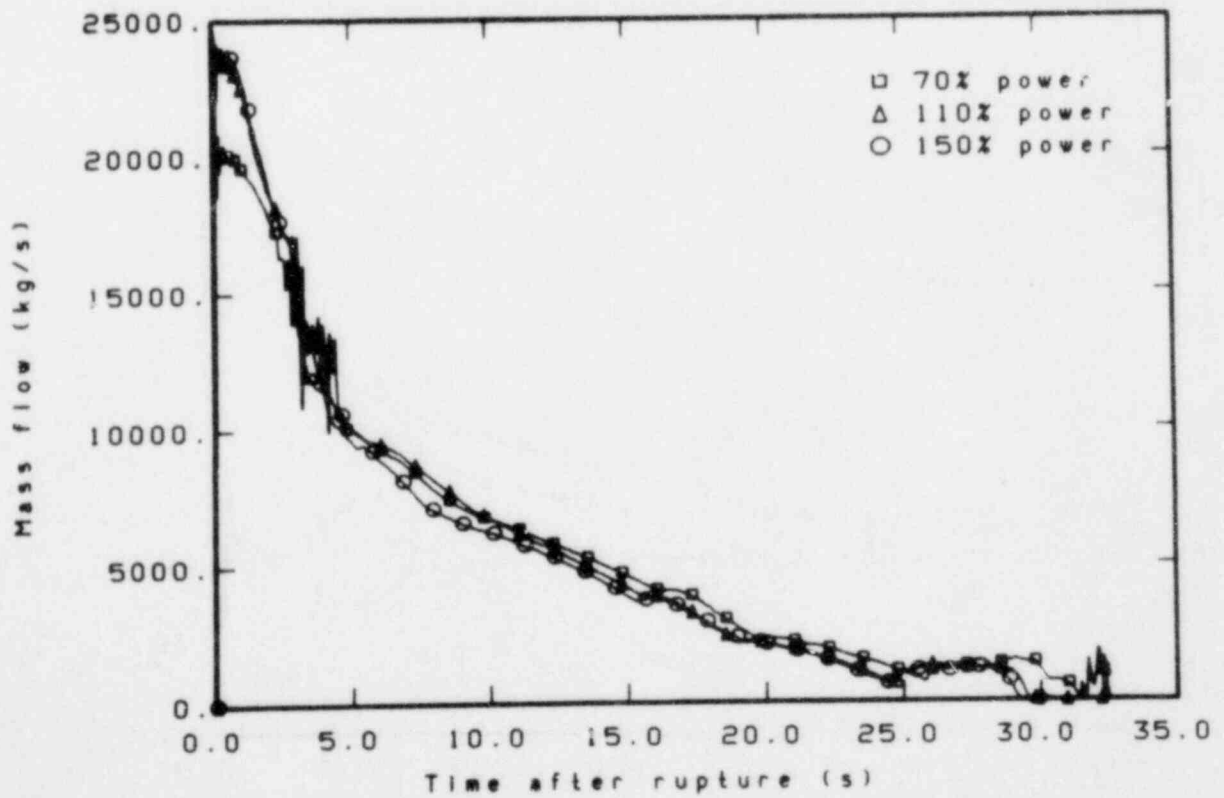
Figure 8.   Break flow in the cold leg for Zion 1 calculations.

19
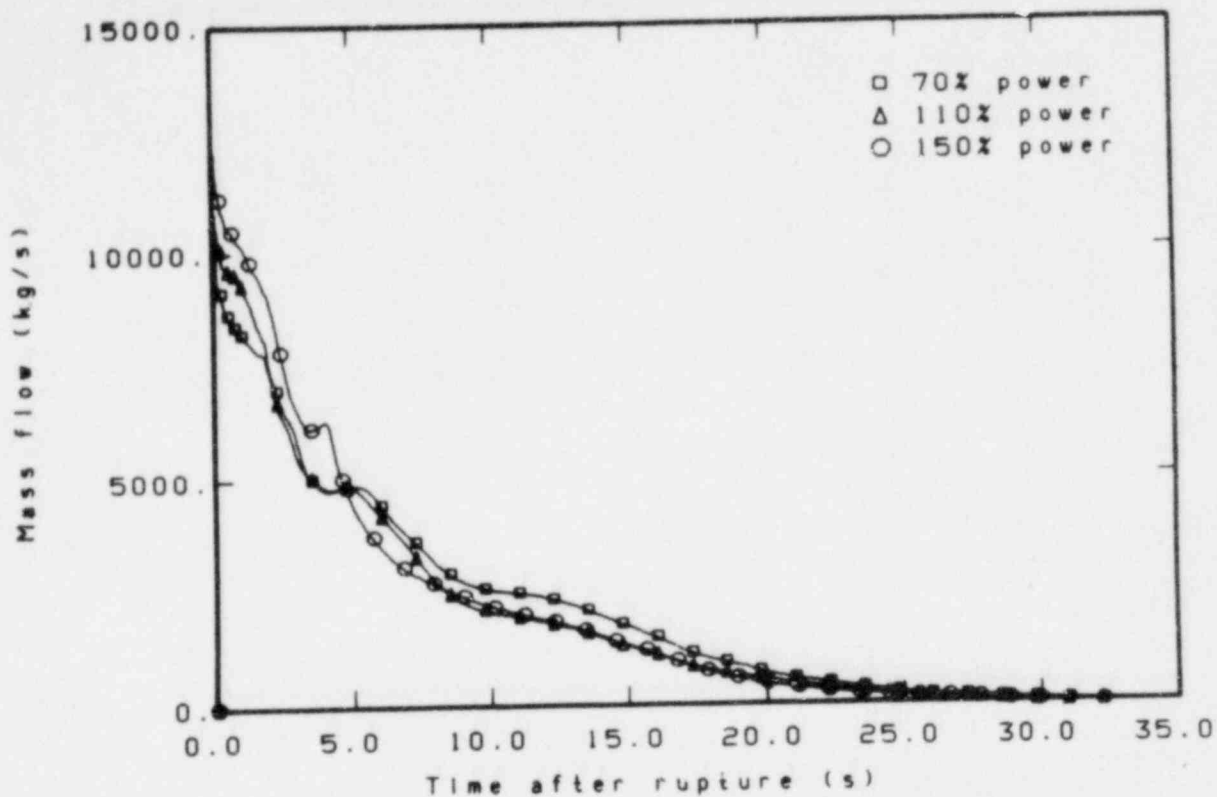
Figure 9. Break flow in the hot leg for Zion 1 calculations.
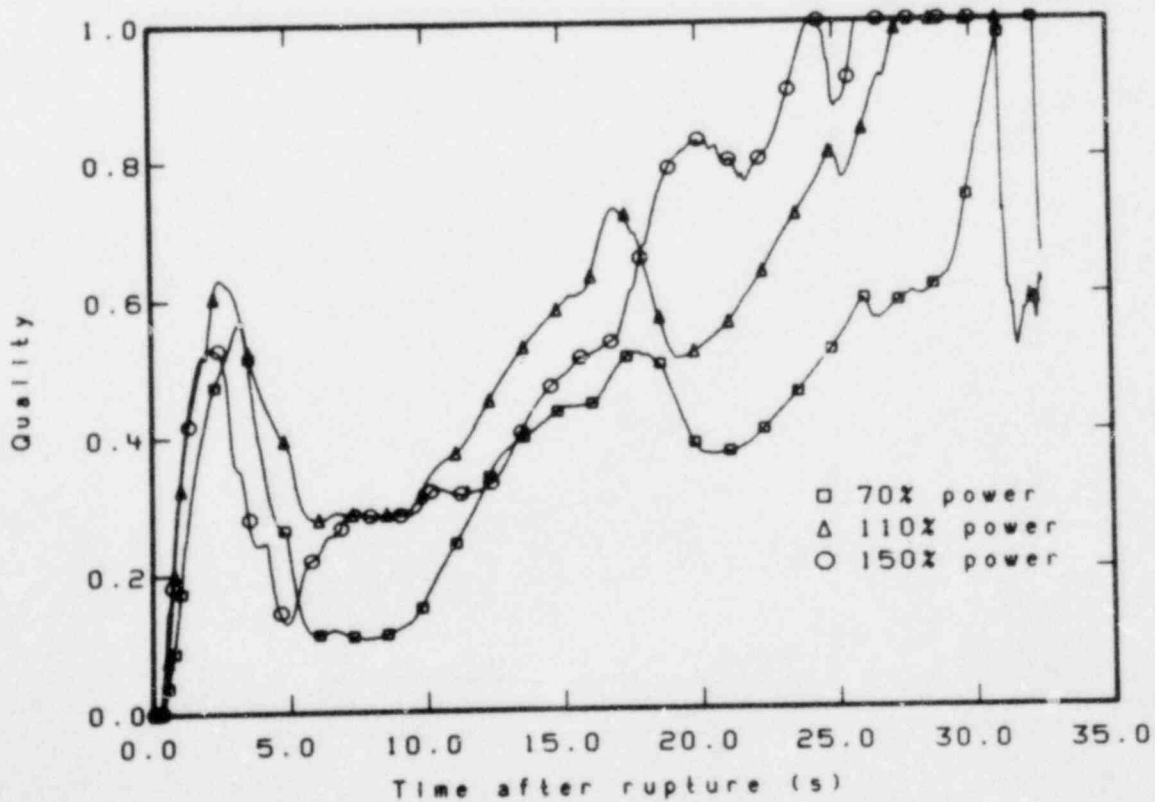
Figure 10. Fluid quality in middle part of core for Zion 1 calculations.
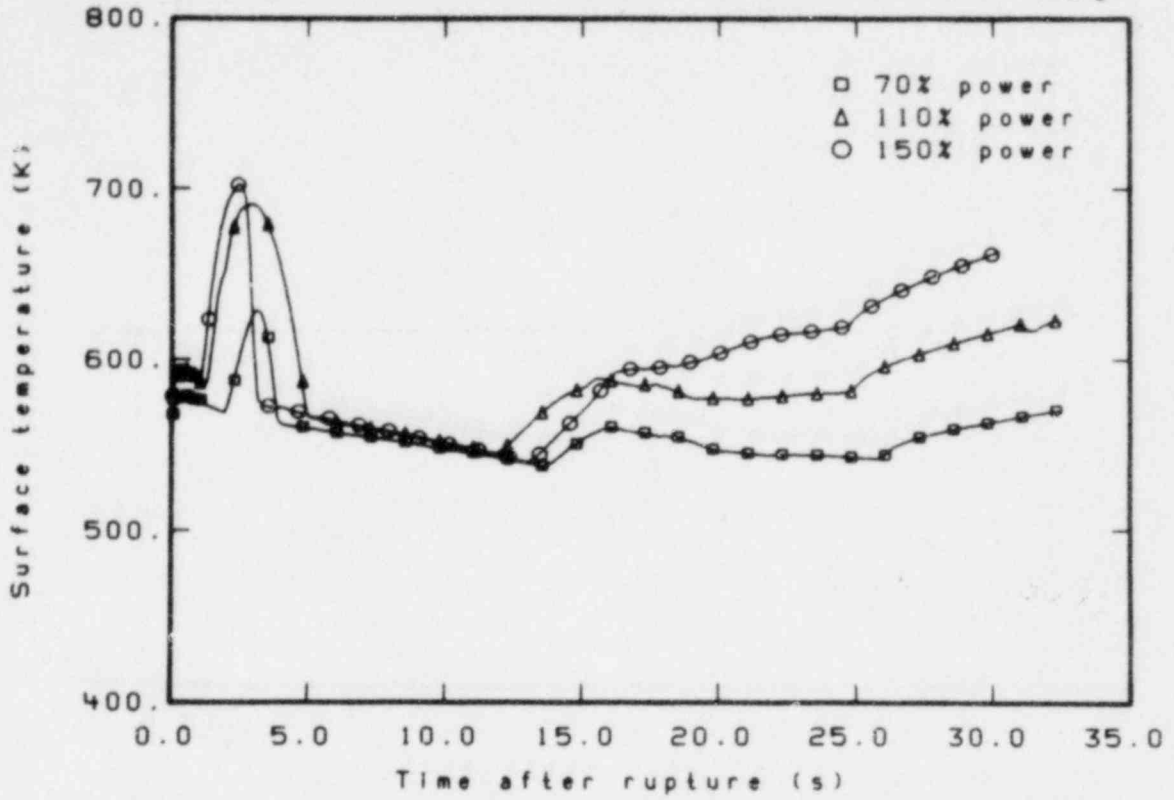
Figure 11. Cladding temperature in lower part of core for Zion 1 calculations.
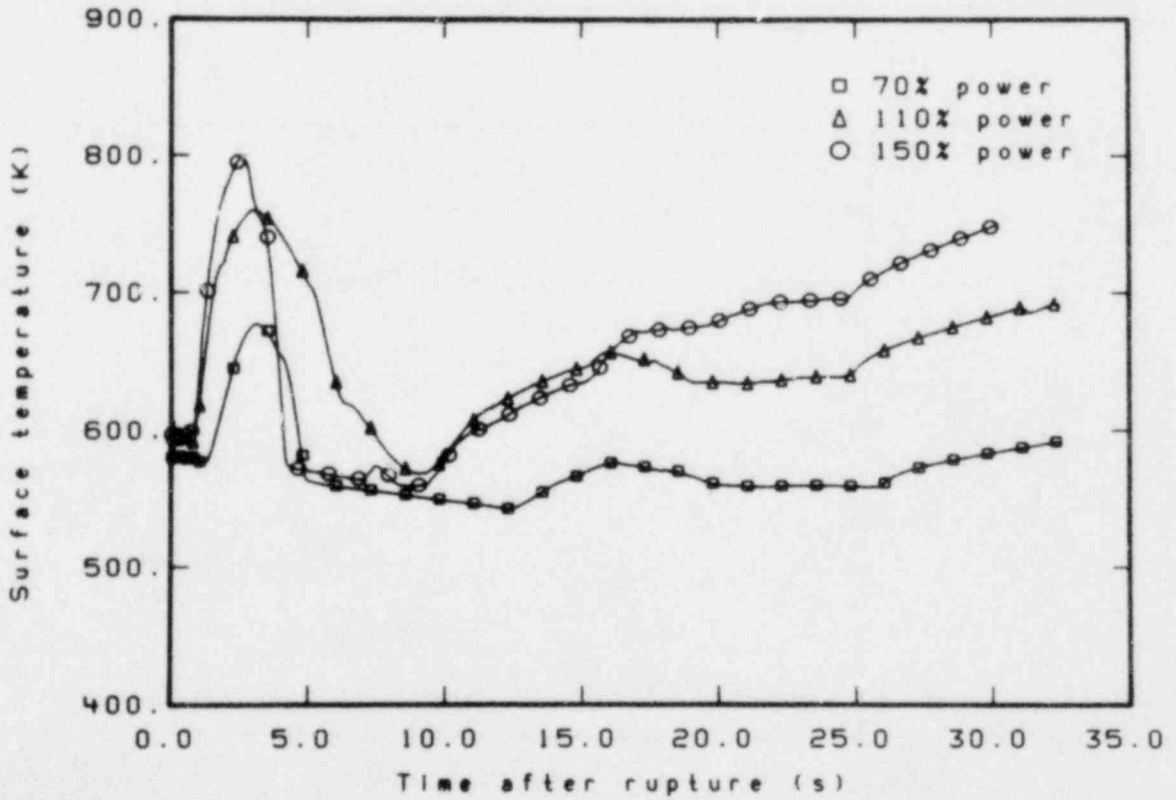
Figure 12. Cladding temperature in middle part of core for Zion 1 calculations.

21
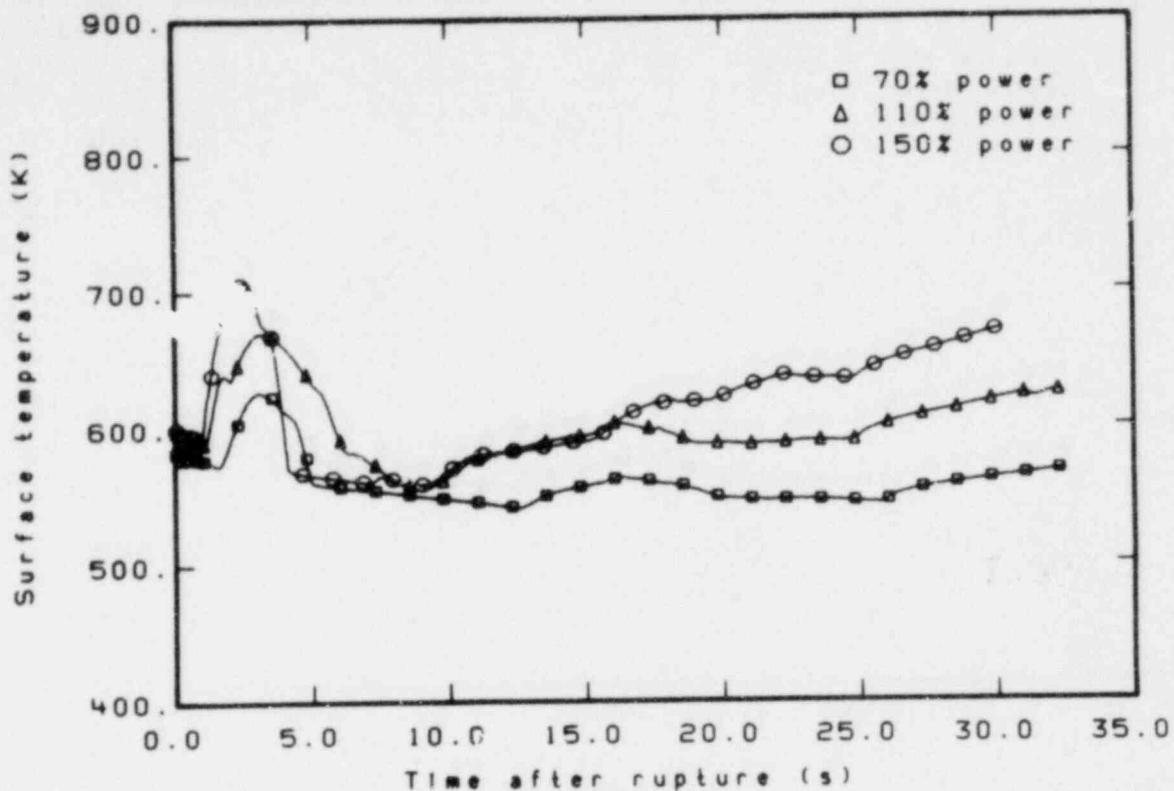
Figure 13. Cladding temperature in upper part of core for Zion 1 calculations.
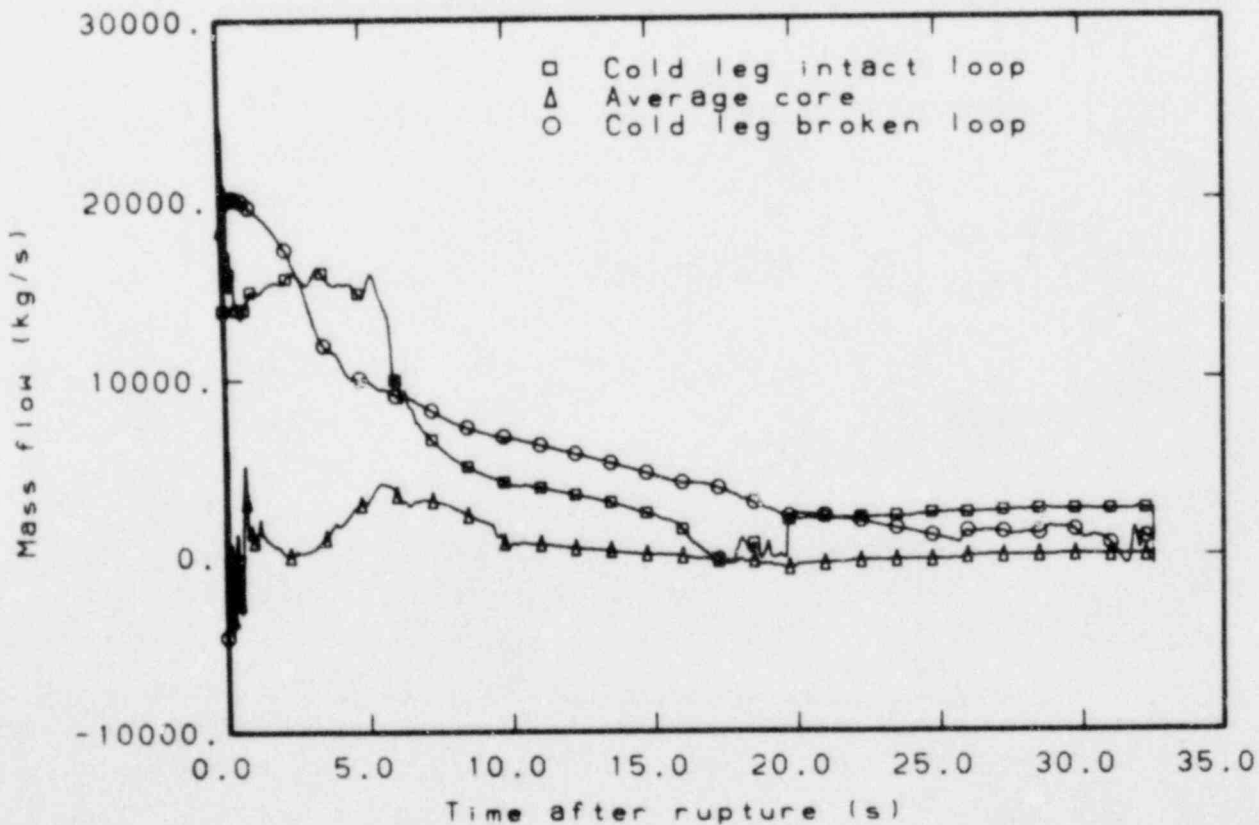
Figure 14. Mass flow in core and cold legs for Zion 1, 70% power calculation.
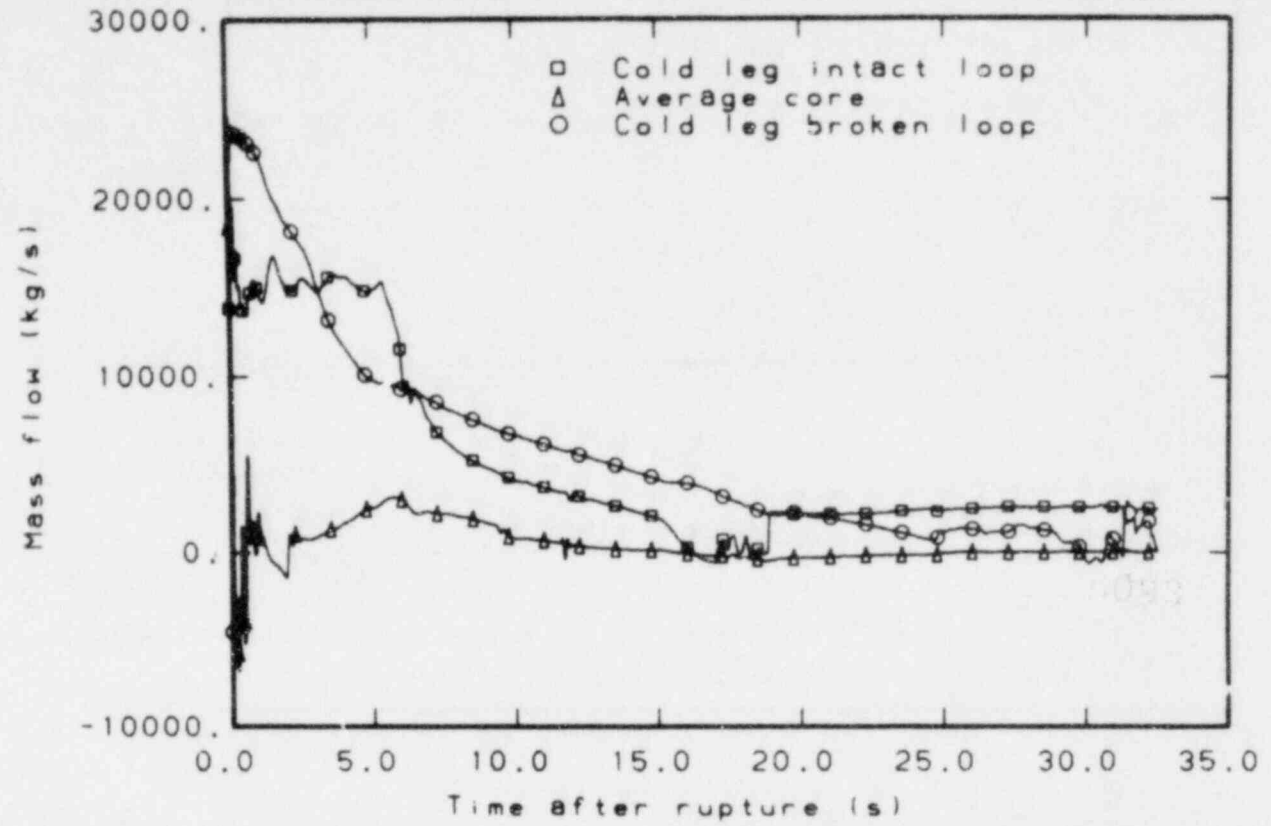
Figure 15. Mass flow in core and cold legs for Zion 1, 110% power calculation.
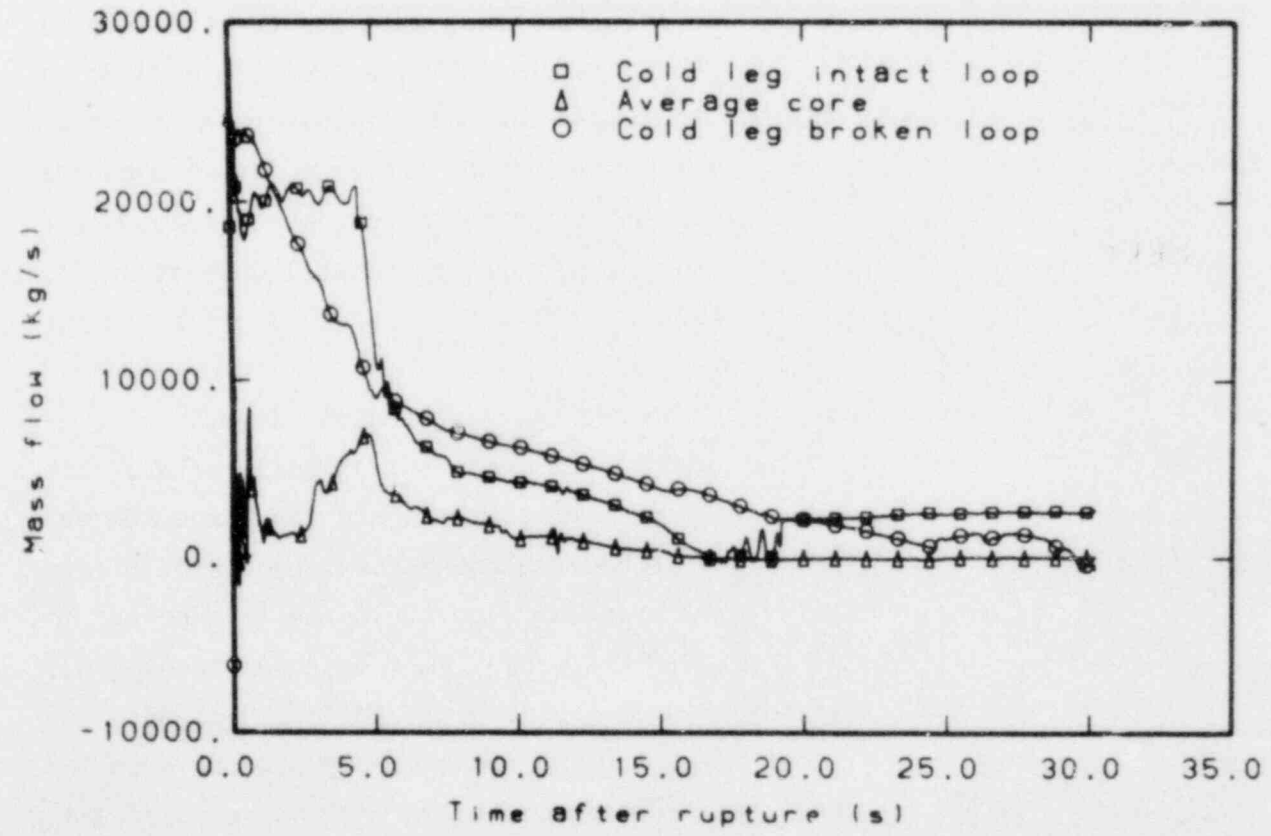
Figure 16. Mass flow in core and cold legs for Zion 1, 150% power calculation.
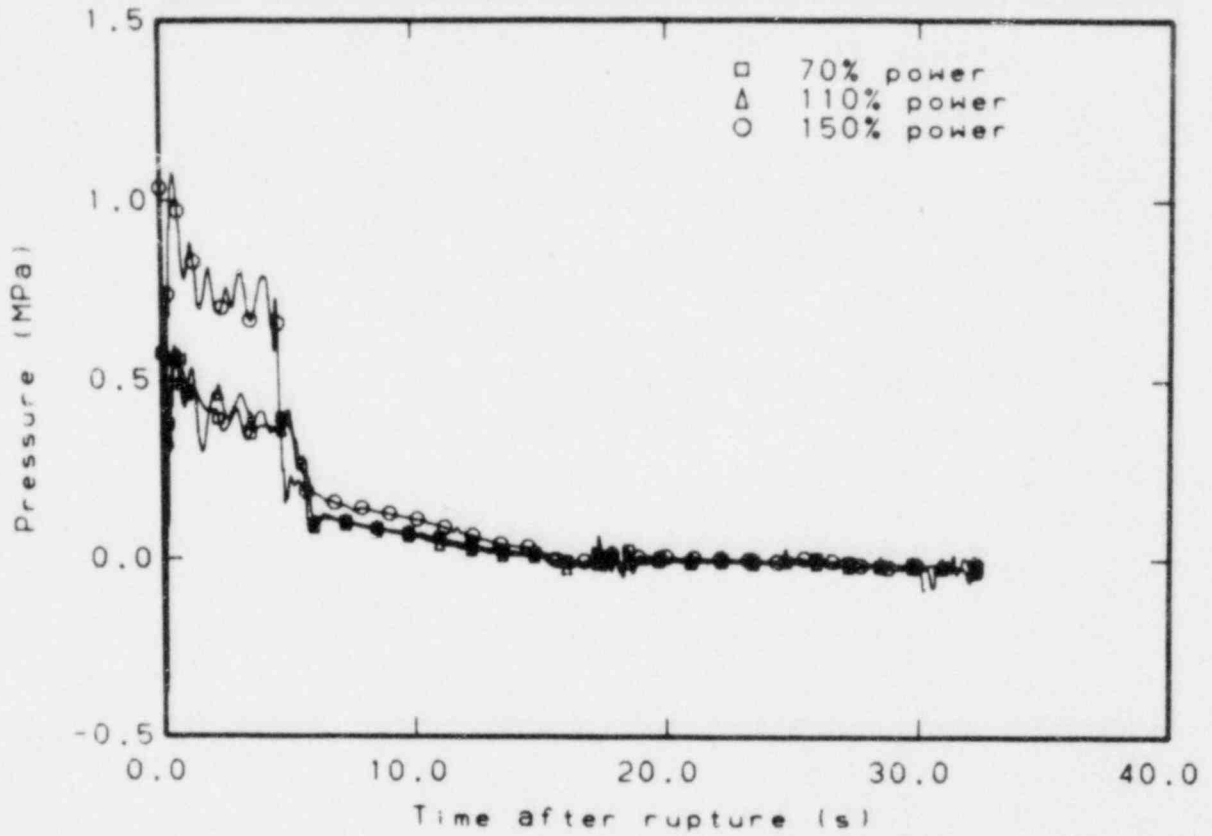
Figure 17. Pump head in intact loop pump for Zion 1 calculations.

reverse the positive core flow to a smaller negative flow. The negative core flow caused a slight decrease in cladding temperature for the 70 and 110% power calculations, but the negative flow in the 150% power calculation was insufficient to decrease the cladding temperature (in all cases the heat transfer was controlled by film boiling). In all cases, when core flow was almost zero, a strong increase in cladding temperature was noted at approximately 25 s.

For the first 5 s, the cold leg break flow for the 150 and 110% power calculations was equal, while the 70% power cold leg break flow was less (higher saturation pressure in the hot leg for 150 and 110% power calculations than for the 70% power calculation, see Figure 8). In addition to the higher saturation pressure, another explanation for the hot leg break flow differences was the speed of the pump in the broken loop. After 5 s into the transient, the 70% power case had a larger break flow because there was more water left in the system.

These system calculations concluded that the pump speed was an important parameter for the maximum cladding temperature. The maximum cladding temperature for the 150% power calculation was lower than expected from the results of the 70 and 110% power calculations. The higher pump speed caused an increased core flow; therefore, a lower maximum cladding temperature resulted. Moreover, there was a complete return to nucleate boiling which did not occur for the 110% power calculation.

3.2 Hot Pin Calculations

A hot pin calculation for each system was completed. In order to get a hydraulic and energetic well balanced initial condition, some small adjustments were made in the core mass flux compared to the system core mass flux. The mass fluxes for the different hot pin and system calculations are given in Table 8.

TABLE 8.   SYSTEM AND HOT PIN CALCULATIONS OF CORE MASS FLUX FOR ZION 1
CALCULATIONS

Calculation	Core Mass Flux $(kg/s \cdot m^2)$	
	System Calculation	Hot Pin Calculation
70% power	3707.4	3678.3
110% power	3707.4	3627.3
150% power	4980.7	4873.7

One calculation was done with the same power as for the system calcula-
tion. Results from this calculation showed that the hydraulic behavior in
the hot pin calculation is the same as in the system calculation.

Results of the three hot pin calculations are given in Figure 18. In
this plot, the temperature of the hottest spot in the core (heat Slab 7) is
given as a function of time. This figure shows that the hot spot tempera-
ture of the 150 and 110% power calculations were about the same during the
first 15 s of blowdown. The higher core flow (Figure 6) of the 150% power
calculation compensates for the higher stored energy. After 15 s, when
the core flows are small and the core is voided, the higher decay heat caused
a steeper temperature increase for the 150% power calculation. The hot spots
of the 150 and 110% power calculations did not return to nucleate boiling
after the first dryout as did the hot spot of the 70% power calculation.

The time to reach first and second dryout, peak temperature, and quench-
ing as a function of the axial position in the core is given in Figure 19 for
the 70% power hot pin calculation. This figure shows that the entire upper
half of the core reached uniform DNB at the same time, while the lower part
of the core dried out later. The peak temperature was reached throughout
the core at the same time. Both the time to reach the peak temperature and
the time to reach the first dryout support the fact that the average flow in
the core was almost stagnant during the first few seconds. Quenching of the
core started from the bottom, due to the positive core flow, and the second
dryout started at the top of the core. The behavior of the 110 and 150%
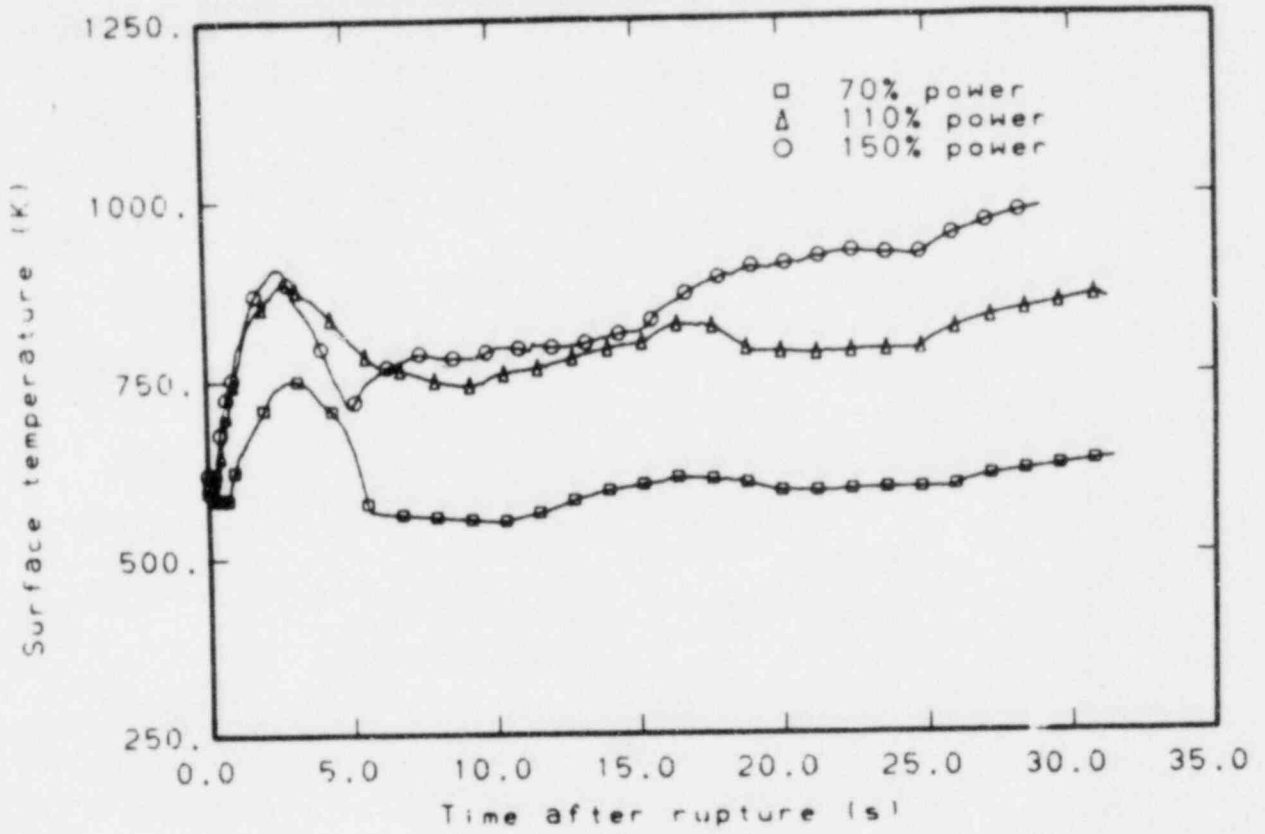
Figure 18. Temperature of hot spot in the core for Zion 1 hot pin calculations.
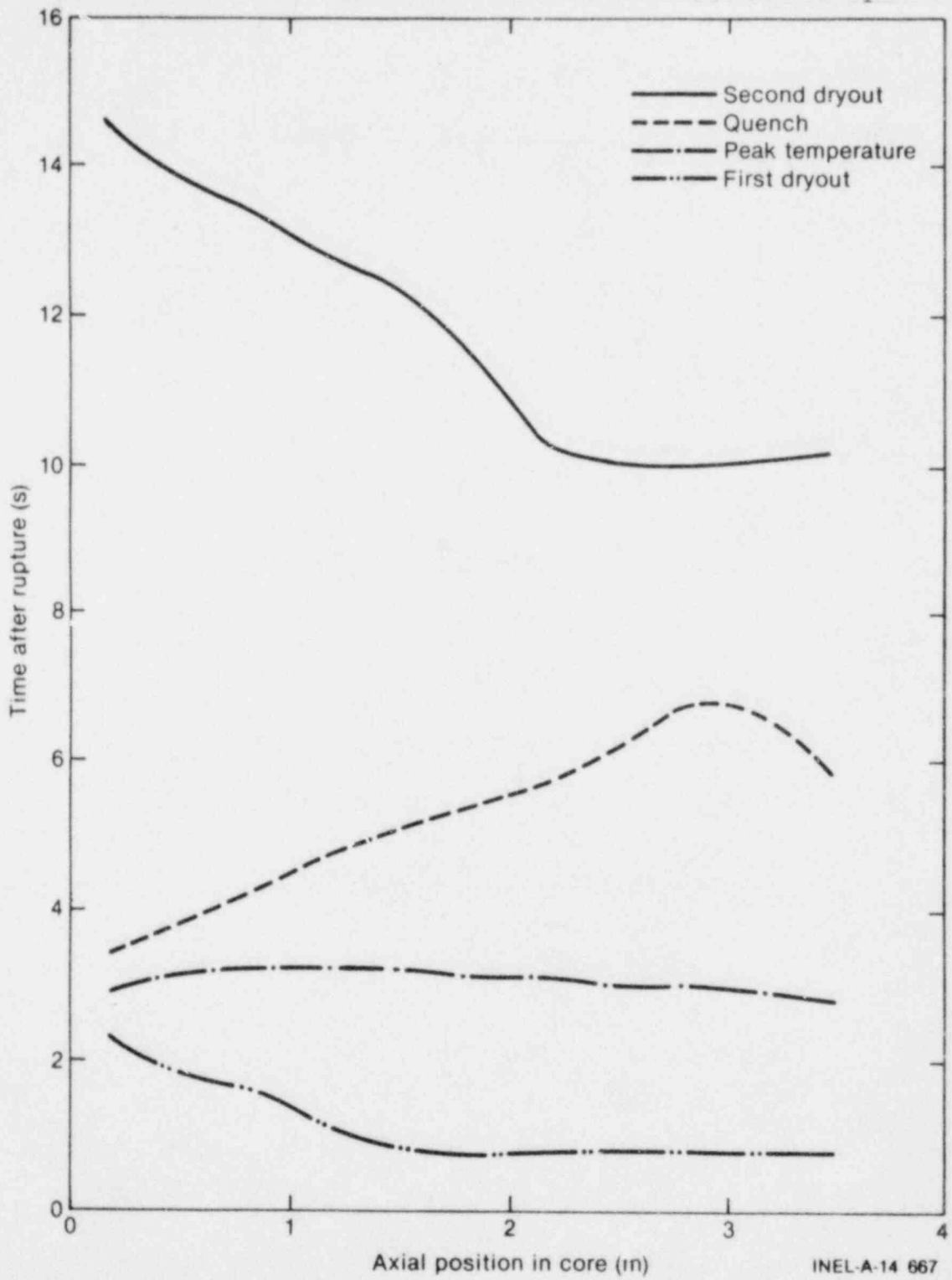
Figure 19. Thermal-hydraulic behavior in the core for Zion 1, 70% power hot pin calculation.

power calculations was about the same, but quenching and second dryout did not occur for the upper part of the core. For this part, however, there was a decrease followed by an increase in temperature after peak temperature was reached.

4. COMPARISON OF ZION 1 CALCULATIONS WITH LOFT EXPERIMENTAL DATA

With the temperature difference across the core as a base, the 70% power calculation can be compared with LOFT Experiment L2-2 and the 110% power calculation with Experiment L2-3. The 150% power calculation had the same temperature difference across the core as is planned for LOFT large break Experiment L2-4.

In this section, a comparison is made between data from LOFT Experiments L2-2 and L2-3 and the 70 and 110% power calculations, respectively. In Table 9, a number of the major parameters for Experiments L2-2 and L2-3 are given together with the parameters for the 70 and 110% power calculations. A map showing fuel rod position designations in the LOFT core is provided in Figure 20.

TABLE 9. COMPARISON OF EXPERIMENT AND CALCULATION PARAMETERS

Parameter	Experiment		Calculation	
	L2-2	L2-3	70% Power	110% Power
System volume (m^3)	7.22	7.22	355.7	355.7
Power [MW(t)]	24.88	36.0	2 296.63	3 540.0
Initial core mass flow (kg/s)	194.2	199.8	18 395.2	18 395.2
Initial core mass flux ($kg/s \cdot m^2$)	1 181.0	1 215.1	3 867.3	3 867.3
ΔT across core (K)	22.7	32.2	23.9	35.8
Core length (m)	1.68	1.68	3.66	3.66
Number of fuel rods	1 300	1 300	39 372	39 372

TABLE 9. (continued)

Parameter	Experiment		Calculation	
	L2-2	L2-3	70% Power	110% Power
Average linear heat generation rate (kW/m)[a]	11.4	18.0	15.94	24.57
MLHGR (hot pin) (kW/m)	26.4[b]	39.0[b]	25.56	39.40
MLHGR (average pin)(kW/m)	15.4[c]	23.0[c]	18.68	28.79
Peaking factor (hot pin)	2.4[b]	2.4[b]	1.60	1.60
Peaking factor (average pin)	1.4[c]	1.4[c]	1.17	1.17

a. Total generated power/total length of fuel rods.

b. Center fuel module.

c. Fuel rods 1C7 and 3C7 (see Figure 20).

The axial power profile from Experiment L2-2 (fuel Rod 5M3) and the 70% power hot pin calculation is given in Figure 21. These two profiles are characteristic of the axial power profiles for both the Zion 1 calculation and the LOFT experiments. The power profile in the Zion 1 calculation represents a "middle-of-life" core; the LOFT core has a sharper profile and is skewed to the bottom of the core. Results of LOFT Experiments L2-2 and L2-3 are given in References 7 and 8.

Main conclusions from LOFT Experiment L2-2 are:

1. There was a core-wide rewet ending at about 8 s into the transient. This early rewet was caused by resumption of the positive core flow at 2.5 s into the transient and by introduction of relatively cold water from the intact loop cold leg into the core region. The general pattern of the rewetting between 6 to 8 s was from the bottom of the core upward.
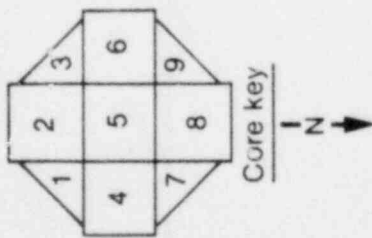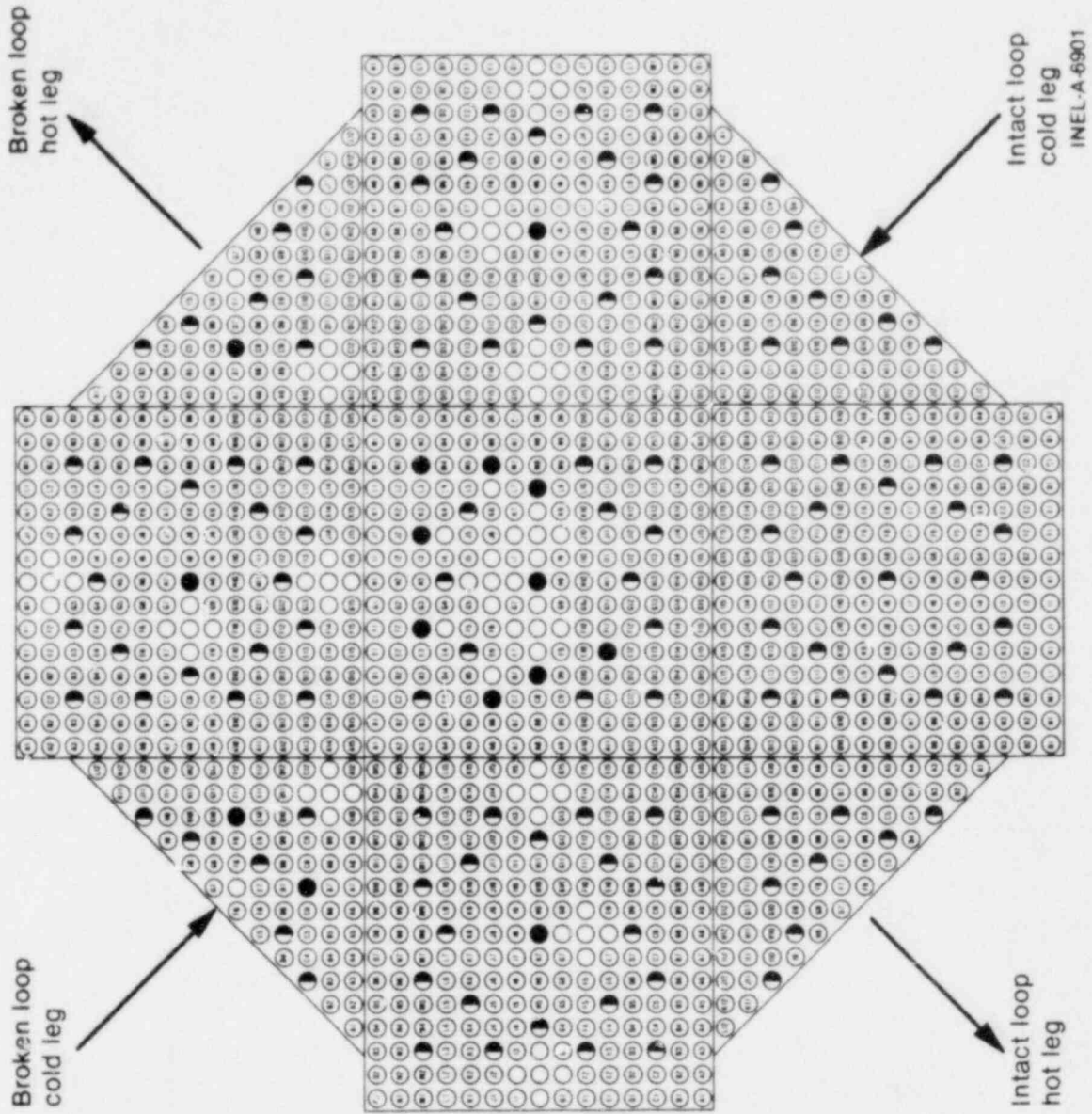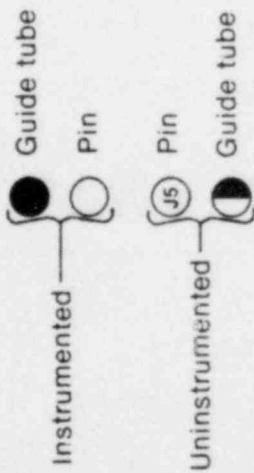
Figure 20. LOFT core map showing fuel rod position designations.
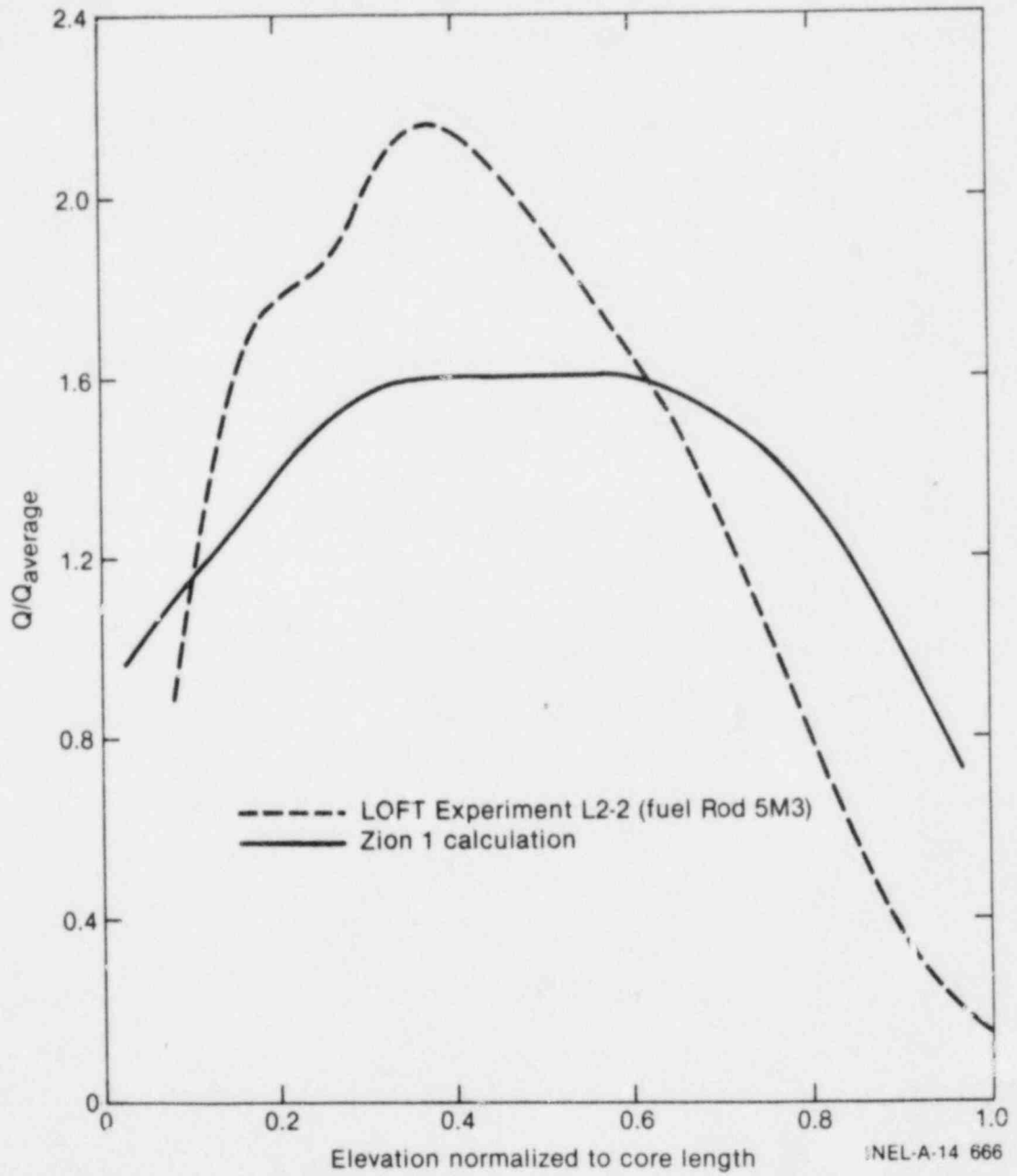
Figure 21. Axial power profile for Experiment L2-2 and Zion 1, 70% power hot pin calculation.

2. There was a second dryout of the core between about 12 and 20 s
    into the transient (starting time depends upon the axial location
    in the core). A number of thermocouples underwent a rewet after
    the second dryout. The entire core was reflooded after about
    55 s into the transient.

Next is a comparison of data from LOFT Experiment L2-2 and the 70%
power calculation for the Zion 1 plant. The two LOFT volume-scaled
calculated break flows from the cold leg and hot leg are compared with the
measured mass flows in the cold leg and hot leg of the broken loop during
Experiment L2-2 in Figures 22 and 23. The cold leg break flow indicates
good agreement; however, the calculated hot leg break flow is higher
during the first 10 s of the transient than the measured flow. The reason
for this difference is the active running pump in the broken loop in the
calculation and the passive pump simulator in the experiment.

A detailed comparison between calculated total ECC system flow and
measured flow is difficult because there were two nonqualified measured
mass flows (maximum accumulator mass flow as measured by the orifice was
approximately 48 l/s and as measured by the liquid level detector in the
accumulator was about 60 l/s). The maximum calculated accumulator mass
flow was 47 l/s.

The above comparisons conclude that the external occurrences, loss and
addition of fluid to the system, were about the same for the experiment and
the Zion 1 calculation.

Figure 24 shows the pressure response in the hot leg of the intact
loop for both the calculation and Experiment L2-2. This figure indicates
that the subcooled depressurization was lower in the calculation than in
the experiment. This is due to the initial temperature being 8 K lower in
the calculation. The overall behavior of the pressure was approximately
the same.

Figure 22. Break mass flow in the cold leg for Experiment L2-2 and scaled break mass flow for Zion 1, 70% power calculation.

Figure 23. Break mass flow in the hot leg for Experiment L2-2 and scaled break mass flow for Zion 1, 70% power calculation.

34

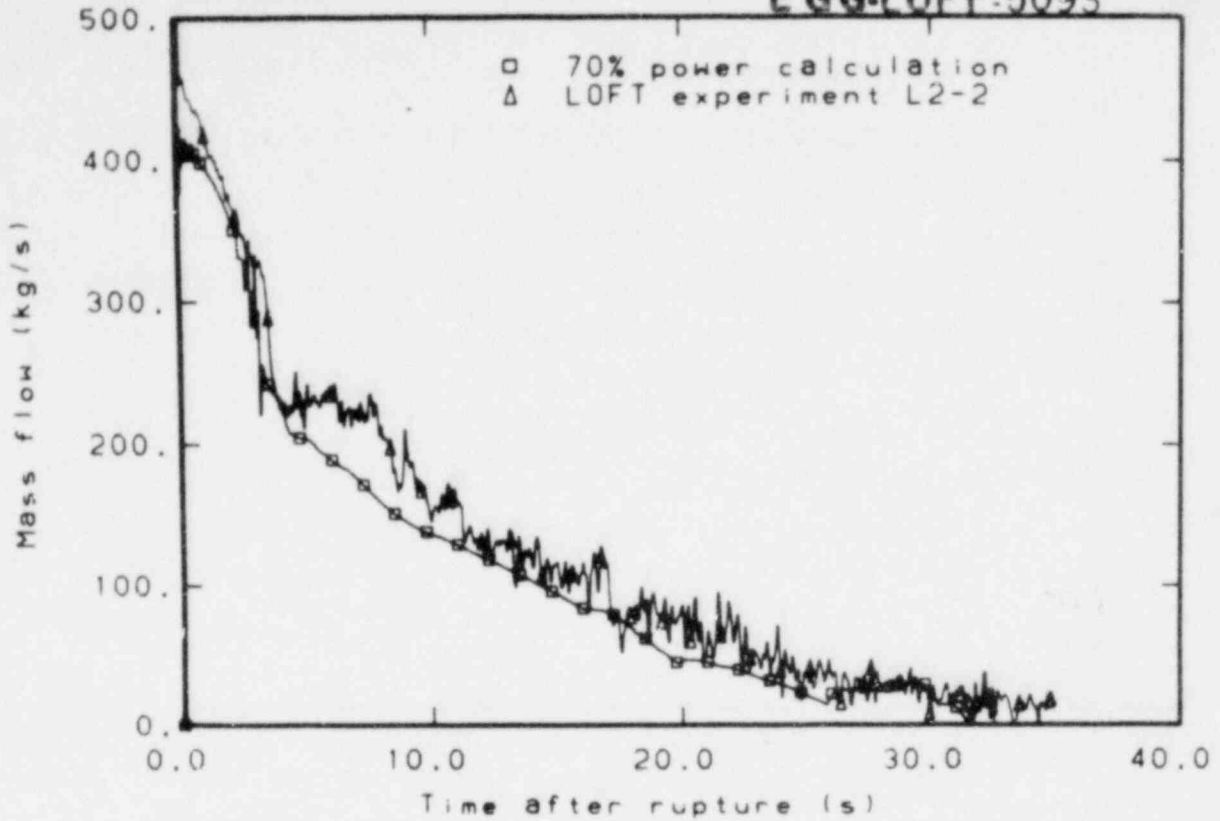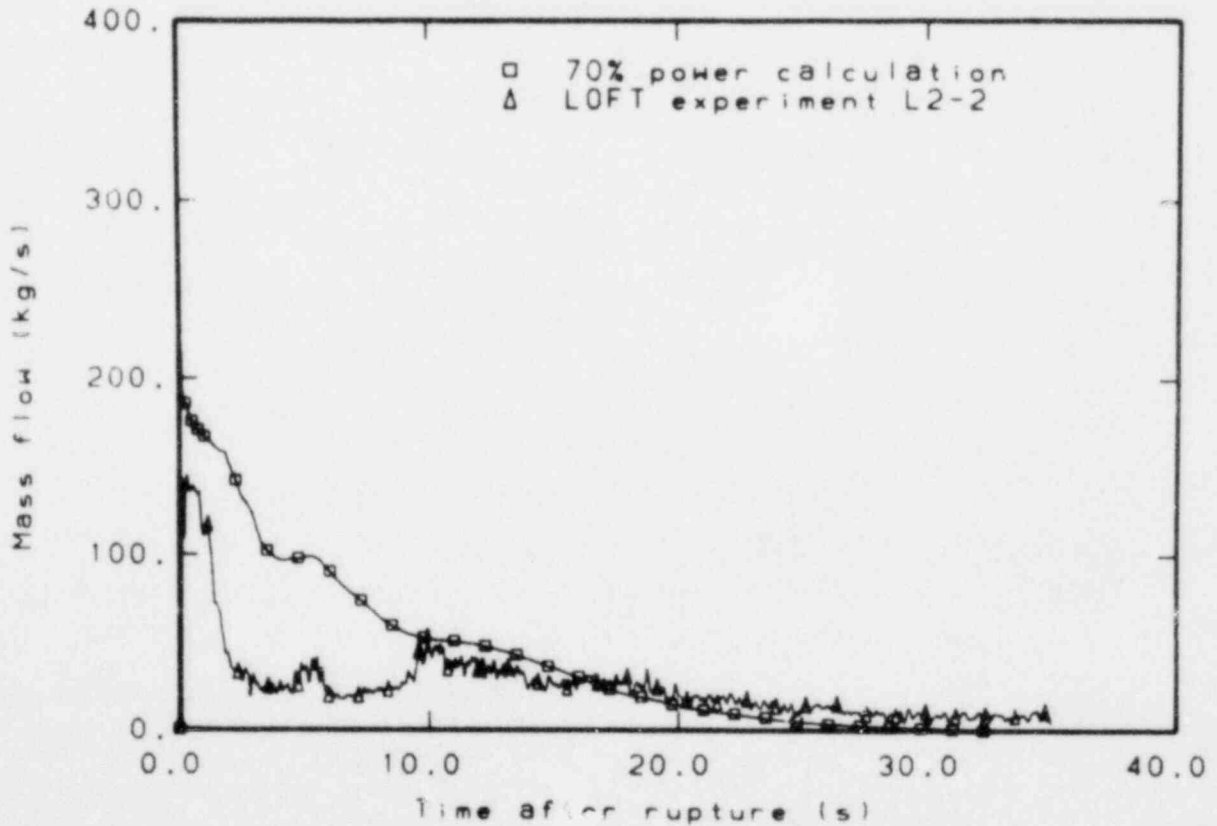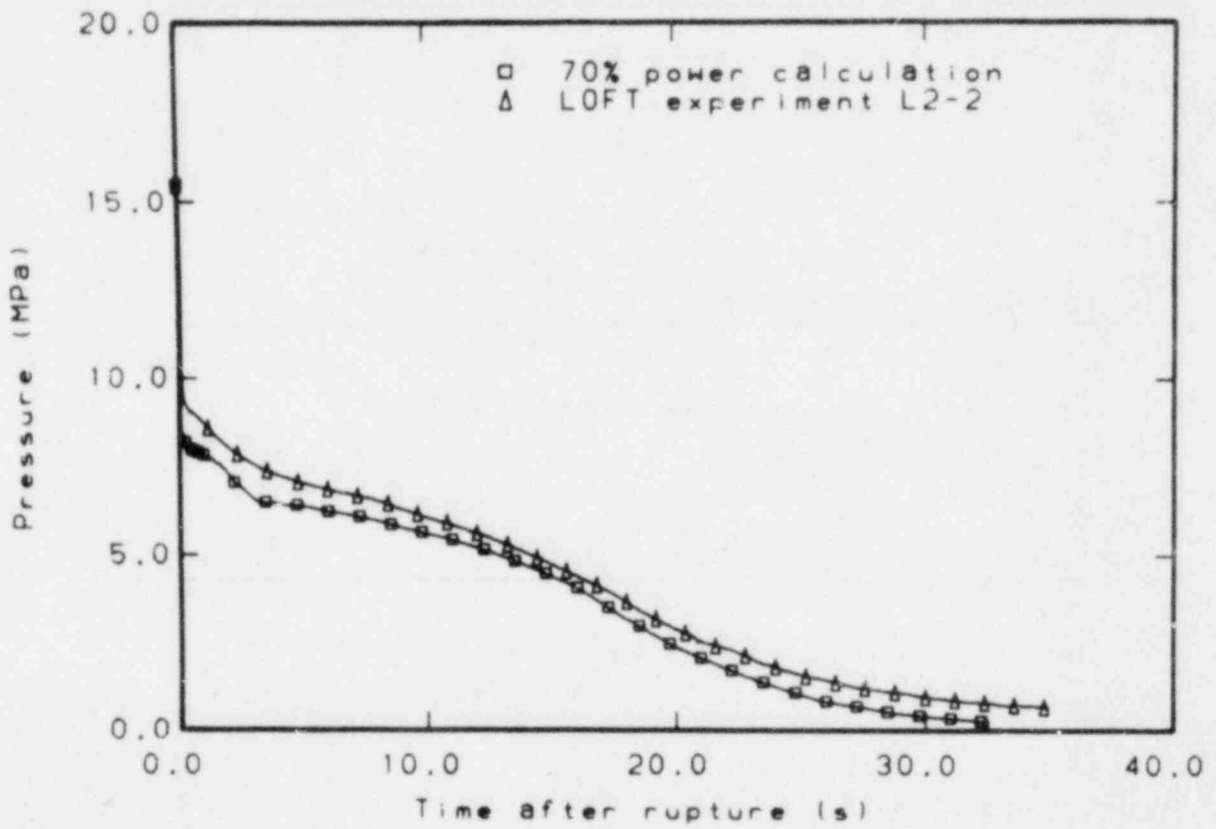Figure 24. Pressure in intact loop hot leg for Experiment L2-2 and Zion 1, 70% power calculation.

In Figure 25, the calculated average core mass flow is compared with the momentum flux as measured in Experiment L2-2 in the upper plenum, just above the core. The measured momentum flux has been qualified as trend data. The behavior of the momentum flux was close to the behavior of the calculated core mass flow. During the transient, there was a small positive flow between 0 and 2.5 s, an increase in the positive core flow with a maximum flow at around 5 to 6 s, followed by a gradual decrease in the flow. At the start of accumulator injection into the system, there was again a zero or small reversed flow. The decrease of core mass flow after 5 s into the transient was caused by the pump delivering less mass to the vessel because of two-phase degradation in the intact loop pump.

An important factor for the core mass flow, especially after the core started voiding, is the difference between the intact and broken loop cold leg flows. Figure 14 shows that between 3 and 6 s the calculated cold leg intact loop flow was larger than the calculated break flow; therefore, a surplus of relatively cold water was delivered to the core. This slug of cold water was important for the rewetting after 5 to 6 s. The difference in mass flows between the two cold legs, calculated and measured in Experiment L2-2, is shown in Figure 26 and indicates that the behavior was about the same.

A comparison of the measured and calculated densities in the hot and cold legs of the intact and broken loops is shown in Figures 27 through 30. Comparisons of measured and calculated cladding temperatures are shown in Figures 31 and 32 for the 70 and 110% power calculations, respectively. In Figure 31, the calculated hot pin cladding temperatures, for the 70% power calculation, at four axial positions are compared with the measured hot spot temperature (Rod 5J4 in the center fuel module at 0.76 m above the bottom of the core) from Experiment L2-2. In Figure 32, the calculated hot pin temperatures, for the 110% power calculation, at four axial locations are compared with the measured hot spot temperature from LOFT Experiment L2-3 (Rod 5J4 in the center fuel module at 0.76 m above the bottom of the core). Comparison of the calculated data for the system calculations (representative for the average core) give the same trends; however, it is hard to define which fuel rod was representative for the
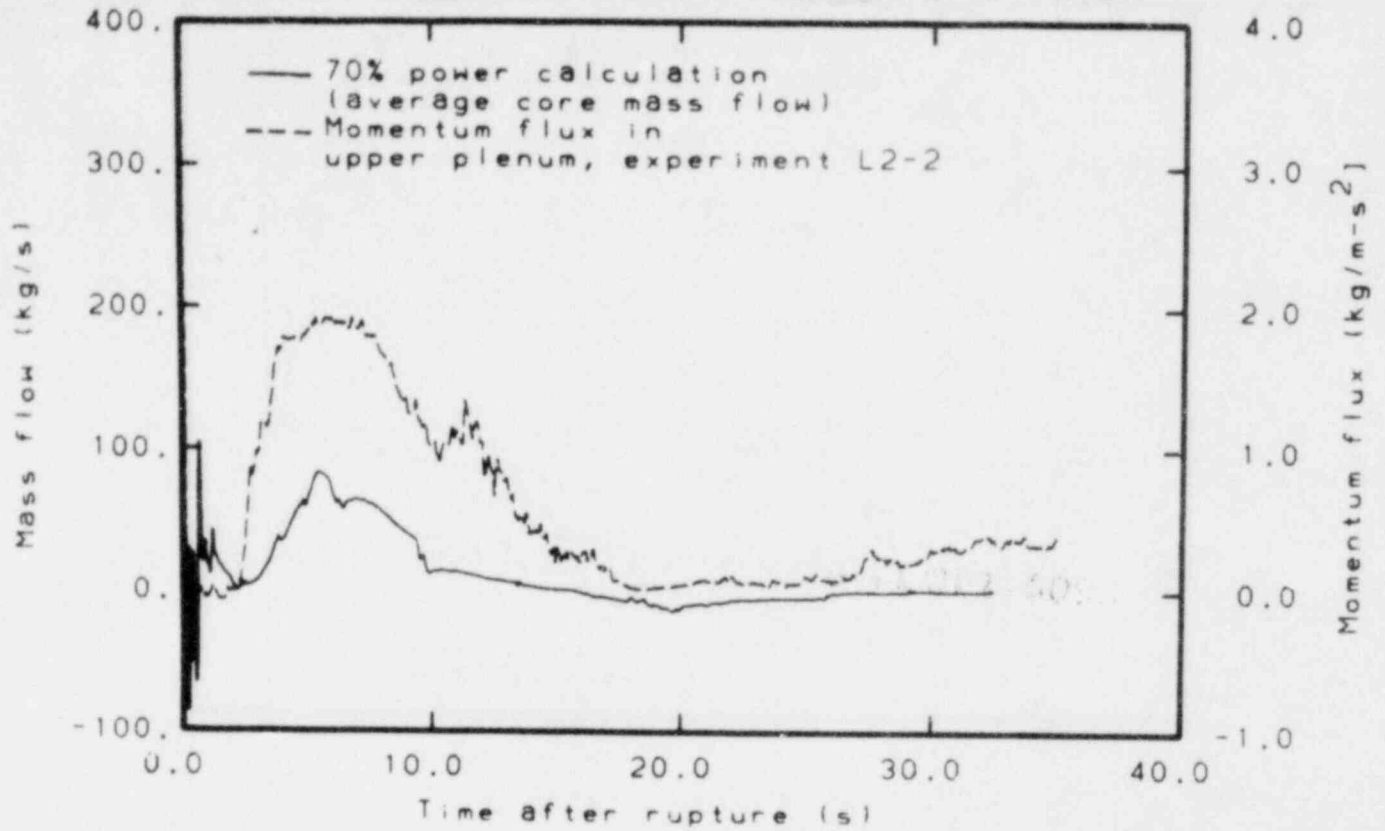
Figure 25.   Average core scaled mass flow for Zion 1, 70% power calculation and momentum flux in upper plenum for Experiment L2-2.
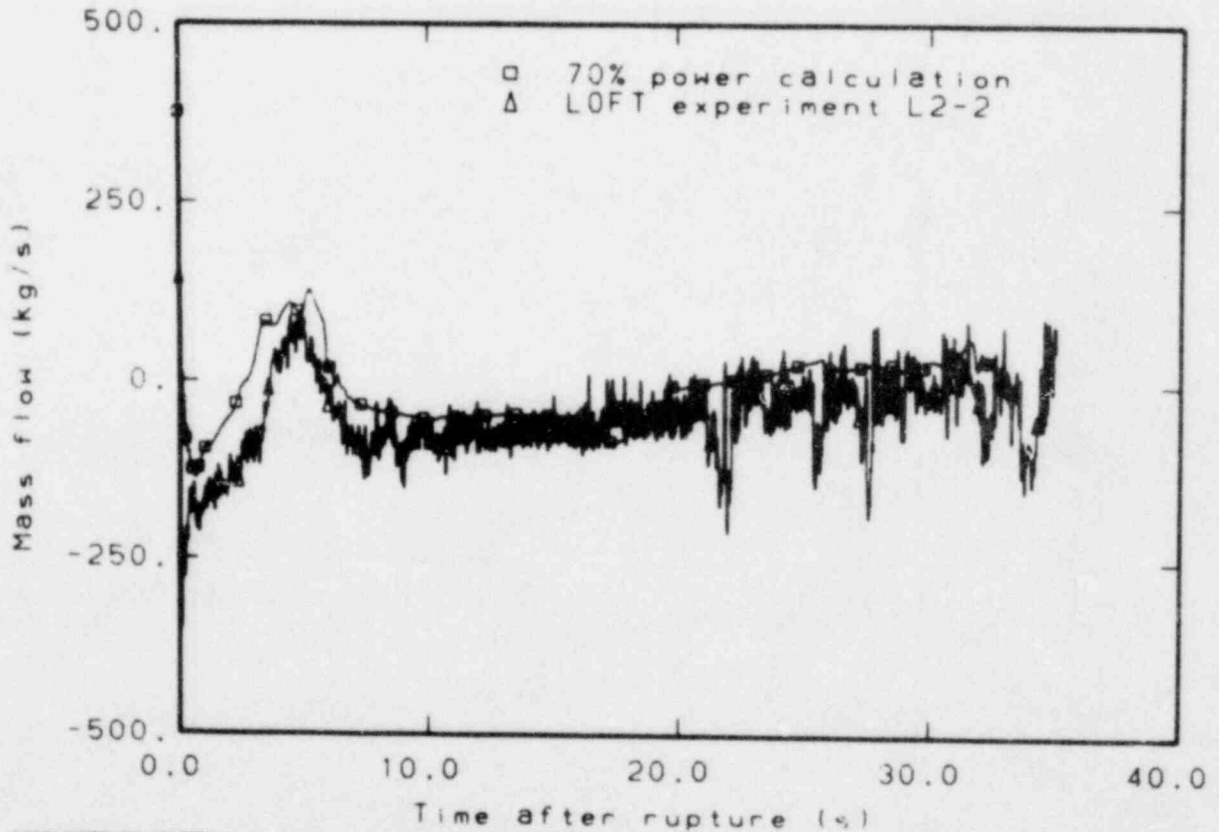
Figure 26.   Mass flow difference between intact and broken loop cold legs for Experiment L2-2 and scaled mass flow difference for Zion 1, 70% power calculation.
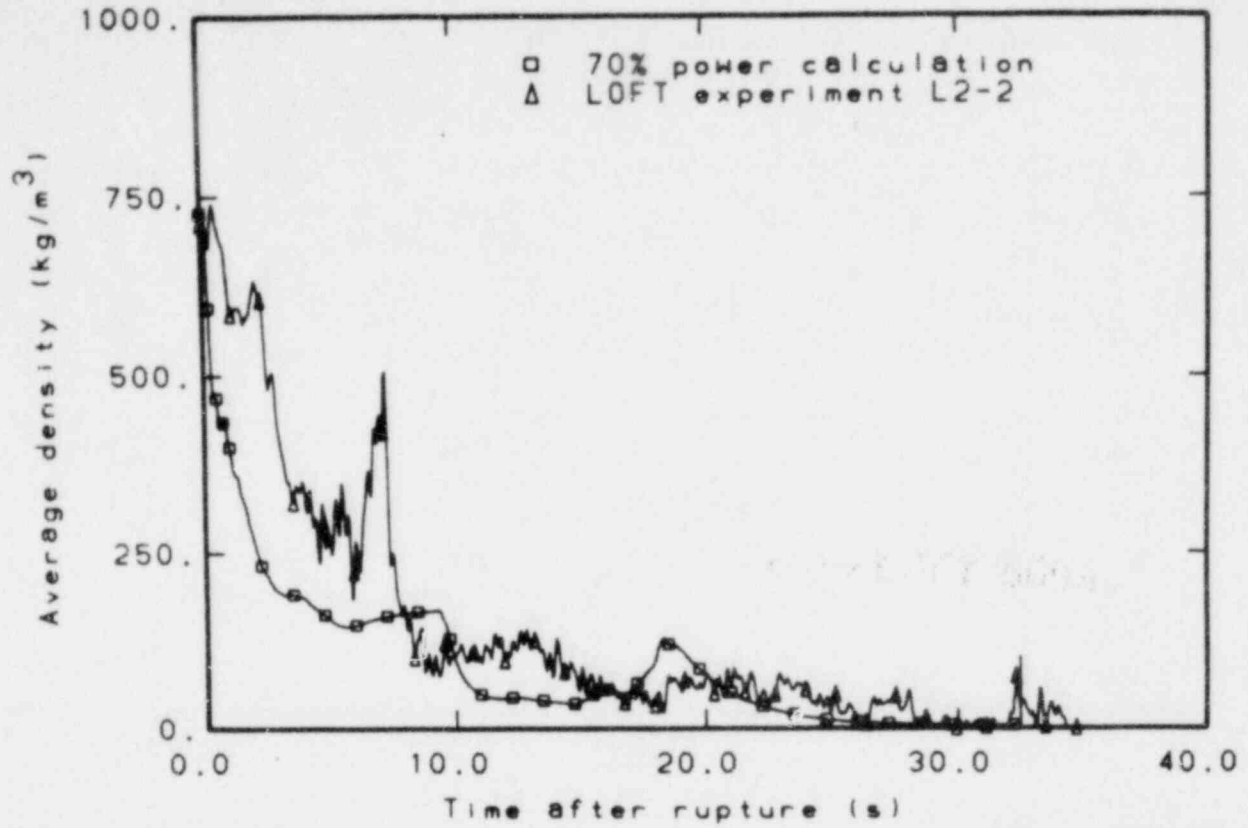
Figure 27. Density in intact loop hot leg for Experiment L2-2 and Zion 1, 70% power calculation.
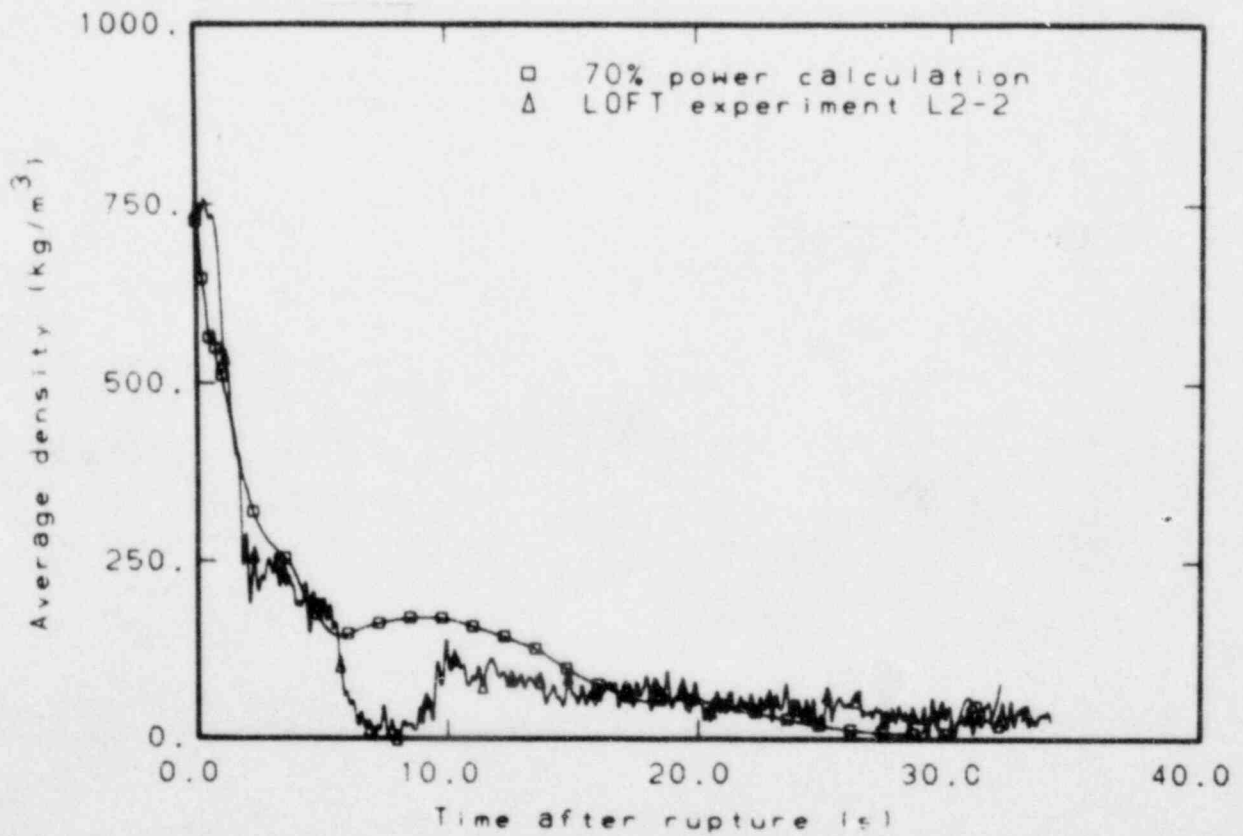
Figure 28. Density in broken loop hot leg for Experiment L2-2 and Zion 1, 70% power calculation.
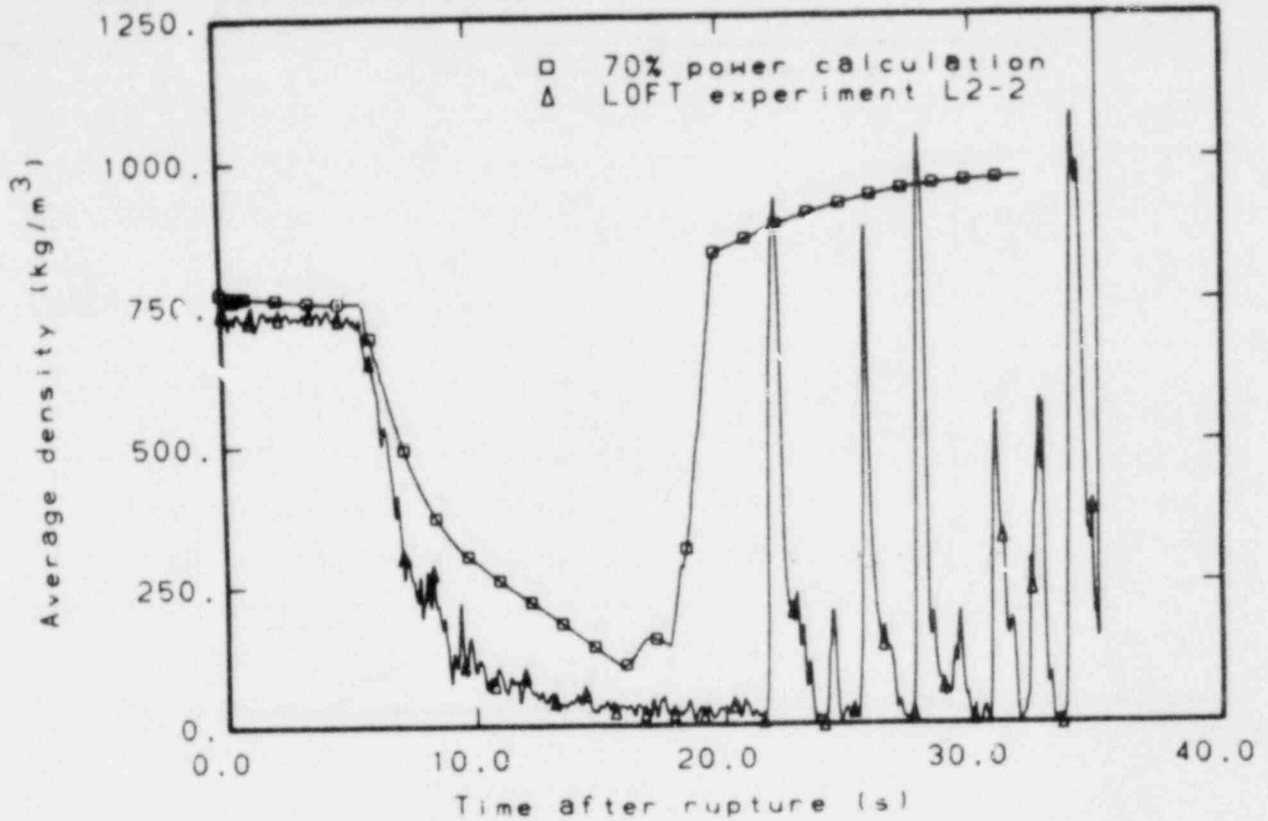
Figure 29. Density in intact loop cold leg for Experiment L2-2 and Zion 1, 70% power calculation.
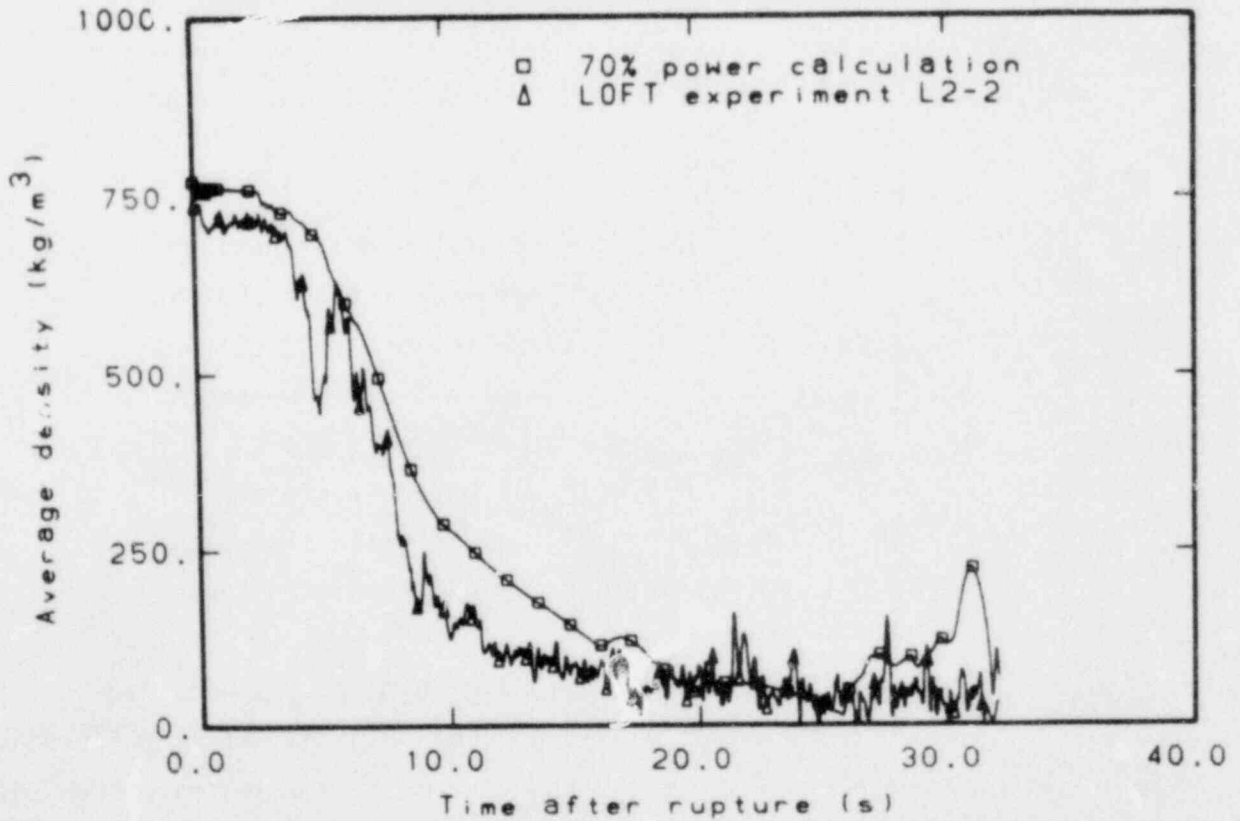
Figure 30. Density in broken loop cold leg for Experiment L2-2 and Zion 1, 70% power calculation.
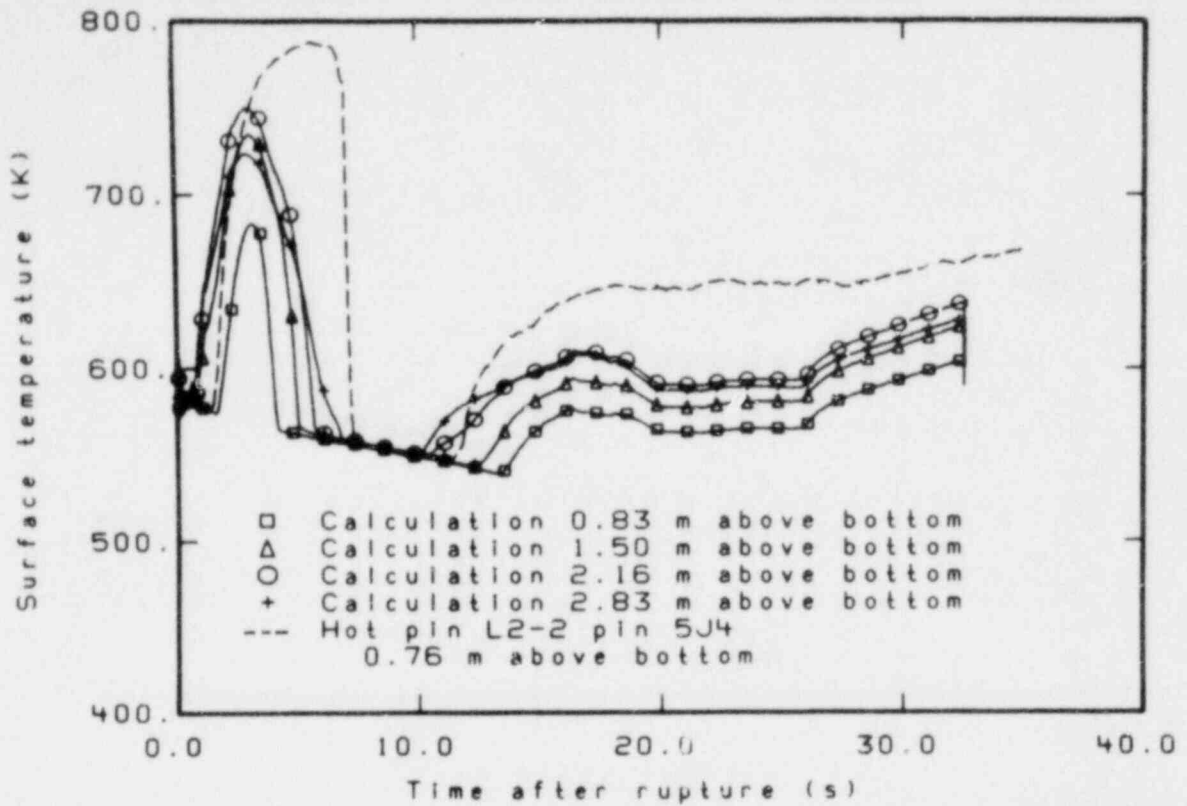
Figure 31. Temperatures at various elevations in the core for Experiment L2-2 and Zion 1, 70% power hot pin calculation.
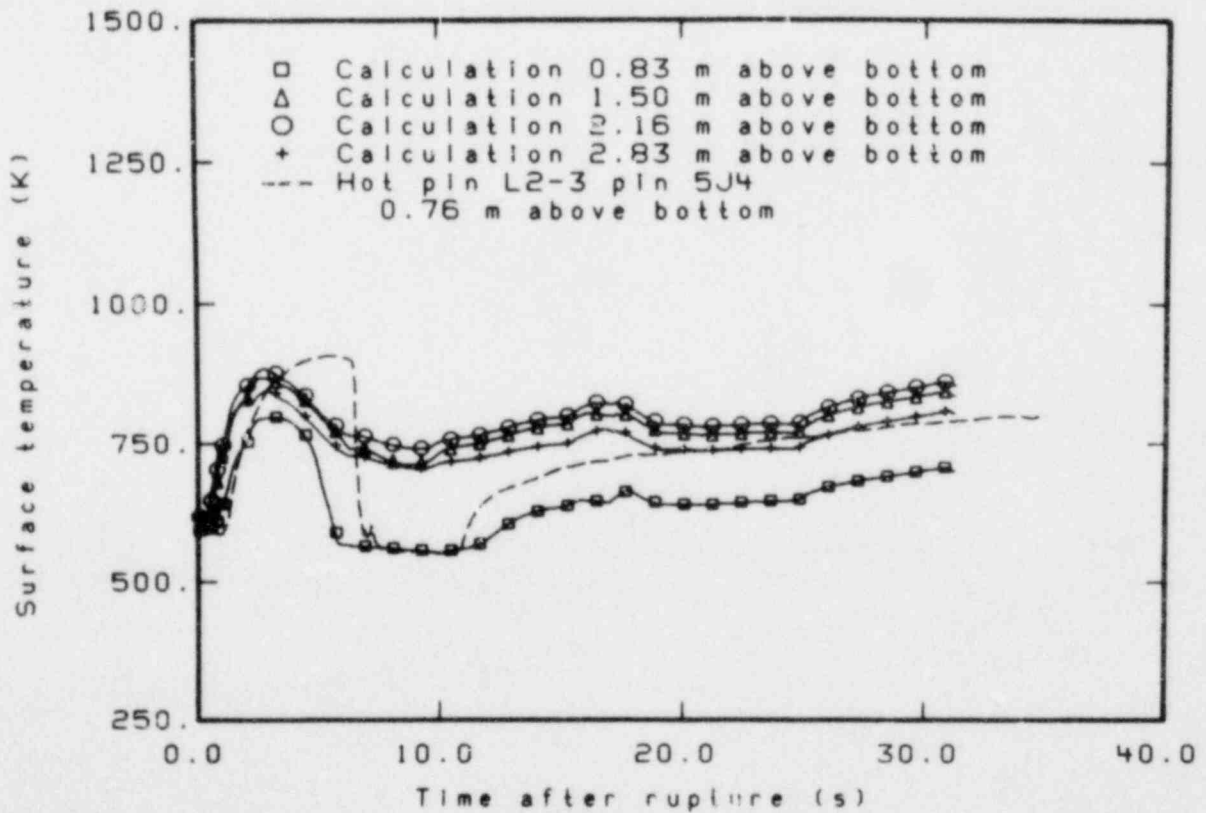
Figure 32. Temperatures at various elevations in the core for Experiment L2-3 and Zion 1, 110% power hot pin calculation.

average rod. Fuel rods in the center of the outer, square fuel modules
have about the average power but a number of them rewet after 5 s, while
others did not. In the calculation, all the fuel rods representing the
average pin rewet. When there was a rewet shown in the experimental data,
the peak temperature was close to the calculated temperature. In the cal-
culation, there was a second dryout between 13 and 14 s into the transient.
In Experiment L2-2, there was a second dryout (or first if there was no
early DNB) between 12 and 30 s.

It is concluded from the comparison of the Zion 1 calculations with
LOFT experimental data that the calculated hydraulic behavior in Zion 1
was close to the hydraulic behavior seen in Experiment L2-2. The cladding
temperature behaviors of the calculation and Experiment L2-2 were quite
close; however, the Zion 1 calculation with Experiment L2-3 initial condi-
tions did not show as strong a rewet tendency at the hot spot of the core
as did Experiment L2-3. Differences in temperature response can probably
be attributed to the different power profiles for LOFT and Zion 1.

5. SENSITIVITY STUDIES

The sensitivity studies are divided into three main parts. The first
part gives information about the influence of specific RELAP4 code options
on a LPWR LOCA blowdown calculation. Calculations were done with a differ-
ent film boiling correlation and with changes in the break flow multiplier
and the transition region for the break flow. These calculations were done
for the case with nominal plant conditions, and the results are compared
with the base calculation described earlier in this report.

The second part consists of a pair of calculations which investigated
the influence of the pressurizer level and the steam generator design on a
LPWR LOCA calculation.

The third part consists of a number of calculations performed to answer
the question: "Are the calculations described in the first part worst case
accidents for this kind of a LOCA?" Different axial power profiles and the
maximum allowable hot leg temperature cases were calculated. Some final

calculations were done to provide information for future planning of experiments in the LOFT large break experiment series (L2 series). Different pump operation and some changes in initial mass flow were the parameters for these final calculations.

5.1 Code Options

The RELAP4 pretest prediction for LOFT Experiment L2-2 gave a reasonable prediction for the hydraulic behavior of the system; however, the thermal response of the core was much too conservative.[4] The cladding temperature predictions showed DNB at the same time as in the experiment, but there was no rewet after about 5 s and the predicted temperature level was much higher than the temperature level in the experiment. To achieve a better agreement, the following major changes in the RELAP4 options were made for the posttest analysis:

1. A multiplier of 1.0 had been used for the cold leg break flow; this multiplier was applied to both the saturated and the subcooled part of the critical flow. In the posttest analysis, a multiplier of 0.848 was used for all qualities of the cold leg break flow.

2. The transition region between subcooled critical flow and the saturated critical flow had been defined as between 0.0 and 2.0% quality. In the posttest analysis, this transition region was decreased to values between 0.0 and 0.25% quality.

3. The correlation used for high flow film boiling had been the Groeneveld correlation. In the posttest analysis, the Condie-Bengston correlation was applied for this regime.

These changes, together with other minor changes, gave a much better prediction of the thermal behavior of the core for LOFT Experiment L2-2.[9] The major contributor of this improved prediction was the transition region change. The new transition region caused a significantly higher core flow which gave the same early rewetting as seen in the experiment.

To investigate the influence of the above mentioned option/parameter changes on the Zion 1 calculations, a sensitivity study was done for the 70% power calculation.

5.1.1 Groeneveld Film Boiling Correlation

Using the RELAP4/MOD6 blowdown heat transfer package, there is an option of the Condie-Bengston correlation or the Groeneveld correlation for the high flow film boiling heat transfer. Usually the Condie-Bengston correlation will yield larger heat fluxes than the Groeneveld correlation. To investigate the sensitivity of the cladding temperature of the fuel rods for this film boiling heat transfer correlation, both system and hot pin calculations for the 70% power case were done. Results of these calculations are shown in Figures 33 and 34. In Figure 33, the hot spot temperature (heat Slab 7 in the hot pin calculation) is given and in Figure 34 the cladding temperature of the middle part of the core is given for the system calculation (this temperature is representative for the average core). The calculations show that change of the film boiling correlation from Condie-Bengston to Groeneveld had no effect on the core mass flow.

Because the Condie-Bengston correlation transfers more heat to the coolant, the temperature peak during first dryout was lower and it returned earlier to nucleate boiling than in the calculation with the Groeneveld correlation. The second dryout occurred at about the same time, but the decrease in temperature, which is seen in the Condie-Bengston correlation after about 17 s, is not seen in the Groeneveld calculation due to the higher heat fluxes given in the Condie-Bengston correlation than in the Groeneveld correlation.

5.1.2 Break Flow Multiplier and Transition Region

In the LOFT Experiment L2-2 posttest analysis,[9] the break flow multiplier and in particular, the transition region, had a big influence on the core mass flow and, therefore, on the heat transfer in the core. In RELAP4, the possiblity exists to multiply the junction area by a certain number (CONCO on the junction data cards). In this calculation, the
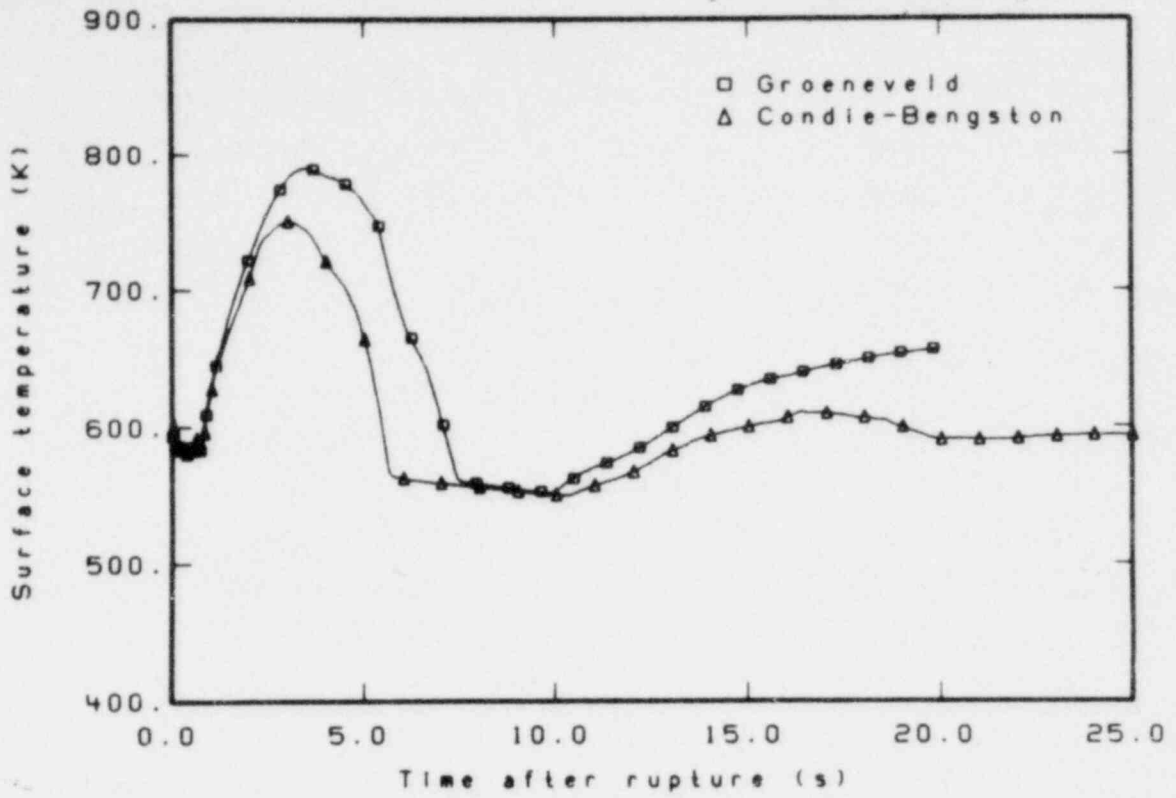
Figure 33. Hot spot cladding temperature calculated for Zion 1 using RELAP4 with Groeneveld and Condie-Bengston film boiling correlations.
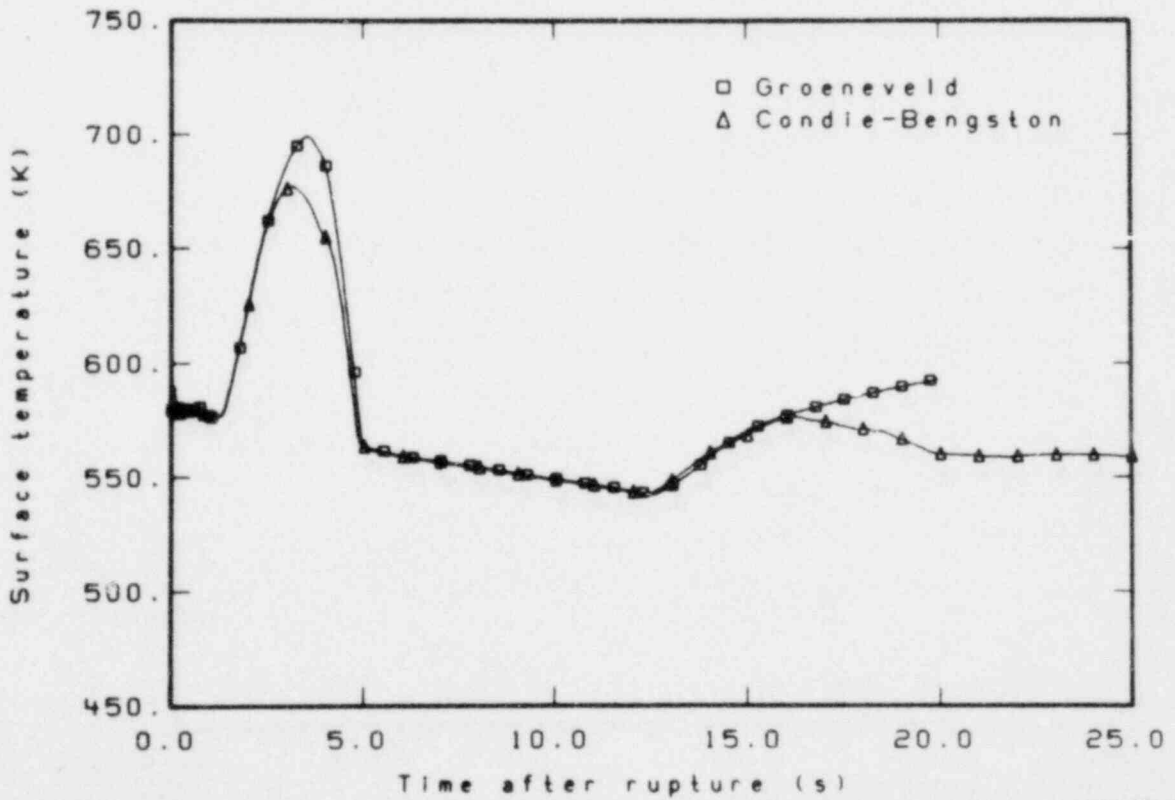

Figure 34. Cladding temperature in middle part of core calculated for Zion 1 using RELAP4 with Groeneveld and Condie-Bengston film boiling correlations.

contraction coefficient was used as a multiplier for the flow area of the break junction and it can be seen as a multiplier for the critical mass flow. One calculation has been done for the 70% power case system calculation in which the contraction coefficient for the cold leg break junction was changed from 1.0 to 0.8.

Using a critical flow model, the transition region has to be specified. This transition region is a quality region in which a smooth transition between a critical flow model for subcooled and saturated conditions was established. A calculation has been done in which the base case quality transition region was changed from 0 to 0.25% into 0 to 2%. Comparisons of the base case 70% power system calculation with the two above mentioned calculations are shown in Figures 35 through 38.

5.1.2.1 Break Flow Multiplier. The break flow multiplier of 0.8 instead of 1.0 was used only in the cold leg. The hot leg contraction coefficient has not been changed. The hot leg and cold leg break flows are given in Figures 35 and 36. Use of the 0.8 multiplier gave, as expected, a smaller mass flow from the cold leg break (Figure 36). Because less water was leaving the system, the system pressure tended to be higher (especially after the pressurizer was empty), and this is one of the reasons that the hot leg break flow was higher after about 9 s into the transient (Figure 35). Figure 37 gives the average mass flow in the core. The larger core mass flow compared to the base case calculation was due to the smaller flow from the cold leg break, an almost unchanged and even higher mass flow from the hot leg break, and an unchanged delivery from the pumps to the downcomer. The overall balance of these three flows gave a higher core mass flow in the positive direction. The temperature response of the middle part of the core is given in Figure 38. The higher core mass flow and, therefore, the greater heat transfer in the core caused an approximate 30 K lower peak temperature at 3.5 s into the transient. The return to nucleate boiling was at about the same time, but also, due to the higher core mass flow, the second dryout started about 4 s later. The top part of the core behaved in the same way as

Figure 35. Break flow in the hot leg for Zion 1, 70% power base case, break flow multiplier, and transition region calculations.

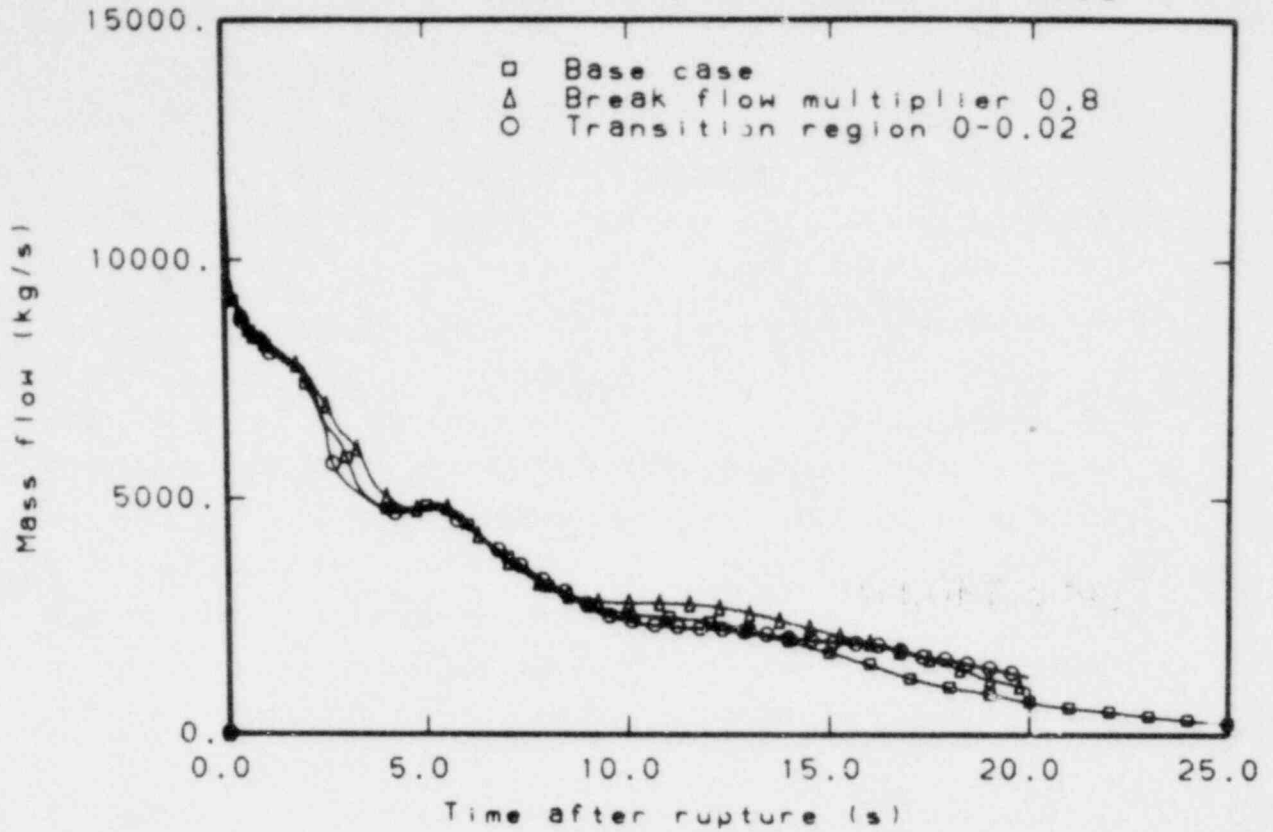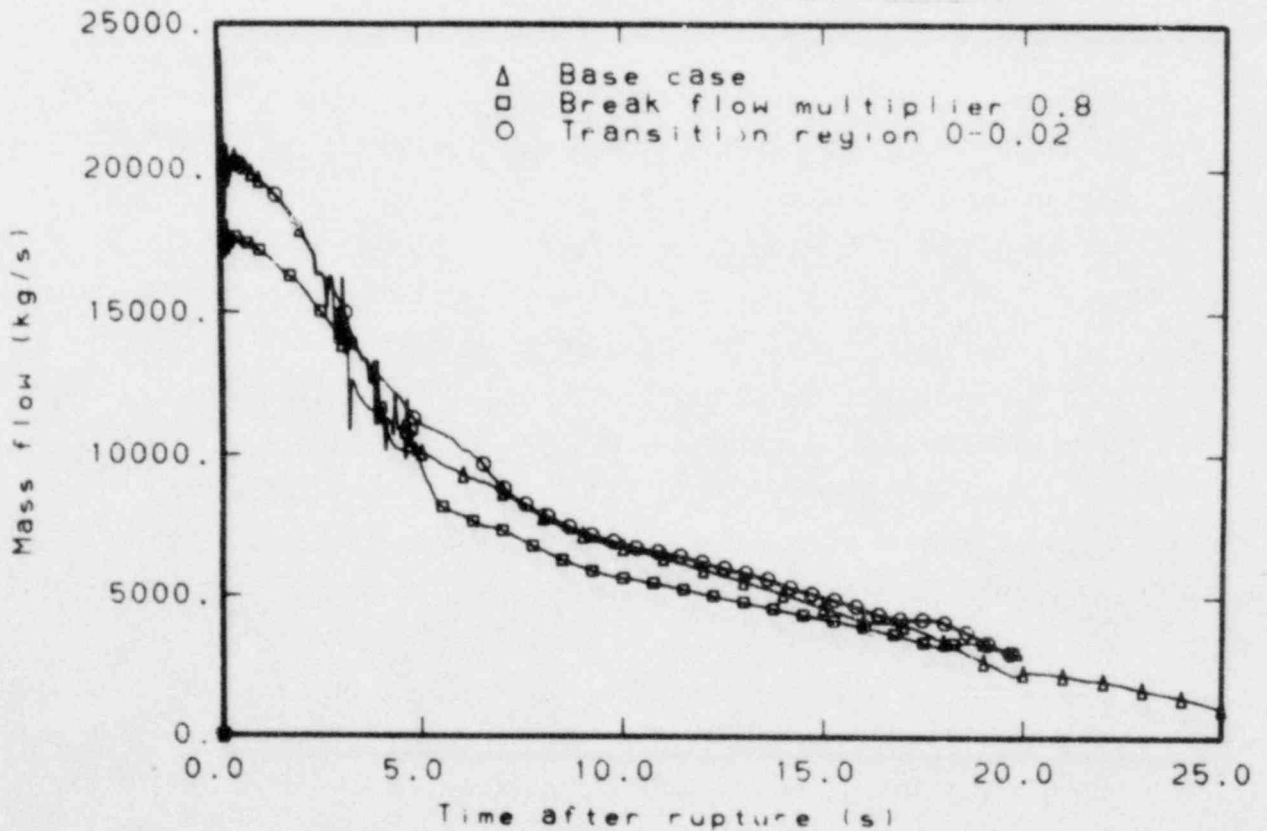Figure 36. Break flow in the cold leg for Zion 1, 70% power base case, break flow multiplier, and transition region calculations.
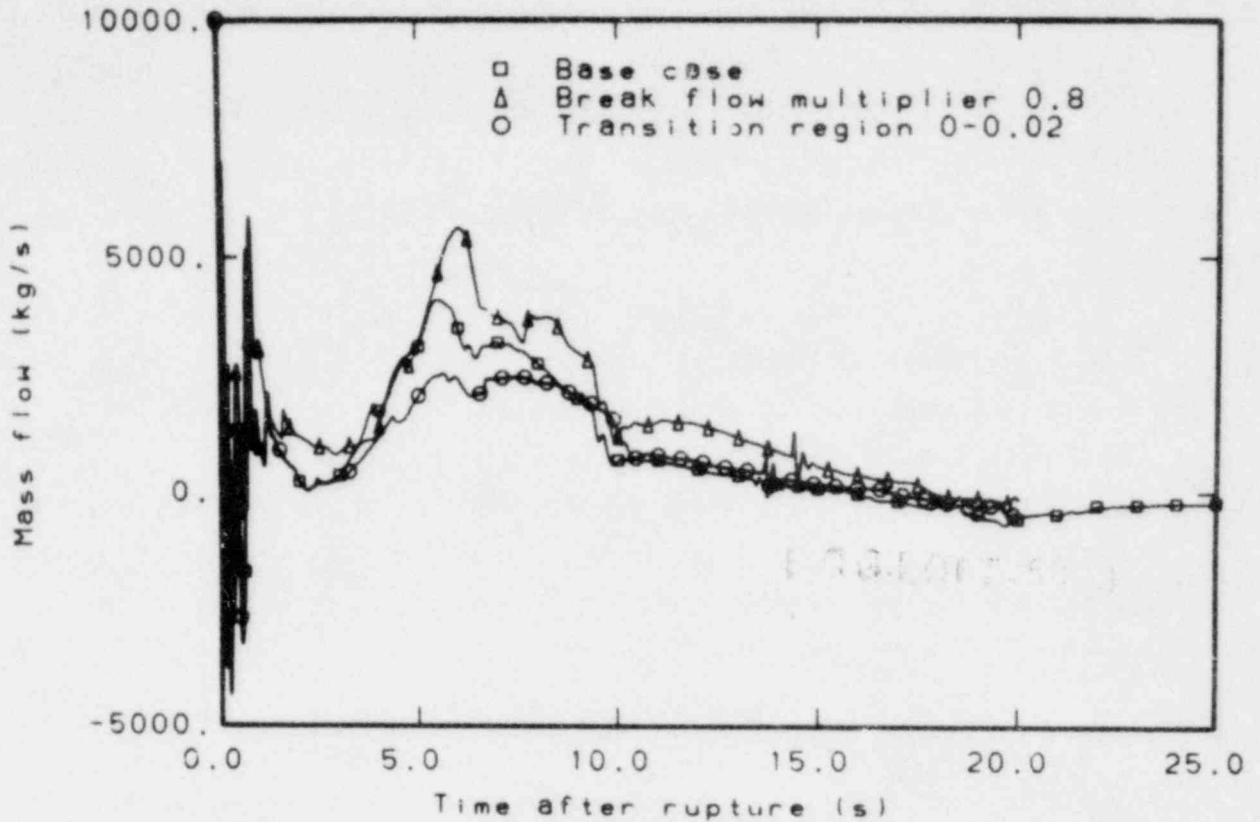
Figure 37. Average core mass flow for Zion 1, 70% power base case, break flow multiplier, and transition region calculations.
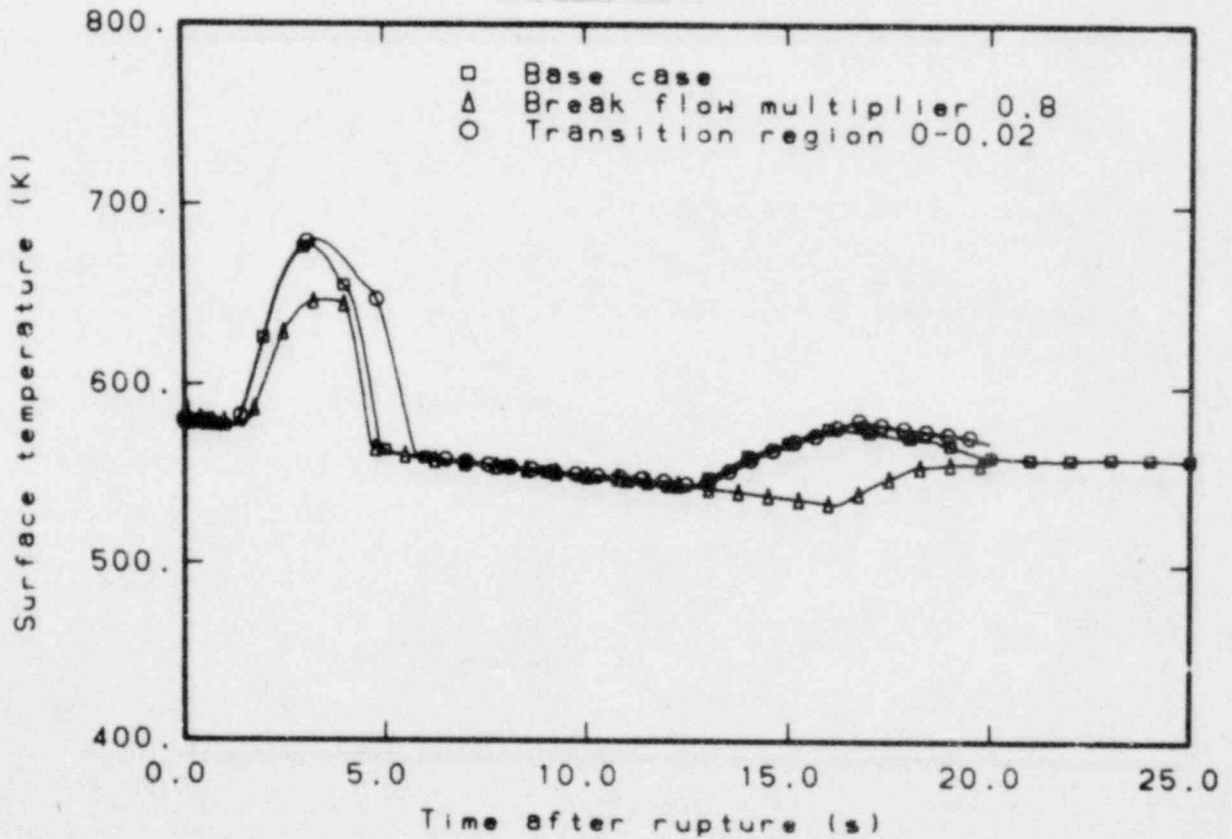

Figure 38. Surface temperature in middle part of core for Zion 1, 70% power base case, break flow multiplier, and transition region calculations.

47

the middle part. In the lower part of the core the higher core mass flow was able to transfer more heat; therefore, this part did not have an early DNB, and the first dryout occurred at about 17 s into the transient.

5.1.2.2 Transition Region. The change of transition region from 0 to 0.25% quality to 0 to 2% quality for all locations where choking occurred had only a small effect on the critical break flows (Figures 35 and 36). This effect only occurred during the time that the break flow was in the transition region and a short period thereafter (between 2.5 and 7 s into the transient). The changes in the break flows were small and had no influence during the rest of the transient. The core mass flow was lower during this period (Figure 37) but was still high enough to cause a rewetting. In Figure 38, the peak cladding temperature in the middle part of the core was shown as almost not affected, but the smaller core flow gave a 1-s delay in returning to nucleate boiling. The temparature behavior for the rest of the transient was exactly the same as for the base case calculation.

The conclusions from the sensitivity calculations to study the effect code options might have on a LPWR LOCA blowdown calculation are as follows.

1. A change of break flow multiplier in the cold leg from 1.0 to 0.8 gives a higher positive core mass flow while the peak cladding temperature (average core) is about 30 K lower.

2. The change in the transition region from 0 to 0.25% quality to 0 to 2% quality gives a lower core flow in the first period of the blowdown, and the early rewetting occurs about 1 s later with no effect on peak cladding temperature.

5.2 Plant Conditions

The second part of the sensitivity studies consists of calculations to investigate the influence of the pressurizer level and steam generator design on a LPWR LOCA calculation.

5.2.1 Pressurizer Water Level

To investigate the influence of the pressurizer level on the behavior of the system under LOCA conditions, a calculation was done in which the initial pressurizer water level was 10% higher than in the normal case. The calculation was done for the 110% power base case system calculation. In the base case calculation, the initial pressurizer level was 8.95 m, and in the new calculation, 9.85 m. Results of the new calculation compared with the base case calculation are given in Figures 39 and 40. Due to the higher level in the pressurizer and the choked flow from the pressurizer to the system, the pressurizer emptied about 1 s later. This delayed empting of the pressurizer had a small effect on the core mass flow between 9.5 and 10.5 s (the faster decrease of the core mass flow after the pressurizer was empty also happens 1 s later for the new calculation) (Figure 39). The effect on the peak cladding temperature in the middle part of the core is negligible, as shown in Figure 40.

A conclusion from this calculation is that a 10% higher water level in the pressurizer has almost no influence on the temperature response in the core.

5.2.2 Steam Generator Heat Transfer

With the Zion 1 RELAP4/MOD6 model (110% power case) as a base, a few calculations were done to investigate the influence of the steam generator geometry on the overall system behavior after a LOCA.

The base calculation (called Calculation Case 1) was a 200% double-ended cold leg break in the Zion 1 reactor at a power level of 3540.0 MW (calculation is described in Section 2.1 of this report).

Three additional calculations were done as follows:

1. Using the same geometry for the two steam generators, the steam generator tube material was changed from Inconel to Type-316 stainless steel. For this material change, the change in heat
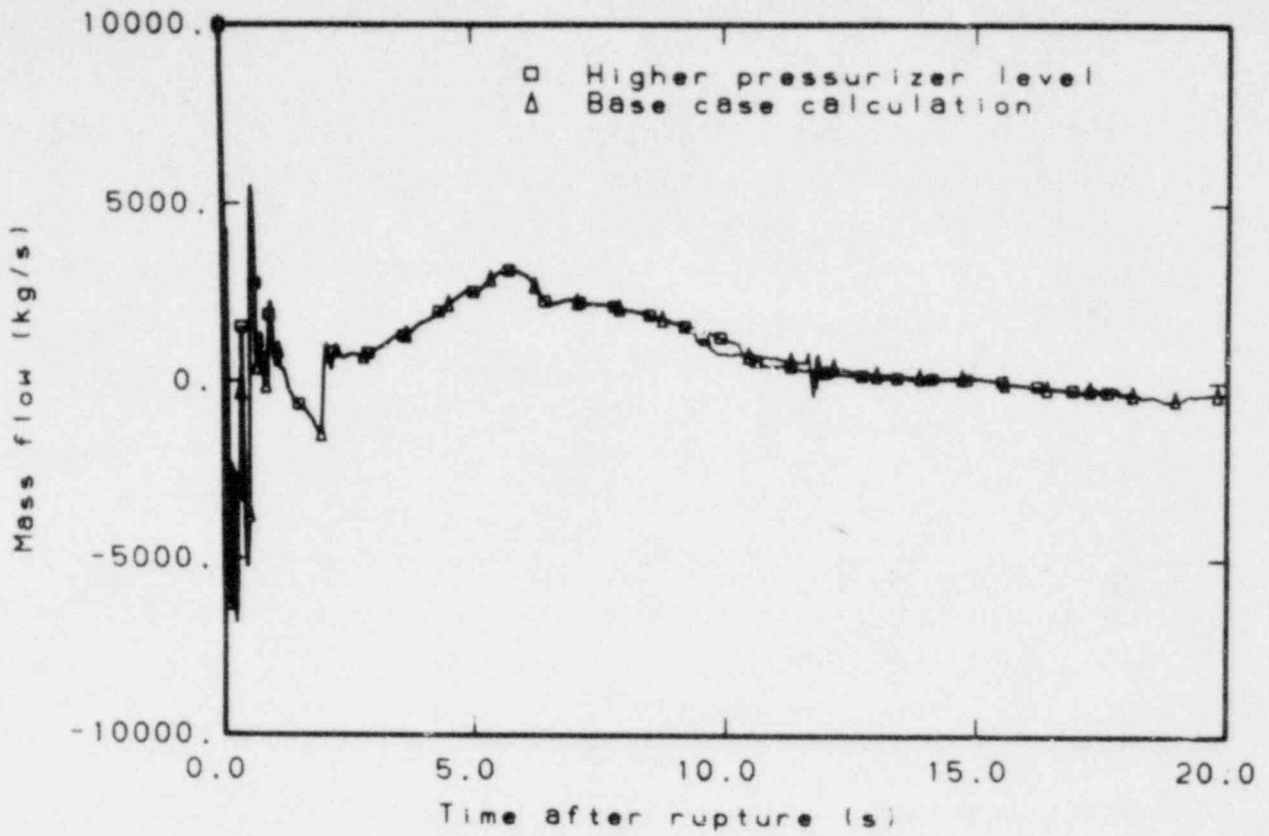
Figure 39. Average core mass flow for Zion 1, 110% power base case calculation and a calculation with a 10% higher pressurizer level.
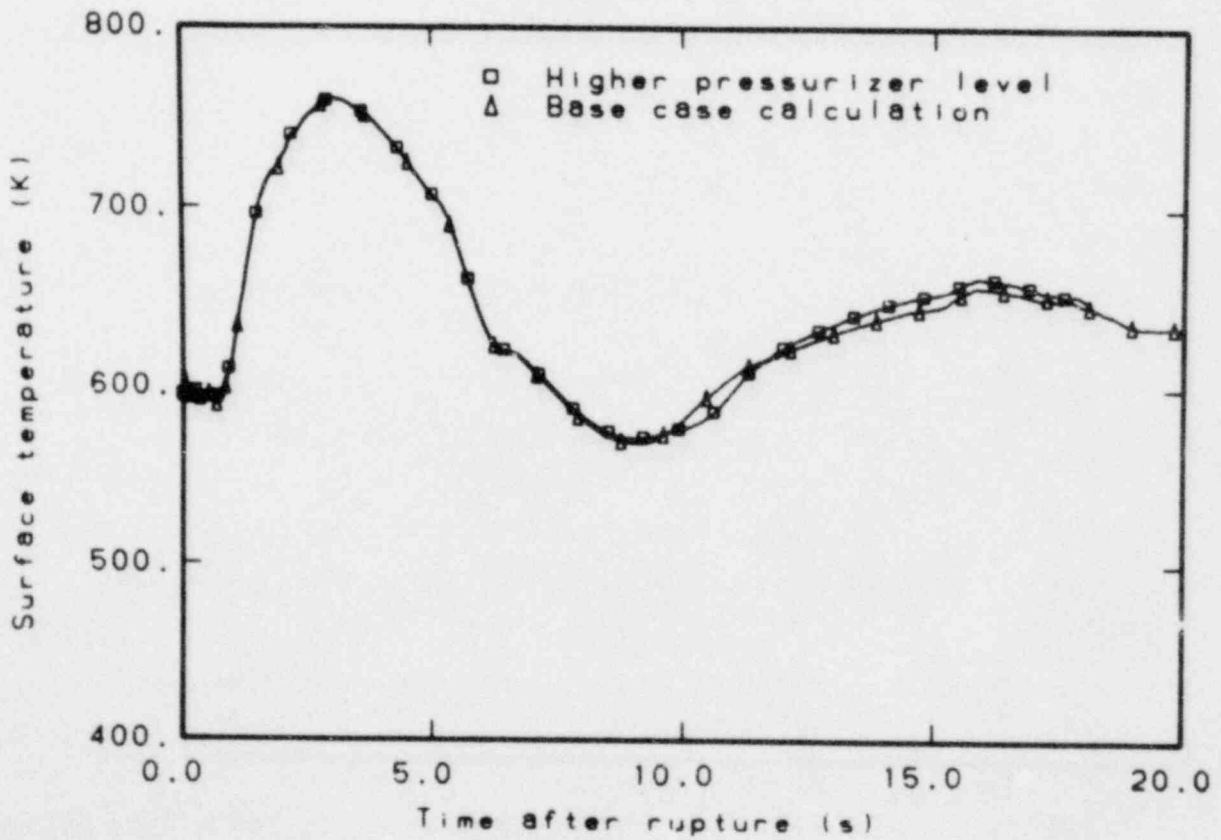

Figure 40. Cladding temperature in middle part of core for Zion 1, 110% power base case calculation and a calculation with a 10% higher pressurizer level.

50

capacity was small, but the change in thermal conductivity was larger. Table 10 gives the heat capacity and thermal conductivity for the 477-to-588-K temperature range. The calculation with this material change is called Calculation Case 2.

TABLE 10. HEAT CAPACITY AND THERMAL CONDUCTIVITY FOR STEAM GENERATOR TUBE MATERIAL

Temperature (K)	Heat Capacity $(Ws/k \cdot m^3)$		Thermal Conductivity $(W/k \cdot m)$	
	Type-316 ss	Inconel	Type-316 ss	Inconel
477.6	$4.098 \ 10^{-6}$	$4.099 \ 10^{-6}$	15.66	17.51
588.7	$4.333 \ 10^{-6}$	$4.276 \ 10^{-6}$	17.12	19.87

2. The calculation was repeated using the steam generator with a different geometry of the tubes and a different number of tubes, but with the same tube material as for the base case calculation (Inconel). This is called Calculation Case 3. Table 11 gives the geometrical data of the steam generator for this case.

3. The calculation was repeated modeling the steam generator with the same geometry as the LOFT steam generator and the same tube material (Inconel). This is called Calculation Case 4. Table 12 gives the geometrical data for this case.

To achieve a well balanced system at time 0.0, the temperature in the primary and secondary sides of the steam generator had to be adjusted. Table 13 gives the temperatures for the different calculation cases (the volume index is the volume number used in the RELAP4 model, Figure 1).

TABLE 11. STEAM GENERATOR GEOMETRICAL DATA FOR CALCULATION CASES 1 AND 3

Parameter	Calculation Case 3	Calculation Case 1
Inner diameter of tubes (m)	0.0227	0.0197
Outer diameter of tubes (m)	0.0257	0.0222
Number of tubes	∿2 430.0	∿3 250.0
Heat transfer area (total):		
Primary side (m^2)	3 668.9	4 237.0
Secondary side (m^2)	4 153.5	4 784.2
Hydraulic diameter for primary side (m)	0.0227	0.0197

TABLE 12. STEAM GENERATOR GEOMETRICAL DATA FOR CALCULATION CASES 1 AND 4

Parameter	Calculation Case 4	Calculation Case 1
Inner diameter of tubes (m)	0.0102	0.0197
Outer diameter of tubes (m)	0.0127	0.0222
Number of tubes	∿12 050.0	∿3 250.0
Heat transfer area (total):		
Primary side (m^2)	8 168.5	4 237.0
Secondary side (m^2)	1 059.8	4 784.0
Hydraulic diameter for primary side (m)	0.0102	0.0197

For the calculations, no changes were made in secondary feed water conditions or in the volume and junction data. Calculation Case 2 was run until 17.5 s into the transient, the remainder of the calculations were carried out to 20.0 s.

The average core mass flow is given in Figure 41, and it is clear from this figure that the influence of the steam generator changes on the average core mass flow are negligible.

TABLE 13. ADJUSTED TEMPERATURE IN PRIMARY AND SECONDARY SIDES OF THE STEAM
GENERATOR

| Volume | Temperature (K) | | | |
	Calculation Case 1	Calculation Case 2	Calculation Case 3	Calculation Case 4
3 and 15	576.4	576.7	576.8	576.1
4 and 16	561.7	562.2	562.3	561.1
6 and 18	553.2	553.2	553.3	552.8
27 and 28	539.11	537.25	536.78	540.54

The surface temperature of the middle part of the core is given in
Figure 42. The maximum cladding temperature in the core was, for the change
to the LOFT geometry, about 30 K lower than in the base calculation; the
other two calculations gave a very small increase in cladding temperature.
This trend was maintained during the first 20 s of blowdown.

Figures 43 and 44 show the total heat added to the primary coolant
system by the steam generators. From these figures, it is clear that the
time at which the steam generator started to put heat into the primary
coolant system was only affected for Calculation Case 4 (LOFT geometry).
For the intact loop, this time changed from 12.5 to 11.5 s into the
transient.

The conclusion from this calculation is that changes in the steam
generator geometry show only a minor influence on the system thermal-
hydraulics during the first part of blowdown for a large pipe break in a
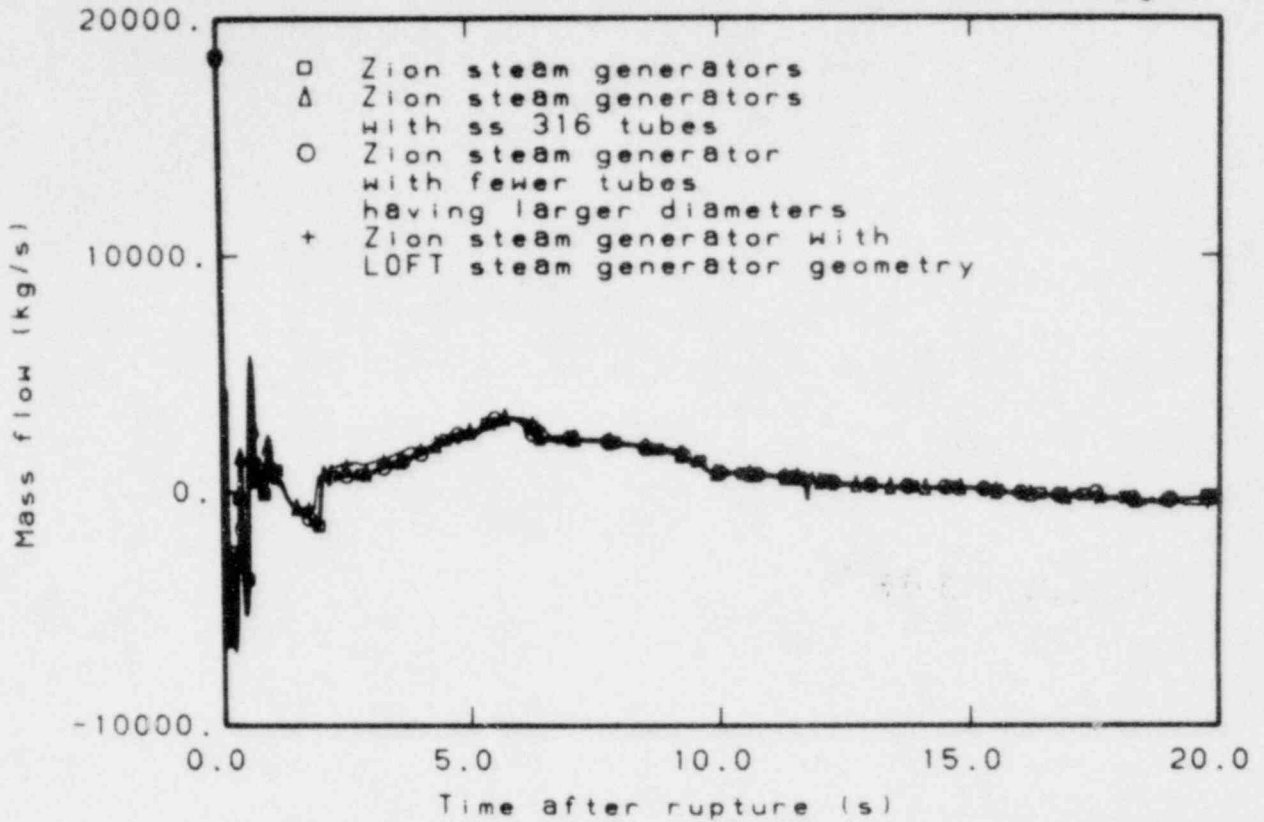LPWR.

Figure 41. Calculated average core mass flow in middle part of core for Zion 1, 110% power case to illustrate the influence of steam generator geometry.
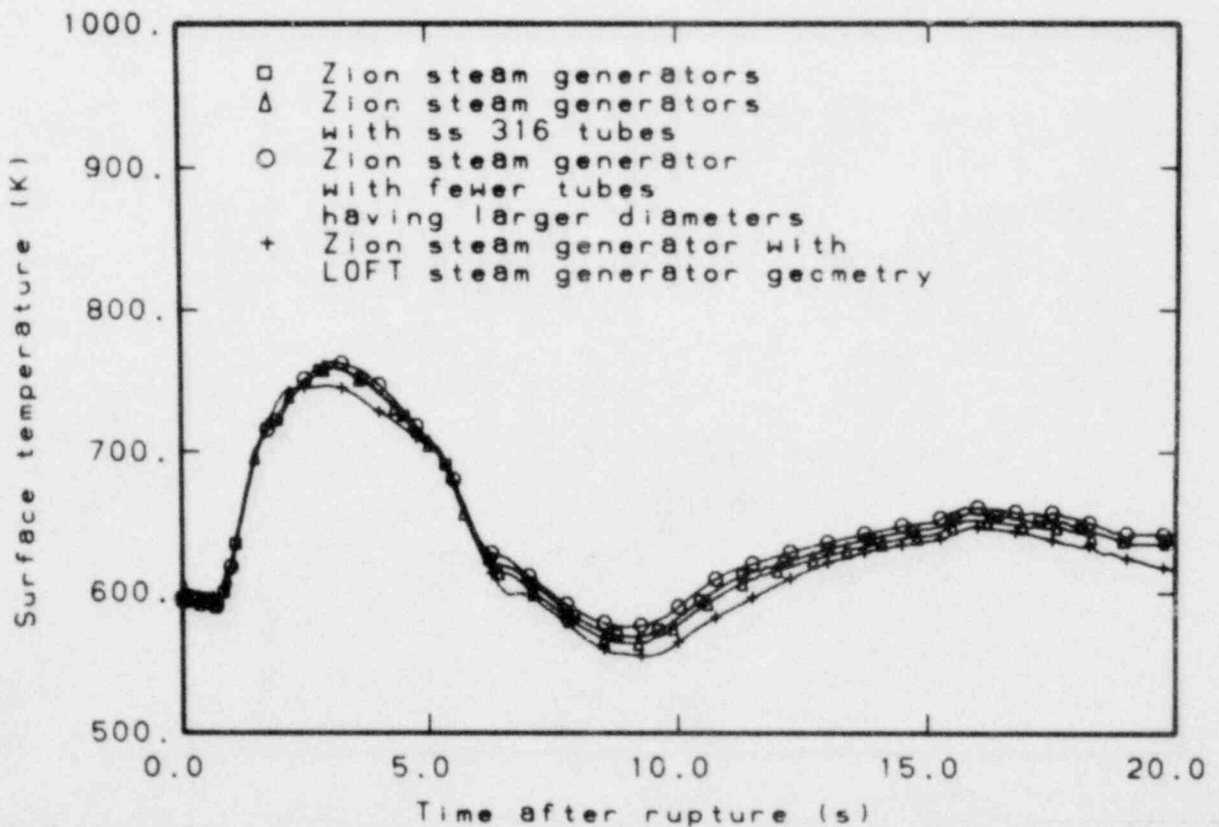

Figure 42. Calculated fuel rod cladding surface temperature in middle part of core for Zion 1, 110% power case to illustrate the influence of steam generator geometry.
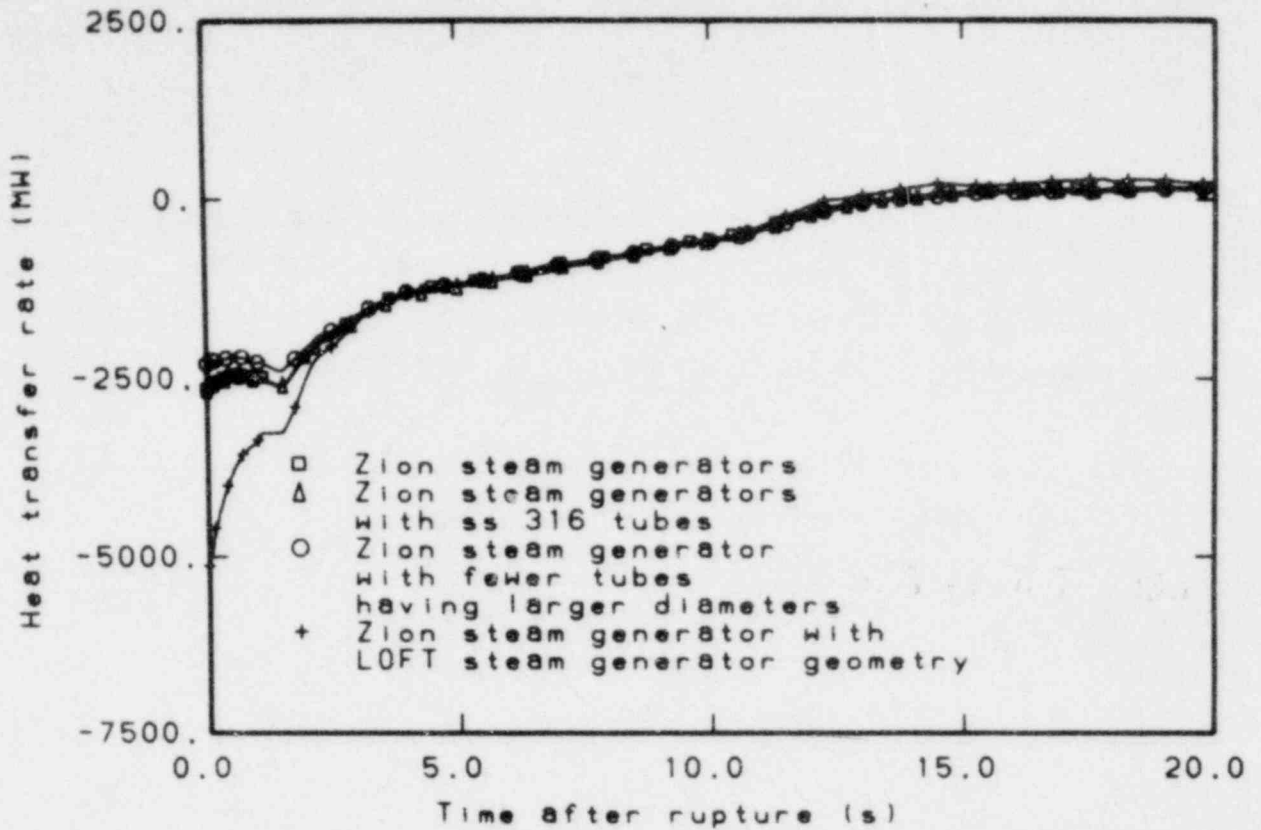
Figure 43. Calculated total heat transfer rate in the steam generator to the primary system intact loop for Zion 1, 110% power case to illustrate the influence of steam generator geometry.
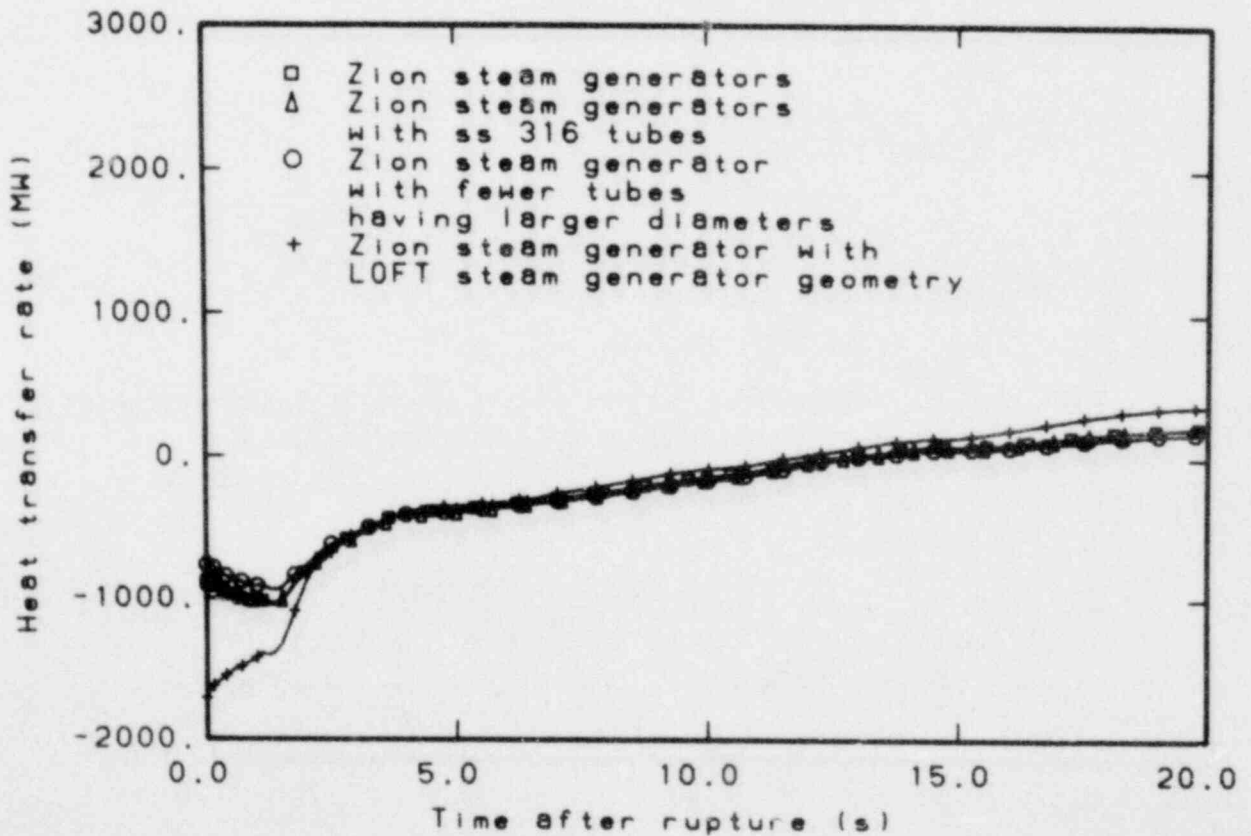

Figure 44. Calculated total heat transfer rate in the steam generator to the primary system broken loop for Zion 1, 110% power case to illustrate the influence of steam generator geometry.

5.3 "Worst Case" and Experiment Planning Calculations

In addition to RELAP4 calculations for the Zion 1 plant operating under the same initial conditions as was established in LOFT for Experiments L2-2 and L2-3, other calculations were done to study the sensitivity of the system behavior for different plant conditions as follows:

1. Calculations to study the influence of the shape of the axial power profile on cladding temperatures (Experiment L2-3 initial conditions, 110% power case)

2. Calculations to study the influence of hot leg temperature on the system behavior (Experiment L2-3 initial conditions, 110% power case)

3. Calculations to study the influence of pump operation (coast down or blocked) on system behavior (Experiment L2-3 initial conditions, 110% power case)

4. Calculation of system behavior under initial conditions planned for Experiment L2-4, however, with a mass flow equal to Experiment L2-3 initial conditions.

The goal of Calculations 1 and 2 was to determine if the base case Zion 1 calculation is representative for the worst case under "normal" plant conditions. Calculations 3 and 4 can be used in defining initial conditions for LOFT Experiments L2-4 and L2-5. All the calculations were stopped between 20 and 30 s into blowdown; therefore, only the first phase of blowdown was investigated.

A schematic of the RELAP4 model used for the system calculations is shown in Figure 1, and a schematic of the model for the hot pin calculations is shown in Figure 3.

5.3.1 Axial Power Profile

Four hot pin calculations (Zion 1, 110% power case at Experiment L2-3 initial conditions) were done to study the influence of the shape of the axial power profile on the surface cladding temperature. The shape of the four different power profiles is given in Figure 45. The total generated power for a fuel rod was the same for the four calculations (122.281 kW → MLHGR = 39.4 kW/m). The RELAP4 system calculation used as the boundary condition for these hot pin calculations was the base case Zion 1 system calculation (110% power case). In this system calculation, the axial power profile (represented by three heat slabs) had the same profile as used in the hot pin calculation (Run 00, Figure 45). Power profile Run 00 from Figure 45 is the base hot pin calculation described in Section 2.2 of this report.

The temperatures calculated agree with the axial power profile (a higher local power gives a higher cladding temperature). The hot spot for all calculations was heat Slab 7. Figure 46 gives the hot spot fuel rod cladding temperature as a function of time for the four calculations. From Figure 46, it is clear that the base case Zion 1 calculation (Run 00) gave the highest peak cladding temperature.

A conclusion from the calculations is that the base case Zion 1 calculation (110% power case, Run 00 in Figure 46) gives the highest peak cladding temperature for different profiles with the same maximum linear heat generation and the same total generated power.

5.3.2 Hot Leg Temperature

The base case Zion 1 system calculation for Experiment L2-3 initial conditions (110% power case) was done ...ch a hot leg temperature of 585.6 K. Specifications of the Zion 1 plant allow the maximum hot leg temperature under normal conditions to be 598.2 K. To investigate the influence of the hot leg temperature on the system behavior, a system calculation was done with a hot leg temperature of 598.2 K. For the calculation, the hot leg temperature was set to 598.2 K (base calculation, 585.6 K) and the power and the mass flow were maintained at base case Zion 1 Experiment L2-3 initial
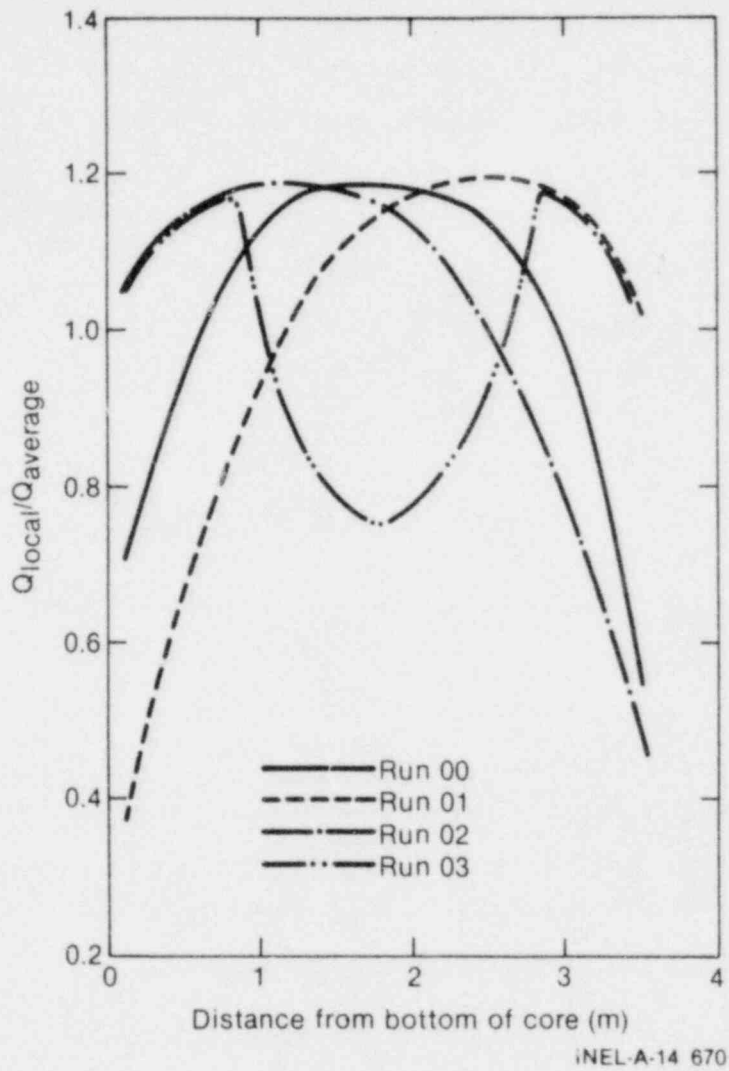
Figure 45. Axial power profiles in the core determined from four hot pin calculations for Zion 1, 110% power case.
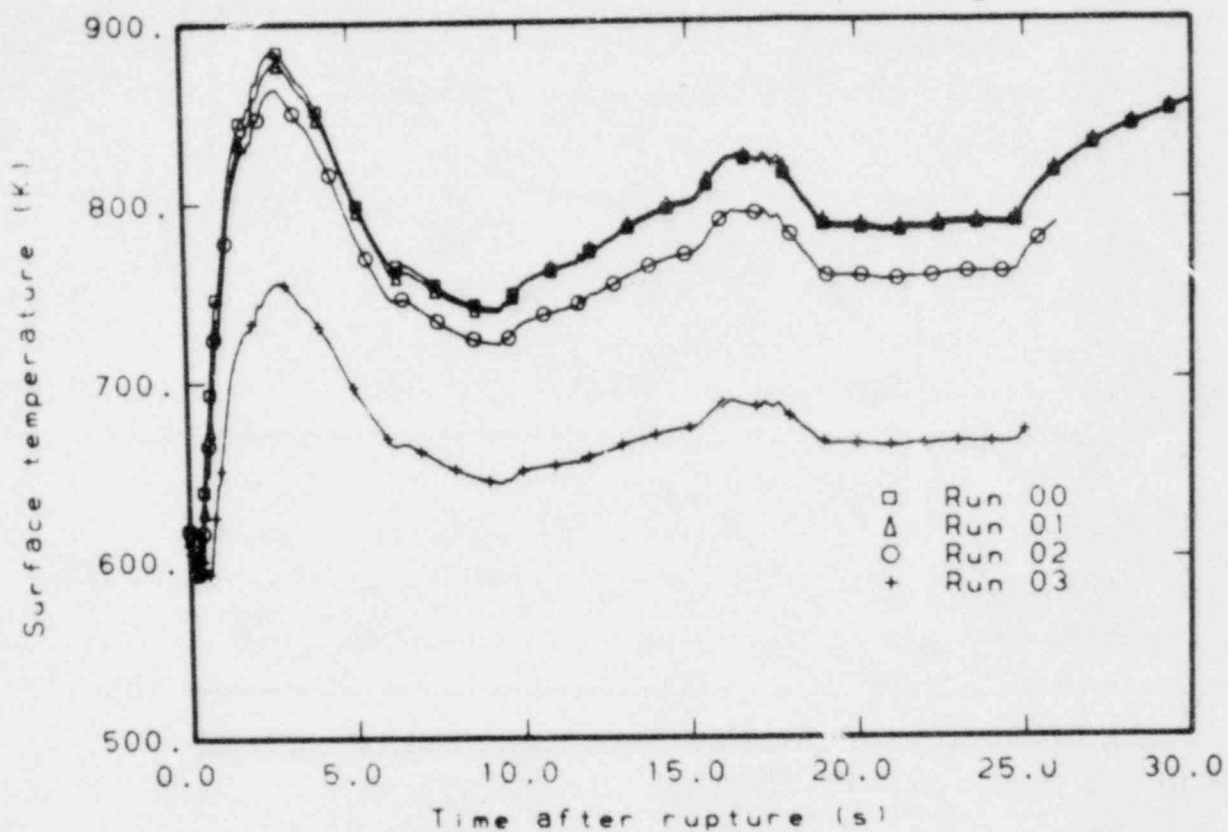
Figure 46. Hot spot fuel rod cladding temperature determined from four
hot pin calculations for Zion 1, 110% power case.

conditions. The steam generator removed all the generated heat; therefore, the cold leg temperature was set to 564.5 K (base calculation, 549.8 K). The temperature difference across the core was 2.2 K smaller than for the base case calculation.

Some results of this calculation are compared with the base case Zion 1 system calculation (110% power case) in Figure 47.

Due to the higher saturation pressure, more mass left the system the first second; therefore, the system depressurized faster during the first 1 or 2 s than was shown by the base case calculation (Figure 47). Also, because the cold leg temperature was closer to the hot leg temperature than in the base case calculation, the cold legs saturated earlier. Therefore, the mass leaving the system through the cold leg break decreased faster from 2 until 4 s into the transient and the pump degraded earlier at about 6 s, see Figures 48 and 49, respectively. These factors caused the balance between the two cold leg flows to be shifted, see Figure 50. Initially the sum of the two flows was larger (less mass leaving the cold leg break); later the sum was smaller (earlier pump degradation in the cold leg intact loop). The average core mass flow for Volume 40, shown in Figure 51, behaved the same as the sum of the two cold leg flows. Figure 52 shows the cladding temperature at the middle part of the core. The peak temperature was slightly higher (about the same amount as the hot leg temperature increase), and the peak was reached a little bit earlier (shifted core mass flow). Between 8 and 16 s into the transient, the core flow in the new calculation was closer to zero and the second temperature increase occurred earlier and gave higher temperatures.

From these calculations, it is concluded that a higher hot leg temperature has only a small influence on the peak cladding temperature in the middle of the core during the first part of blowdown. The influence on the temperature after the first peak is larger because of a smaller average core flow; however, the trend is the same for both calculations.

5.3.3 Pump Operation

To investigate the influence of the pump operation on the system behavior, three additional Zion 1 (110% power case) system calculations
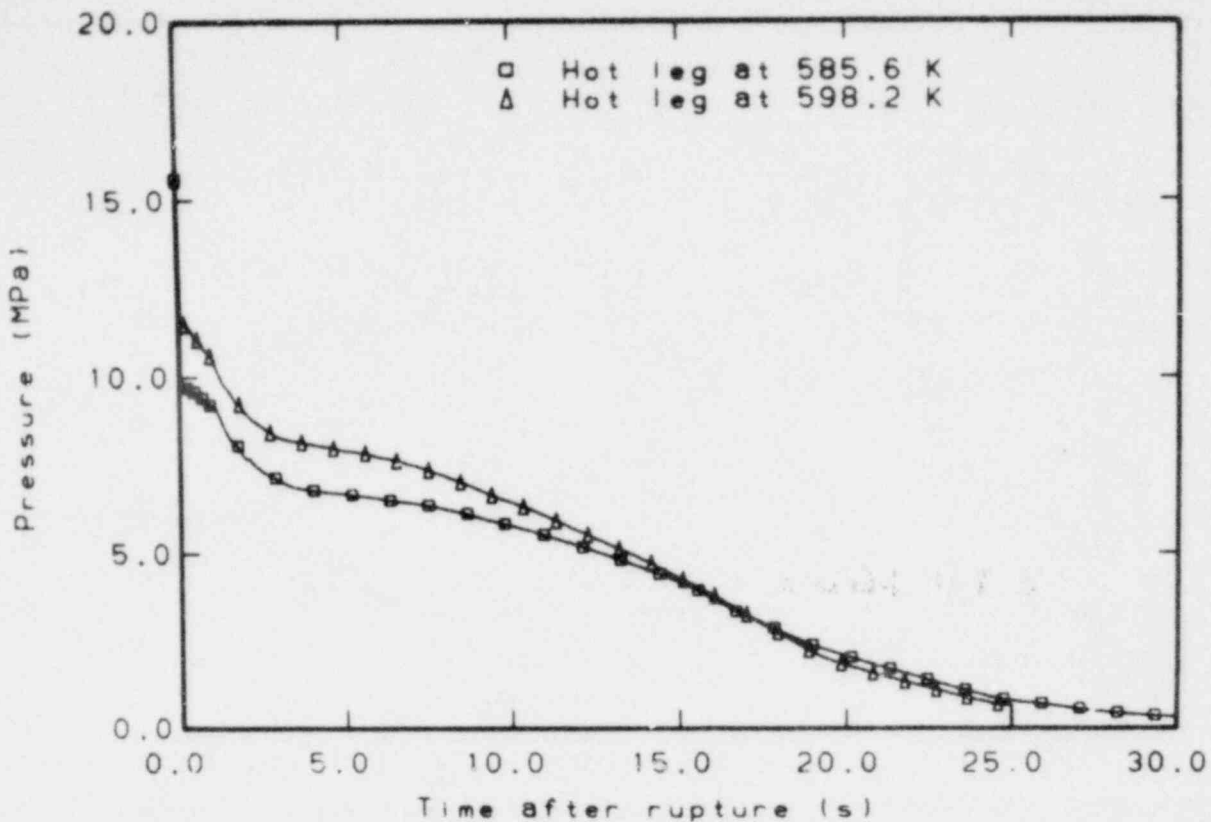
Figure 47. Pressure in upper plenum calculated for Zion 1, 110% power case conditions and for 12.6 K higher hot leg temperature conditions.
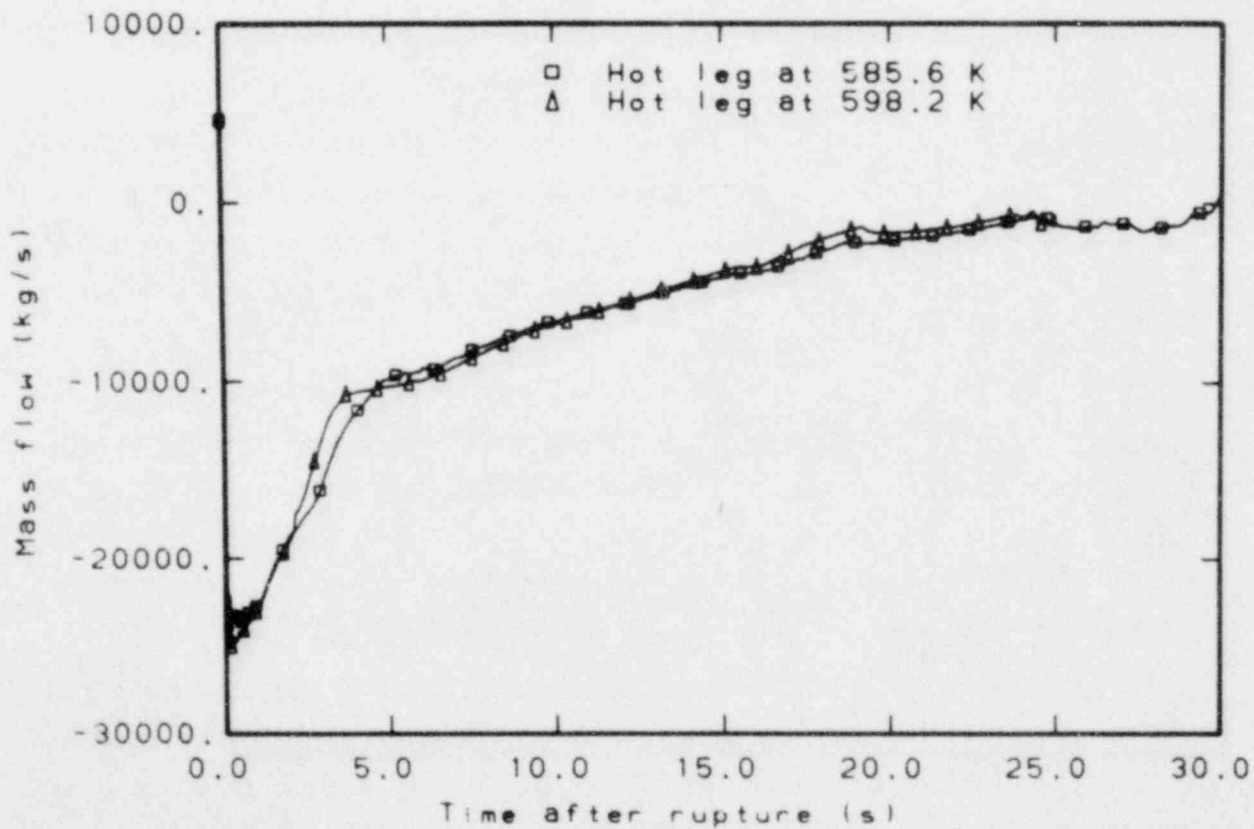

Figure 48. Mass flow in broken loop cold leg calculated for Zion 1, 110% power case conditions and for 12.6 K higher hot leg temperature conditions.
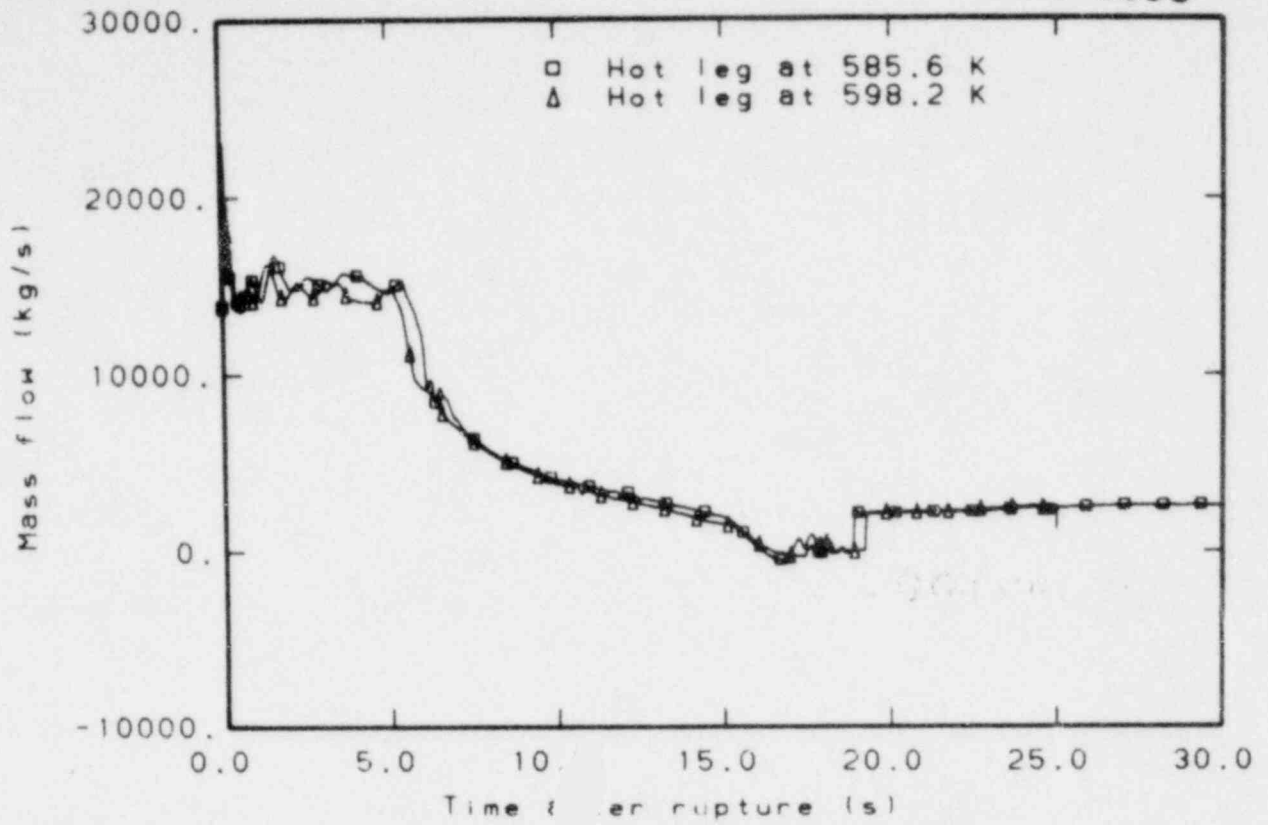
61

Figure 49. Mass flow in intact loop cold leg calculated for Zion 1, 110% power case conditions and for 12.6 K higher hot leg temperature conditions.
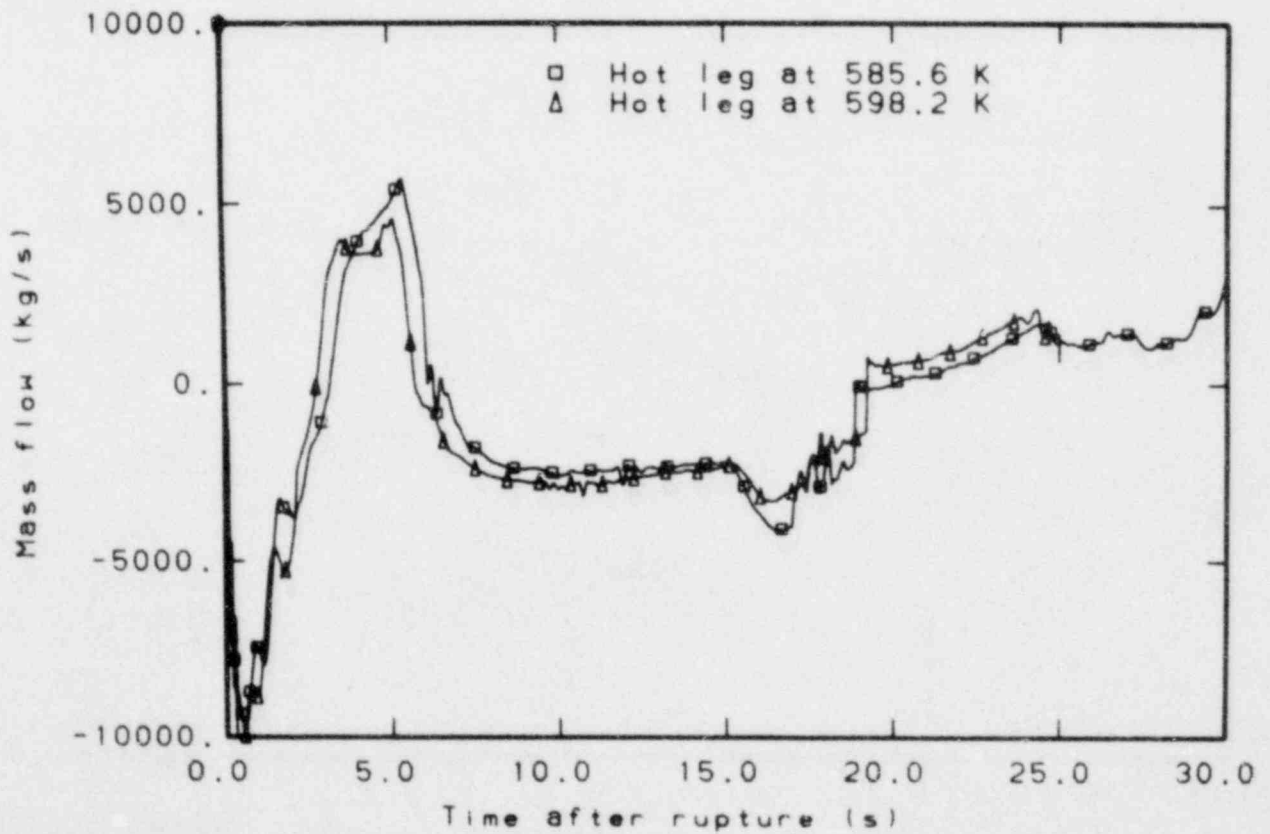

Figure 50. Sum of the two cold leg flows calculated for Zion 1, 110% power case conditions and for 12.6 K higher hot leg temperature conditions.
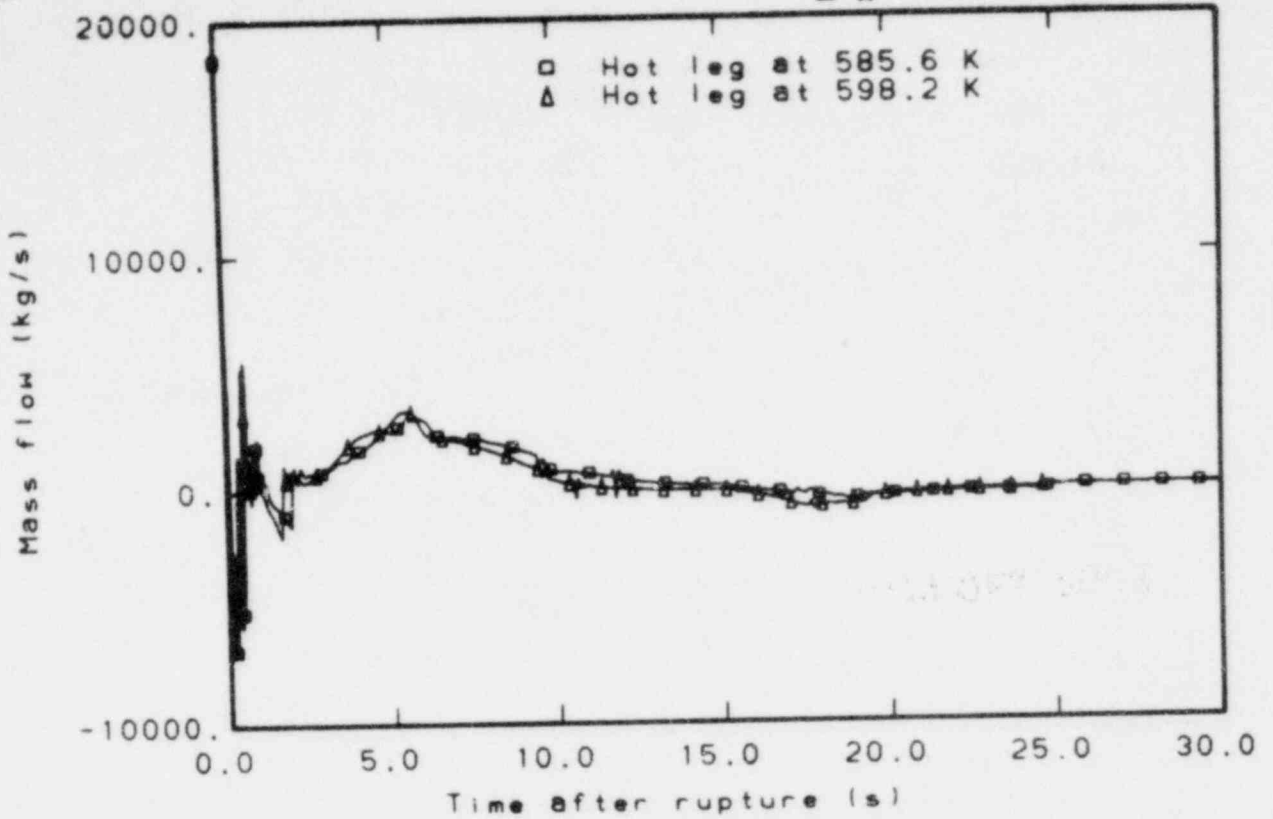
Figure 51. Average mass flow at the middle of the core calculated for Zion 1, 110% power case conditions and for 12.6 K higher hot leg temperature conditions.
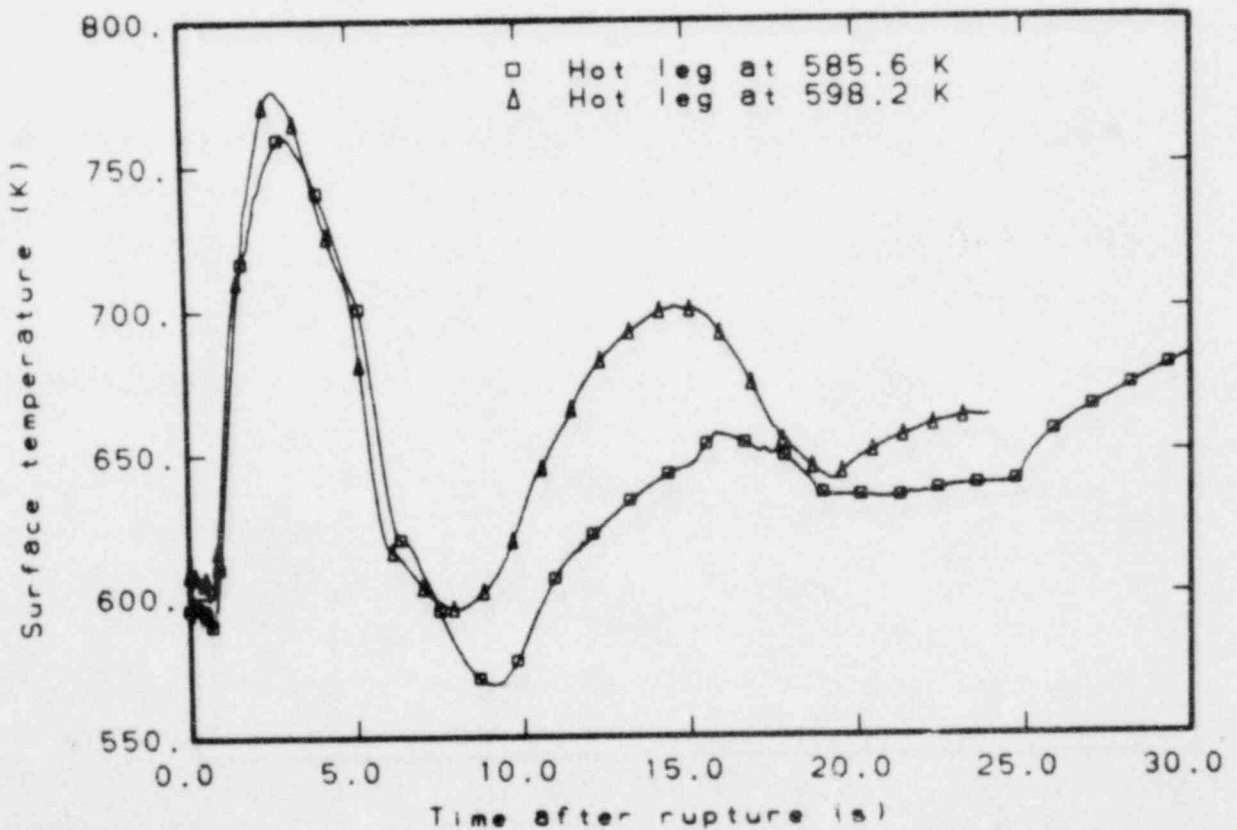

Figure 52. Fuel rod cladding temperature in middle part of core calculated for Zion 1, 110% power case conditions and for 12.6 K higher hot leg temperature conditions.

were done. These calculations are compared with the base case calculations described in Sections 2.1 and 3.1 as follows:

1. Base case calculation - both pumps are powered during the entire transient and keep running

2. Run 0301 - intact loop pump coasting down, broken loop pump running

3. Run 0302 - intact loop pump coasting down, broken loop pump blocked

4. Run 0303 - intact and broken loop pumps blocked.

A blocked pump in the broken loop in the LOFT system was simulated by a high hydraulic resistance in the pump simulator, while a running pump was simulated by a low hydraulic resistance. In LOFT, there is no possibility to block the pump in the intact loop. The calculations were stopped at 20.0 s into the transient. Figure 53 gives the typical pump speed for the different kind of pump trips. Figures 54 and 55 compare the hot and cold leg break flows from the four calculations. Figure 55 shows that the cold leg break flow was only affected by the intact loop pump. There was almost no difference in the cold leg break flow for a running pump and a pump coasting down. A blocked pump in the intact loop had a large influence on the cold leg break flow and gave a much smaller break flow (Figure 55).

Figure 56 shows the intact loop cold leg mass flow. As expected, the blocked pump in the intact loop gave the smallest mass flow. There was a slight difference in the mass flow in the intact loop for the pump coasting down (Runs 0301 and 0302) and the running pump (base case calculation).

Figure 57 shows the sum of the two cold leg mass flows. This sum is important because it gives the mass flow which was available for the core. The behavior of this summed flow was about the same for the running pump and the pump coasting down in the intact loop. The influence of the broken loop pump on this summed flow was very small; calculation Run 0301 (broken loop
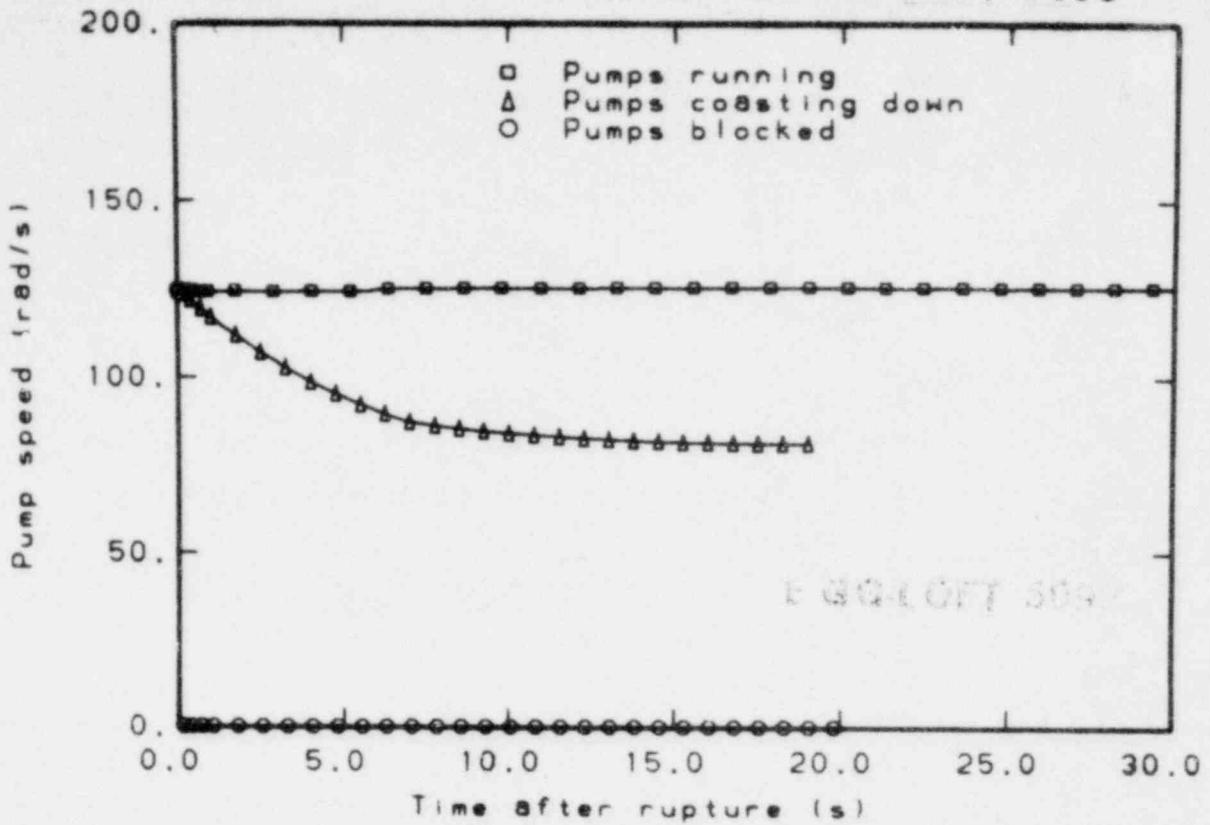
Figure 53. Typical pump speeds for Zion 1, 110% power case calculation with pumps running, coasting down, and blocked.
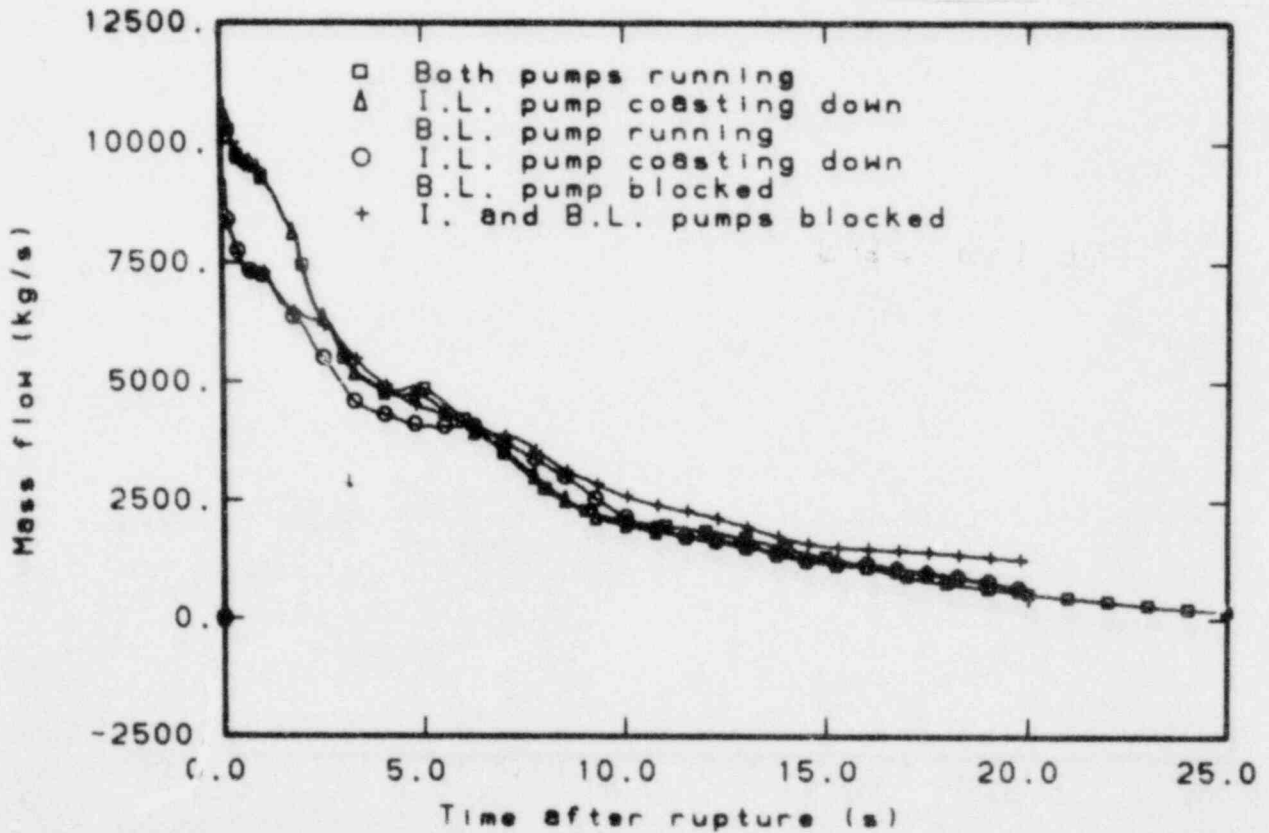

Figure 54. Hot leg break flow for Zion 1, 110% power base case calculation and for calculations with the pumps in various operating modes.
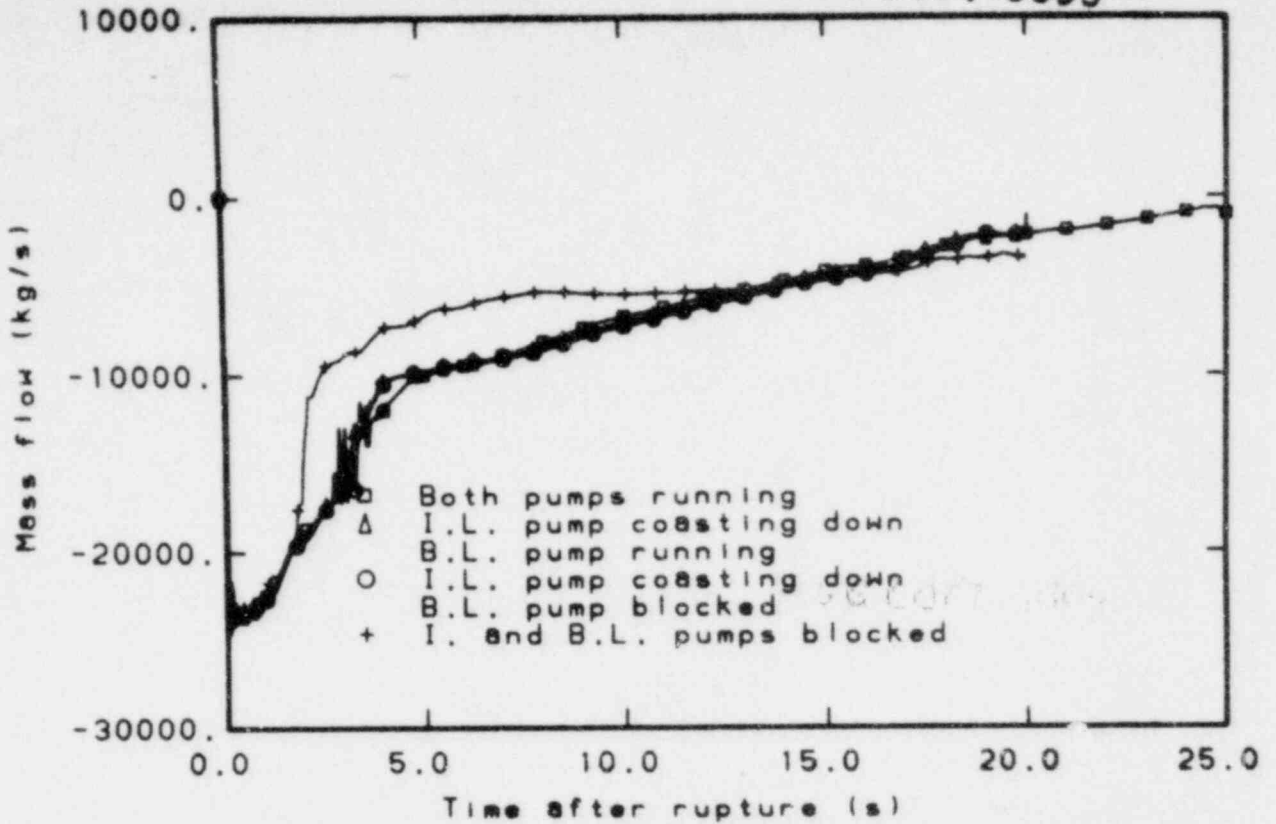
Figure 55. Cold leg break flow for Zion 1, 110% power base case calculation and for calculations with the pumps in various operating modes.
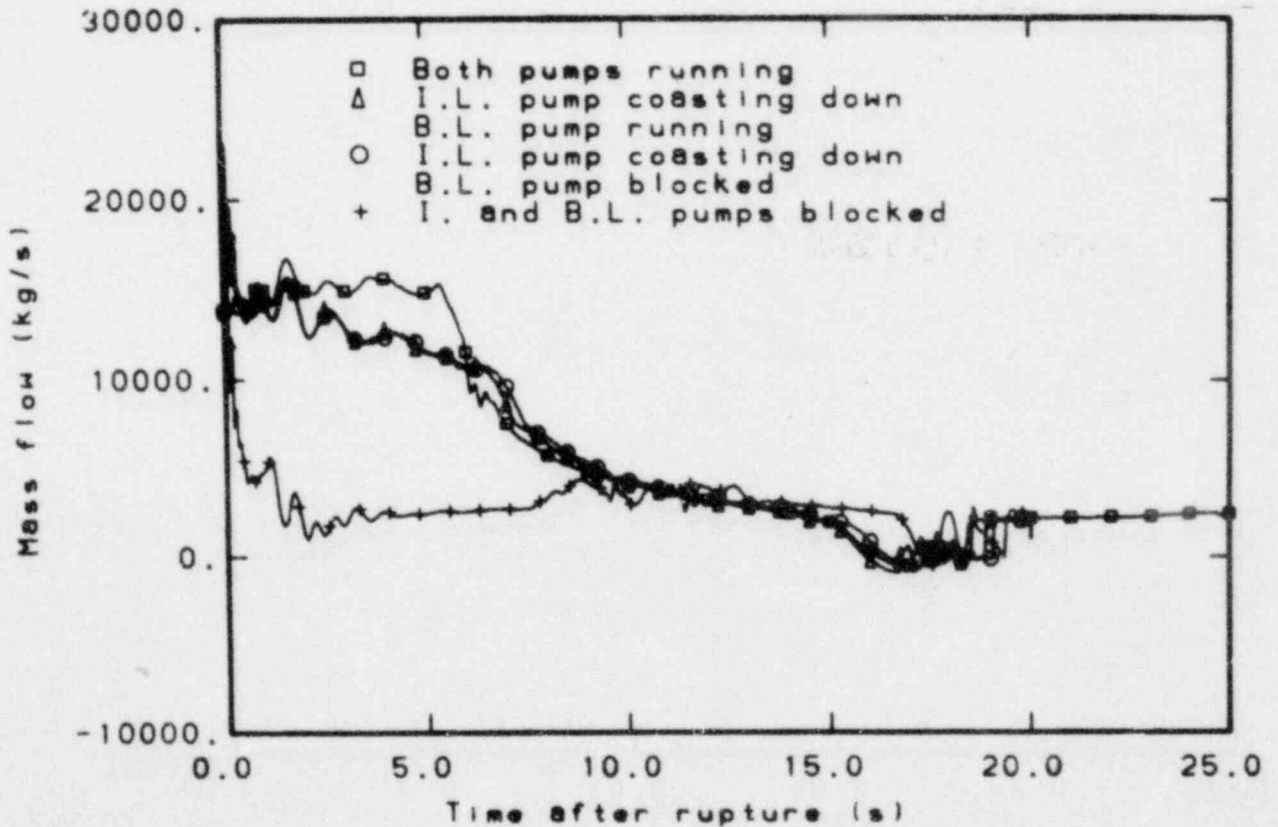

Figure 56. Mass flow in intact loop cold leg for Zion 1, 110% power base case calculation and for calculations with the pumps in various operating modes.
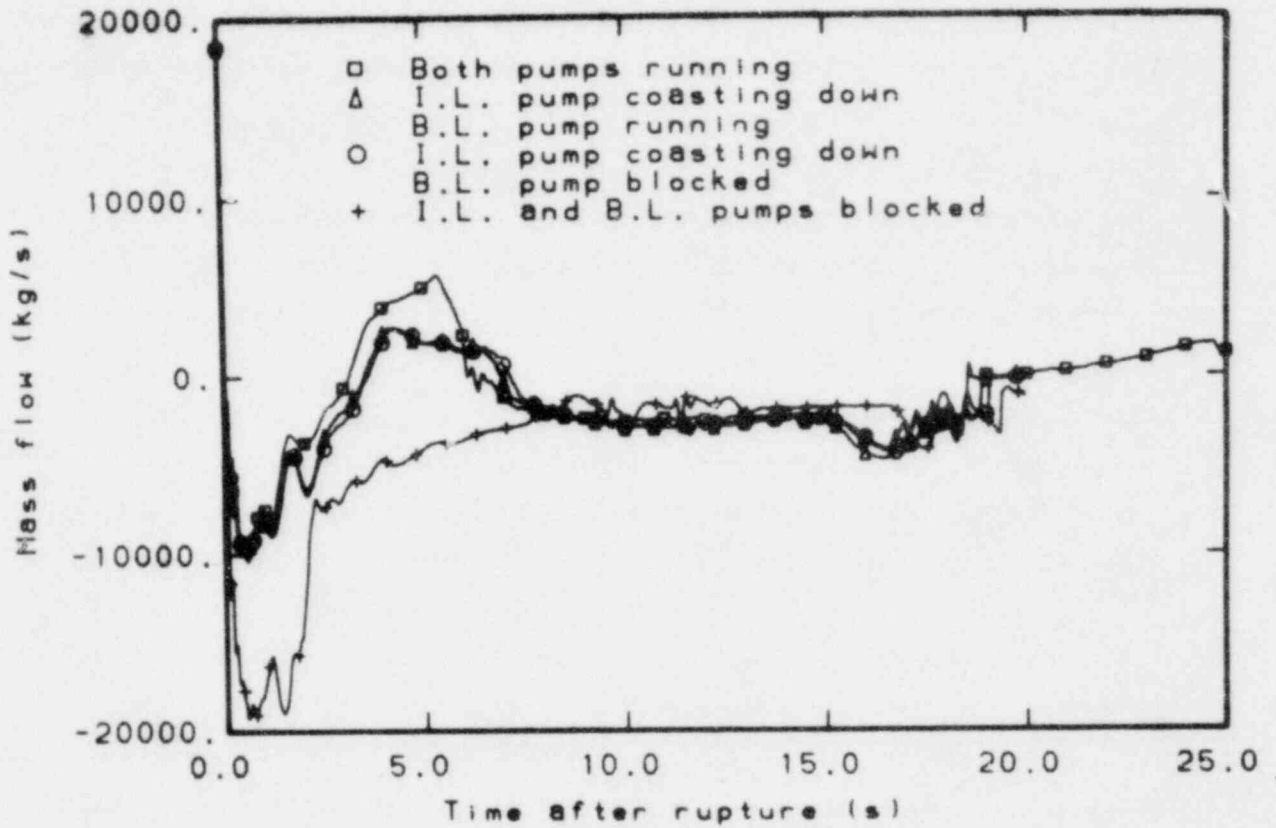
Figure 57. Sum of cold leg flows for Zion 1, 110% power base case calculation and for calculations with the pumps in various operating modes.

pump running) and Run 0302 (broken loop pump blocked) gave the same summed flow. The blocked pump in the intact loop gave a completly different behavior in which there was no flow from the cold leg available for the reactor vessel during the transient. The summed flow indicated that during the entire transient the mass was taken from the vessel.

Figure 58 shows the average core flow in the middle volume of the core. The behavior of this flow was the same as for the sum of the two cold leg flows for all calculated cases (Figure 57).

Figure 59 gives the cladding temperature for the middle heat slab in the core. The behavior of the cladding temperature was as expected from the core mass flow.

The most severe accident, which gives the highest peak cladding temperature, is a LOCA with a pump coasting down in the intact loop. The blocked pump in the intact loop which does not allow positive core flow to be reestablished is less severe because of sufficient core flow to cool the core.

Considering the close connection between the average core mass flow and the cladding temperature, a partial blocking of the intact loop pump could be occurring which causes a core mass flow very close to zero during the entire transient and possibly will lead to high temperatures in the core.

5.3.4 Zion 1 Calculations at Experiment L2-4 Conditions with Low Mass Flow

It is not possible to run LOFT Experiment L2-4 with the same mass flow as in Experiment L2-3 and a power of 50 MW because of safety considerations of the plant. It is perhaps possible to satisfy the plant safety requirements a i perform the experiment with the lower mass flow and 50 MW power if the system temperature is lowered. Three calculations were done with 50 MW power, low mass flow, and cold leg fluid temperatures of 549.8, 533.2, and 516.5 K. When the system was balanced, the core temperature differences across the core for the 549.8-, 533.2-, and 516.5-K cases were 47.0, 49.9, and 52.3 K, respectively. The results of the calculations confirm the results of the Zion 1 calculation (110% power case) with increased hot leg temperatures discussed in Section 5.3.3.
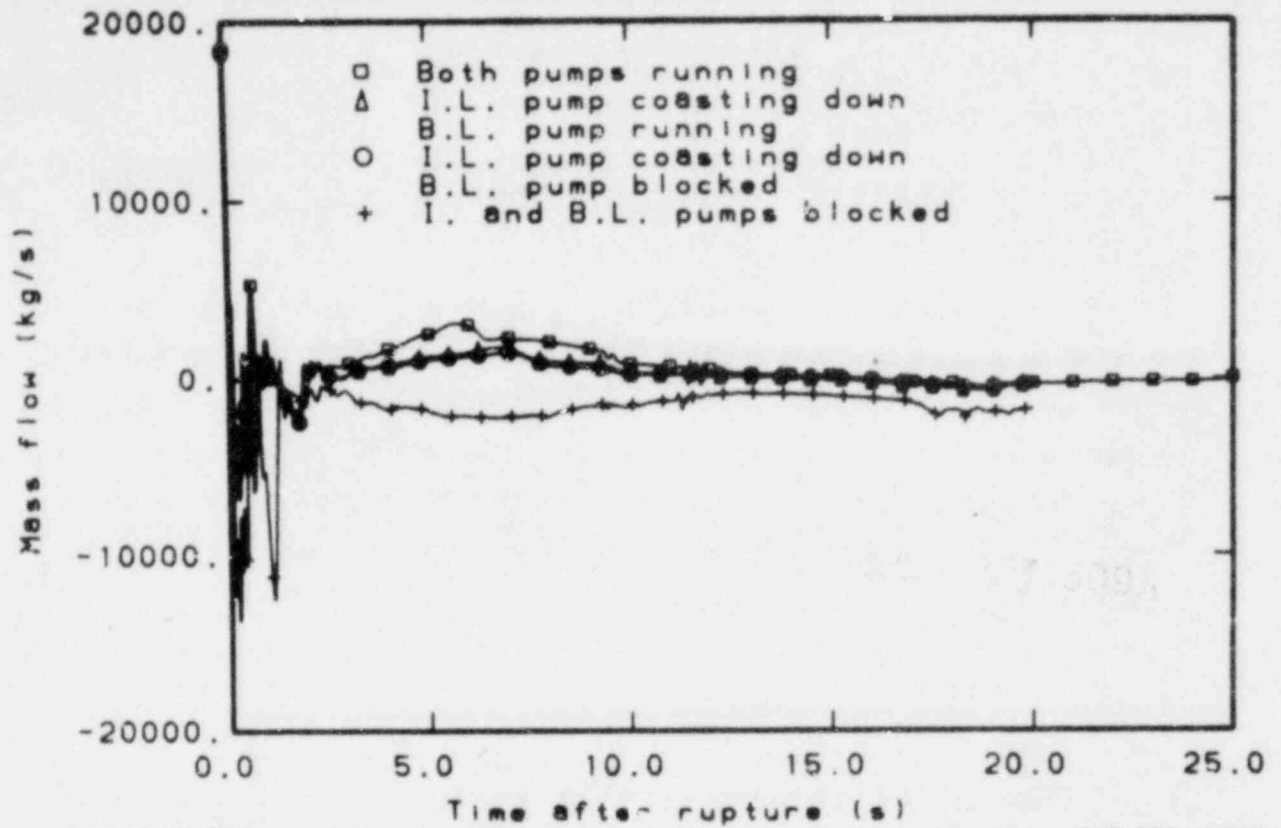
Figure 58.   Average mass flow in middle part of core for Zion 1, 110%
power base case calculation and for calculations with the
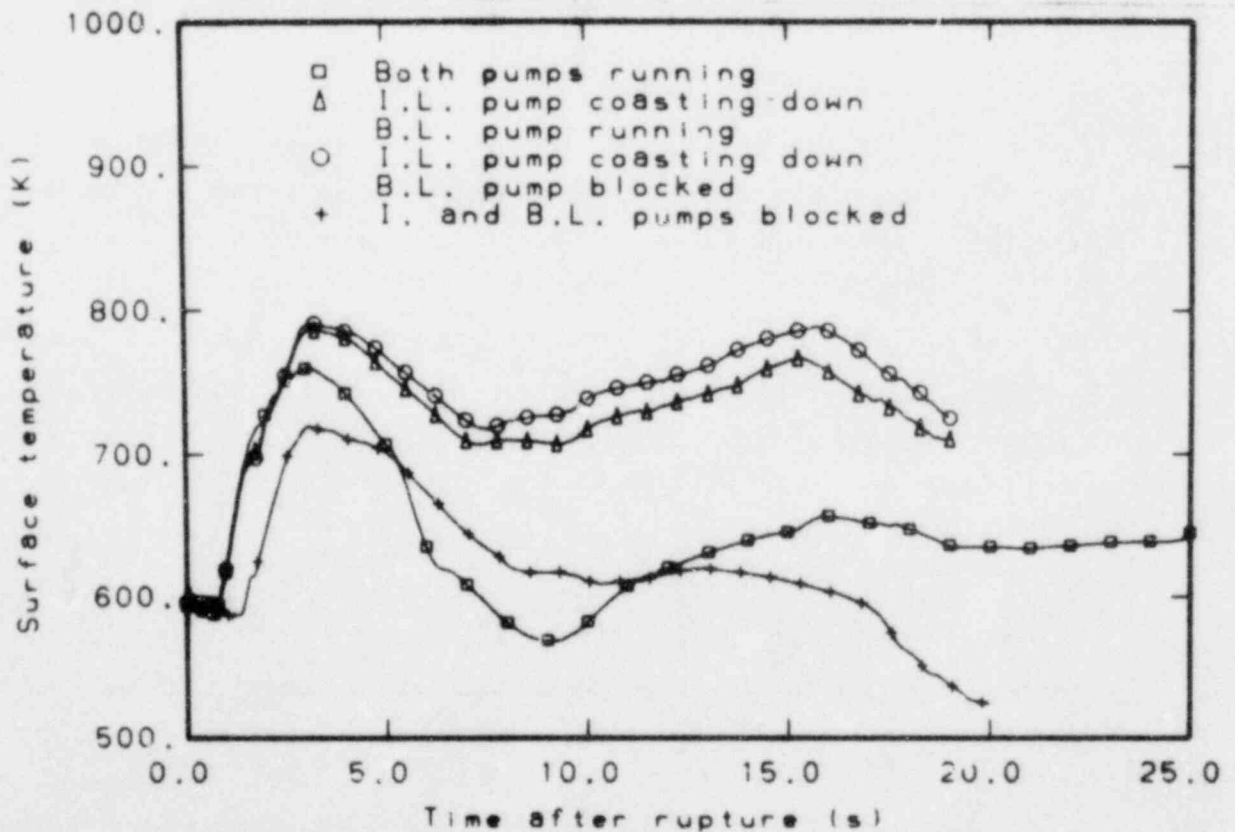pumps in various operating modes.

Figure 59.   Cladding temperature in middle part of core for Zion 1, 110%
power base case calculation and for calculations with the
pumps in various operating modes.

Figure 60 shows the cold leg break flow, and the average core mass flow for the middle volume of the core is shown in Figure 61. Figure 62 shows the pressure in the upper plenum. The average core mass flow, again, reflects the behavior of the cold leg break flow. Between 4 and 7 s into the transient, the break flow for the lowest temperature was the largest and, therefore, the core mass flow was the smallest. Figure 63 shows the cladding temperature in the middle part of the core. The peak temperature at about 3 s was lowest for the lowest hot leg temperature, but the first cooldown of the core which occurs after about 6 s was considerably less for the lower hot leg temperature. Because less heat was transferred from the core during the first 10 s, the later part of blowdown gave substantial higher temperatures for the lower hot leg temperature case. The three calculations show that for the lower hot leg temperature case the peak cladding temperature occurred later in the blowdown phase.

From these calculations it is not clear that an experiment at lower system temperature would be representative of what would happen at higher system temperatures.

6.   CONCLUSIONS

LOFT is prototypical of a LPWR for 200% double-ended cold leg breaks. The early rewet seen in the first two LOFT large break experiments is expected to happen in a LPWR under the same accident conditions.

The behavior of a LPWR with a 200% double-ended cold leg break is sensitive to the pump operation in the intact loop. The behaviors for a running pump and a pump coasting down are quite close. A blocked pump in the intact loop gives a reversed flow and there is no reestablishment of a positive core flow.

The steam generator geometry and the water level in the pressurizer do not have a significant influence on the system behavior after a LOCA with a 200% double-ended cold leg break.
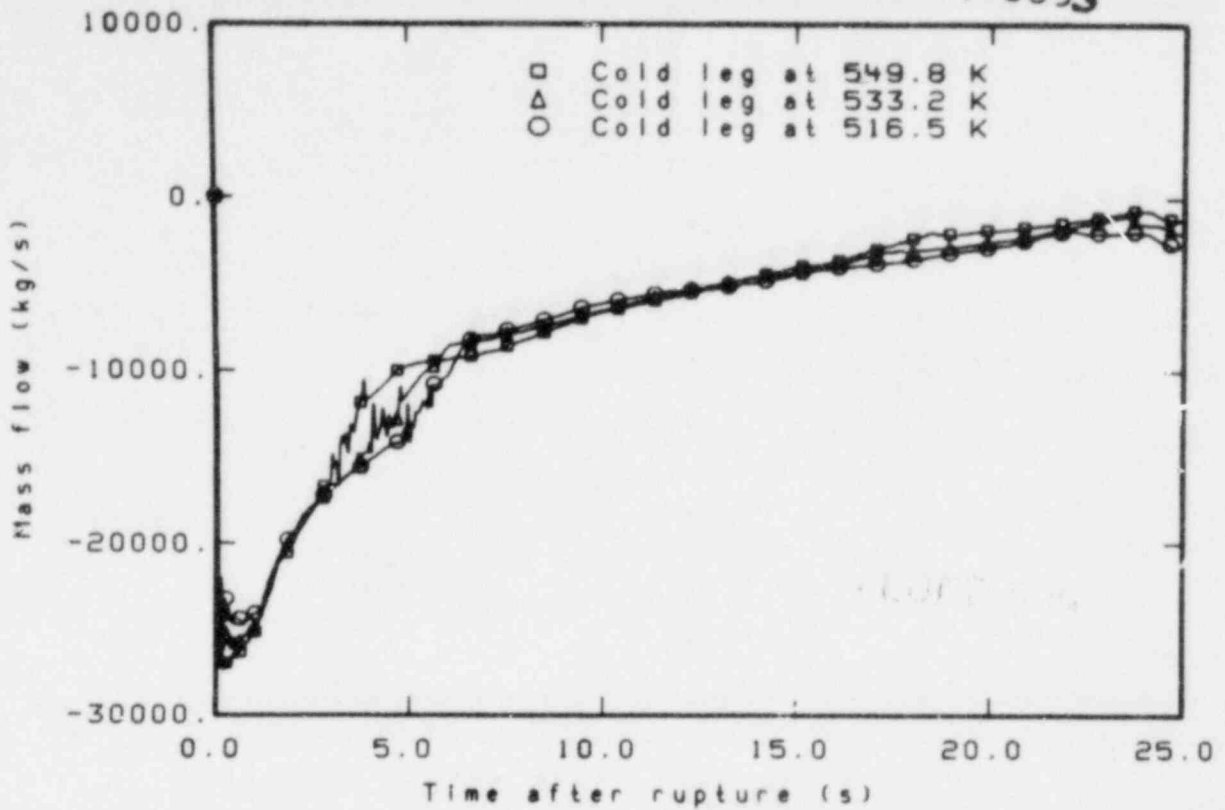
Figure 60. Cold leg break flow for Zion 1, 150% power case calculations with low mass flow and varied cold leg fluid temperatures.
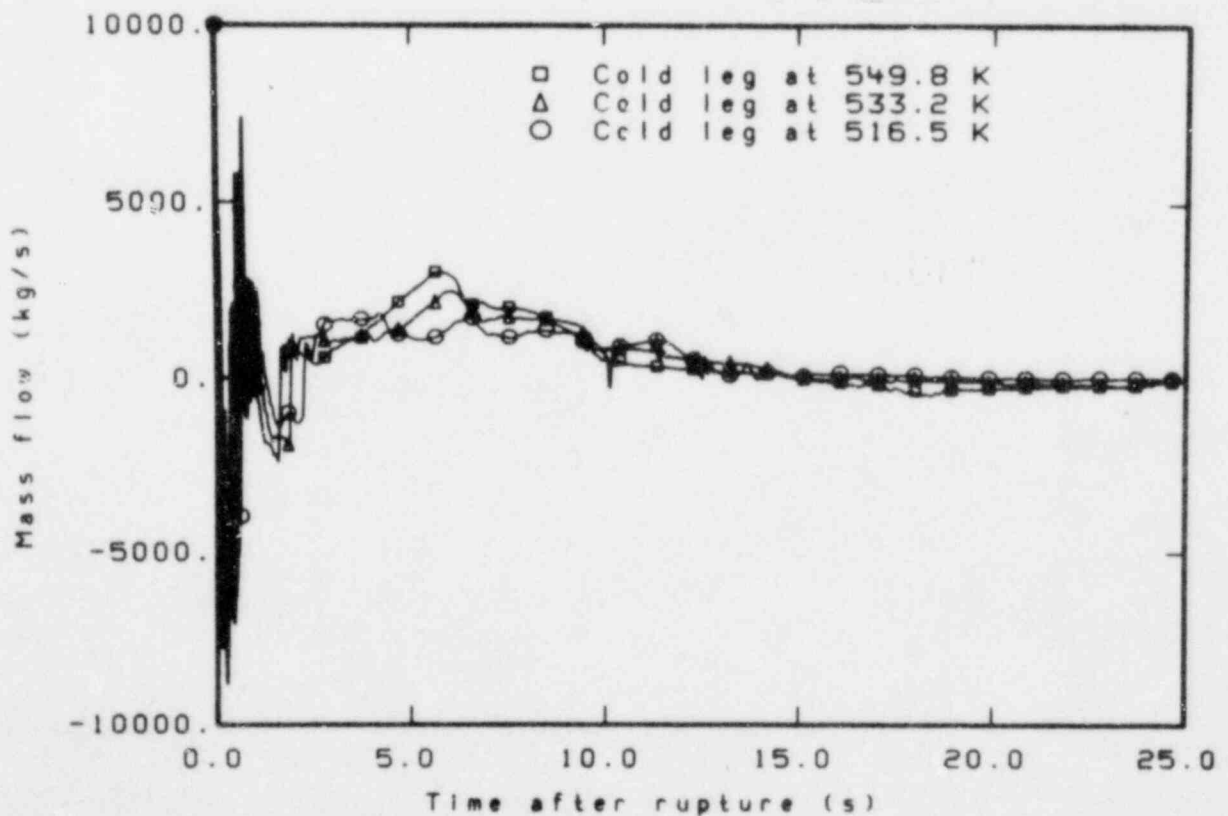

Figure 61. Average mass flow in middle part of core for Zion 1, 150% power case calculations with low mass flow and varied cold leg fluid temperatures.
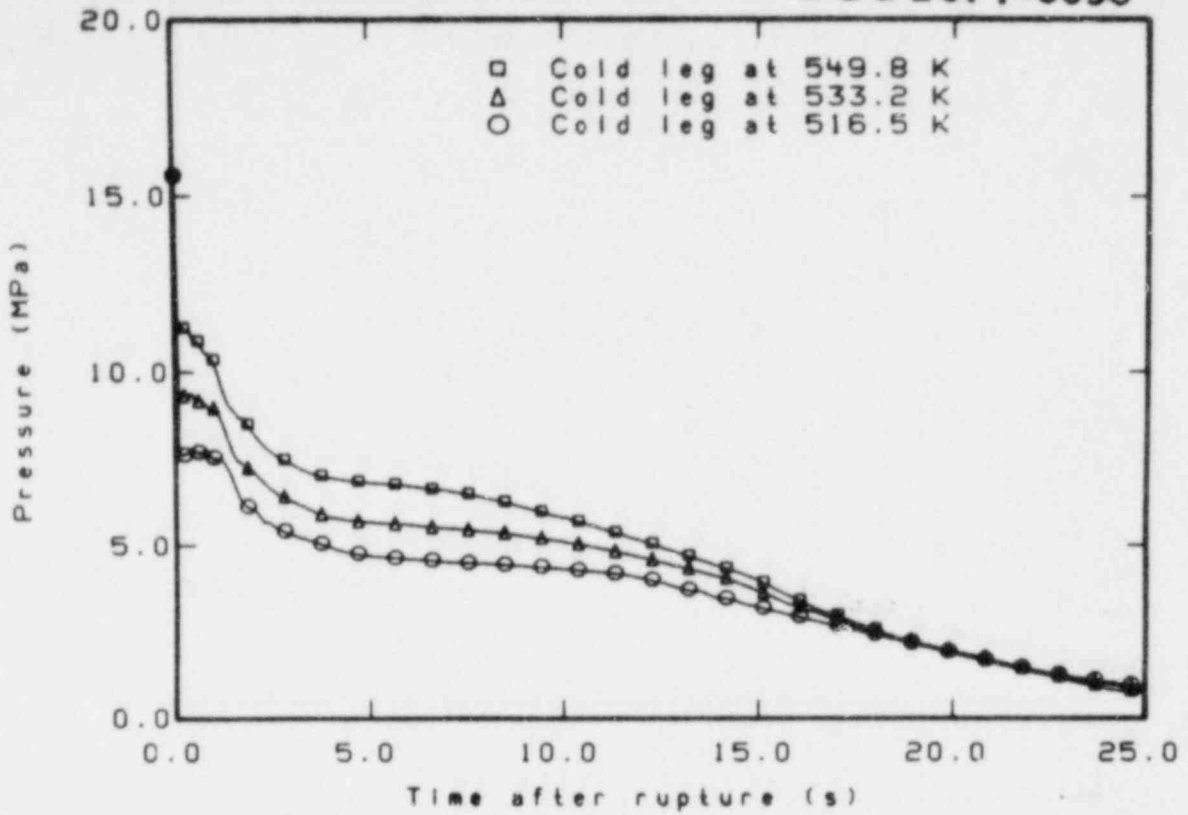
Figure 62. Pressure in upper plenum for Zion 1, 150% power case calculations with low mass flow and varied cold leg fluid temperatures.
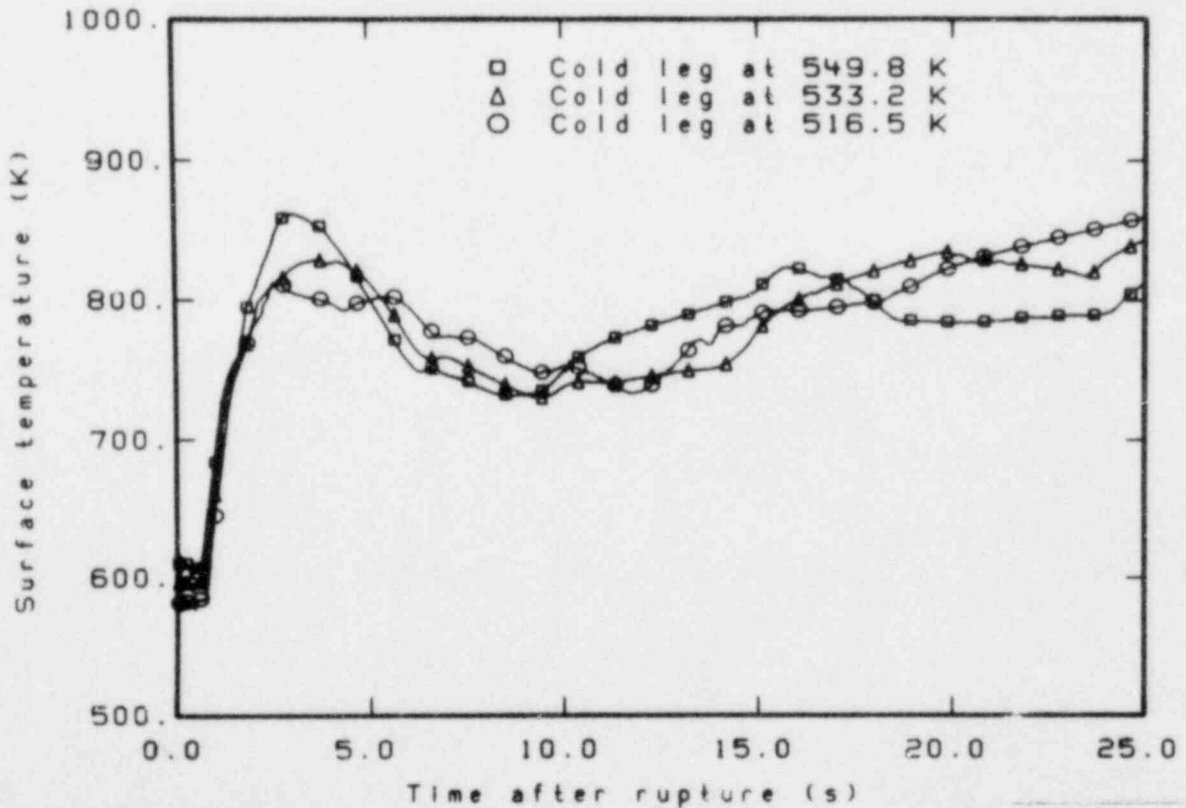

Figure 63. Cladding temperature in middle part of core for Zion 1, 150% power case calculations with low mass flow and varied cold leg fluid temperatures.

72

The calculated LPWR system behavior after a LOCA is less sensitive to the break flow multiplier and transition region used in RELAP4 than was expected from identical sensitivity studies for the LOFT system.

The originally planned LOFT Experiment L2-4 will have the same early rewet tendency as occurred in LOFT Experiments L2-2 and L2-3. The peak temperature, however, will be reached later into the transient, during the refill or reflood phases.

7. REFERENCES

1. D. L. Reeder, LOFT System and Test Description (5.5 ft Nuclear Core 1 LOCEs), NUREG/CR-0247, TREE-1208, July 1978.

2. G. W. Johnsen, F. W. Childs, J. M. Broughton, A Comparison of "Best-Estimate" and "Evaluation Model" LOCA Calculations: The BE/EM Study, PG-R-76-009, December 1976.

3. S. R. Fisher et al., RELAP4/MOD6 - A Computer Program for Transient Thermal-Hydraulic Analysis of Nuclear Reactors and Related Systems - Users's Manual, CDAP-TR-003, January 1978.

4. W. H. Grush et al., Best Estimate Experiment Predictions for LOFT Nuclear Experiments L2-2, L2-3, and L2-4, LOFT-TR-101, November 1978.

5. E. J. Kee and W. H. Grush, Best Estimate Prediction for LOFT Nuclear Experiment L2-3, EP-L2-3, April 1979.

6. W. H. Grush and H. L. O. Holmstrom, Posttest RELAP4 Analysis of LOFT Experiment L1-4, TREE-NUREG-1183, November 1977.

7. D. L. Batt, Quick Look Report on LOFT Nuclear Experiment L2-2, LOFT-TR-103, December 1978.

8. M. McCormick-Barger, <u>Experiment Data Report for LOFT Power Ascension Test L2-2</u>, NUREG/CR-0492, TREE-1322, February 1979.

9. J. R. White, W. H. Grush, C. D. Keeler, <u>Preliminary Posttest Analysis of LOFT Loss-of-Coolant Experiment L2-2</u>, LTR 20-103, June 1979.